



**ORKUSTOFNUN**

National Energy Authority



## Effect of climate change on hydrology and hydro-resources in Iceland

**Tómas Jóhannesson<sup>1</sup>, Guðfinna Aðalgeirsdóttir<sup>3</sup>,  
Helgi Björnsson<sup>3</sup>, Philippe Crochet<sup>1</sup>, Elías B. Elíasson<sup>6</sup>,  
Sverrir Guðmundsson<sup>3</sup>, Jóna Finndís Jónsdóttir<sup>2</sup>,  
Haraldur Ólafsson<sup>5,4,1</sup>, Finnur Pálsson<sup>3</sup>, Ólafur  
Rögnvaldsson<sup>5</sup>, Oddur Sigurðsson<sup>2</sup>, Árni Snorrason<sup>2</sup>,  
Óli Grétar Blöndal Sveinsson<sup>6</sup>, Thorsteinn Thorsteinsson<sup>2</sup>**

<sup>1</sup>Icelandic Meteorological Office

<sup>2</sup>National Energy Authority, Hydrological Service

<sup>3</sup>Institute of Earth Sciences, University of Iceland

<sup>4</sup>University of Iceland

<sup>5</sup>Institute for Meteorological Research

<sup>6</sup>Landsvirkjun/National Power Company

*Client: The VO project*

**OS-2007/011**



## Effect of climate change on hydrology and hydro-resources in Iceland

**Tómas Jóhannesson<sup>1</sup>, Guðfinna Aðalgeirsdóttir<sup>3</sup>,  
Helgi Björnsson<sup>3</sup>, Philippe Crochet<sup>1</sup>, Elías B. Elíasson<sup>6</sup>,  
Sverrir Guðmundsson<sup>3</sup>, Jóna Finndís Jónsdóttir<sup>2</sup>,  
Haraldur Ólafsson<sup>5,4,1</sup>, Finnur Pálsson<sup>3</sup>, Ólafur Rögnvaldsson<sup>5</sup>,  
Oddur Sigurðsson<sup>2</sup>, Árni Snorrason<sup>2</sup>, Óli Grétar  
Blöndal Sveinsson<sup>6</sup>, Thorsteinn Thorsteinsson<sup>2</sup>**

<sup>1</sup>Icelandic Meteorological Office

<sup>2</sup>National Energy Authority, Hydrological Service

<sup>3</sup>Institute of Earth Sciences, University of Iceland

<sup>4</sup>University of Iceland

<sup>5</sup>Institute for Meteorological Research

<sup>6</sup>Landsvirkjun/National Power Company


*Client:*

*The VO project*

**OS-2007/011**

978-9979-68-224-0



<b>Report no.:</b> OS-2007/011	<b>Date:</b> 18.12.2007	<b>Distribution:</b> Open <input checked="" type="checkbox"/> Closed <input type="checkbox"/>
		<b>Conditions:</b>
<b>Title / Main and sub-title:</b> Effect of climate change on hydrology and hydro-resources in Iceland		<b>Number of copies:</b> 500
		<b>Number of pages:</b> 91
<b>Authors:</b> Tómas Jóhannesson, Guðfinna Aðalgeirsdóttir, Helgi Björnsson, Philippe Crochet, Elías B. Elíasson, Sverrir Guðmundsson, Jóna Finndís Jónsdóttir, Haraldur Ólafsson, Finnur Pálsson, Ólafur Rögnvaldsson, Oddur Sigurðsson, Árni Snorrason, Óli Grétar Blöndal Sveinsson, Thorsteinn Thorsteinsson		<b>Project manager:</b> Árni Snorrason
		<b>Project number:</b> 7-690000
<b>Client:</b> The VO project		
<b>Abstract:</b> <p>Future climate change is likely to have pronounced effects on the hydrology and hydro-resources of Iceland. These effects have been investigated by an analysis of climate records, and by modelling of the climate, hydrology and glaciers. The distribution of precipitation in Iceland was modelled and a distributed runoff model was calibrated and used to create a new runoff map for all of Iceland. The modelling of future changes was based on the CE/VO climate change scenario which implies a mean warming of 2.5–3° C between 1961–1990 and 2071–2100 with the greatest warming in the spring and fall. Precipitation changes are comparatively small, with up to 10–20% average increase in the fall between these periods but little change in other seasons. Runoff is projected to increase by 25% between 1961–1990 and 2071–2100, mainly due to increased melting of glaciers, which may disappear almost completely within the next 200 years. Runoff seasonality and flood characteristics are projected to change such that there will in general be more autumn and winter runoff, and spring floods will be earlier and most likely smaller in amplitude. Subglacial water courses and outlet locations of many glacial rivers are likely to change due to the thinning of ice caps and the retreat of glacier margins. A substantial increase in gravitational, potential hydropower is projected and the changes in runoff, seasonality and water courses imply modifications in design assumptions and changes in the operating environment of hydropower plants and other hydrological infrastructure such as bridges and roads.</p>		
<b>Keywords:</b> climate-change energy-production climate-change-scenarios precipitation-modelling mass-balance-modelling glacier-modelling		<b>ISBN-number:</b> 978-9979-68-224-0
		<b>Signature of project manager:</b> 
		<b>Checked by:</b> 



# Contents

<b>1</b>	<b>Introduction</b>	<b>9</b>
<b>2</b>	<b>Recent variations in climate and runoff in Iceland</b>	<b>11</b>
2.1	The climate of Iceland	11
2.2	The hydrology of Iceland	12
2.3	Snow and glaciers	13
2.4	Recent variations in temperature and precipitation	13
2.5	Recent glacier variations	15
2.6	Quantitative analysis of precipitation and discharge variations	16
2.7	Trend analysis by non-parametric methods	17
2.7.1	Temperature	18
2.7.2	Precipitation	18
2.7.3	Discharge	19
2.7.4	Conclusions	19
2.8	Trend analysis by parametric methods	20
<b>3</b>	<b>Climate change scenarios</b>	<b>21</b>
3.1	Precipitation	21
3.2	Winds	22
3.3	Temperature	23
3.4	Scenarios for glaciological and hydrological simulations	24
<b>4</b>	<b>Precipitation modelling</b>	<b>28</b>
4.1	Introduction	28
4.2	Precipitation observations at meteorological stations	28
4.3	Modelling with the MM5 model	29
4.3.1	Verification of simulated precipitation	29
4.4	Modelling with the LT model	37
4.4.1	Model calibration	37
4.4.2	Model validation	37
4.5	Comparison and interpretation of the two sets of model results	37
<b>5</b>	<b>Glacier modelling</b>	<b>43</b>
5.1	Mass balance modelling	44
5.2	Dynamic modelling	45
5.3	Results	46
5.4	Contribution to hydrological modelling	47
<b>6</b>	<b>Runoff modelling</b>	<b>49</b>
6.1	Introduction	49
6.2	Background	49
6.3	Data	49
6.4	Methods	50
6.5	Results of runoff modelling	53
6.6	Summary and outlook	54
<b>7</b>	<b>Energy production</b>	<b>59</b>
7.1	The Icelandic power system	59

7.2	Implications for system planning and component design . . . . .	59
7.3	Magnitude of the climate trend . . . . .	61
7.4	Runoff series . . . . .	61
7.5	Risk analysis . . . . .	62
7.6	Concluding remarks . . . . .	63
<b>8</b>	<b>Summary and conclusions</b>	<b>65</b>
<b>9</b>	<b>Suggestions for further research</b>	<b>69</b>
<b>10</b>	<b>Acknowledgements</b>	<b>72</b>
<b>11</b>	<b>References</b>	<b>73</b>
<b>A</b>	<b>The LT orographic precipitation model</b>	<b>82</b>
<b>B</b>	<b>Daily validation of simulated precipitation</b>	<b>84</b>
<b>C</b>	<b><math>R2</math> and <math>R2log</math> coefficients for measured and simulated discharge</b>	<b>88</b>
<b>D</b>	<b>Runoff maps</b>	<b>90</b>



## List of Tables

1	Comparison of observed and simulated discharge from six watersheds not affected by groundwater flow. . . . .	31
2	Accumulated winter balance and simulated wintertime precipitation at Drangajökull, NW-Iceland. . . . .	36
3	Characteristics of the Langjökull, Hofsjökull and Vatnajökull ice caps. . . . .	43
4	Common model parameters for mass balance modelling of Langjökull, Hofsjökull and Vatnajökull ice caps. . . . .	45
5	Model parameters for mass balance modelling of the Langjökull, Hofsjökull and Vatnajökull ice caps. . . . .	46
C1	Comparison of observed and simulated (WaSiM/MM5) water balance at gauging stations. . . . .	88

## List of Figures

1	Main rivers and glaciers in Iceland. . . . .	12
2	Seasonal discharge variations of three representative Icelandic rivers. . . . .	13
3	Annual average temperature of the northern hemisphere and at Stykkishólmur, W-Iceland, since the 19 <sup>th</sup> century. . . . .	14
4	Annual precipitation at five weather stations in Iceland since the late 19 <sup>th</sup> century or early 20 <sup>th</sup> century. . . . .	14
5	Oblique aerial photographs of Hyrningsjökull and Sólheimajökull. . . . .	15
6	Cumulative variations of the termini of six non-surge-type glaciers in Iceland during the period 1930–2007. . . . .	16
7	Percentage of advancing and retreating termini of glaciers in Iceland from 1930/1931 to 2006/2007. . . . .	16
8	Annual deviations from mean discharge in the Hvítá river at Kljáfoss, W-Iceland. . . . .	18
9	Time of spring and autumn floods at Maríufoss, Tungnaá river. . . . .	19
10	The simulation domain and gridpoints of the HIRHAM dynamic downscaling. . . . .	21
11	Change in annual precipitation in Iceland according to the HIRHAM A2 and B2 downscaling. . . . .	22
12	Change in seasonal precipitation in Iceland according to the HIRHAM A2 and B2 downscaling. . . . .	23
13	Ratio of observed precipitation in mountains with orographic enhancement to lowland areas in the same region without orographic enhancement. . . . .	24
14	Frequency of geostrophic wind directions over Iceland in the control and scenario simulations. . . . .	24
15	Seasonal cycle of temperature 1961–1990 and 2071–2100 in SW-Iceland. . . . .	25
16	Observed seasonal change in temperature in Reykjavík. . . . .	25
17	A scenario for seasonal changes in temperature and precipitation for the 21 <sup>st</sup> century averaged over Iceland. . . . .	26
18	A scenario for seasonal precipitation change for the 21 <sup>st</sup> century for SW-, NW-, NE- and SE-Iceland. . . . .	26
19	Domain setup of the MM5 model. . . . .	30
20	Observed and simulated (MM5) mean annual two-metre temperature. . . . .	32
21	Difference between observed and simulated mean annual two-metre temperature. . . . .	33
22	Location map showing the ice caps and glaciers used for validation of precipitation modelling. . . . .	34
23	Comparison of simulated and measured winter precipitation at Hofsjökull. . . . .	35

24	Comparison of simulated precipitation and observed winter balance for Vatnajökull and Langjökull. . . . .	36
25	Simulated 30-year mean annual precipitation by the LT and MM5 models for 1961–1990. . . . .	39
26	Difference in simulated 30-year mean annual precipitation by the LT and MM5 models for 1961–1990. . . . .	40
27	Simulated 30-year mean monthly precipitation by the LT and MM5 models for 1961–1990 averaged over Iceland. . . . .	40
28	Area-averaged annual precipitation in Iceland for 1958–2005. . . . .	41
29	Location map showing glaciers, meteorological stations and locations of mass balance measurements. . . . .	43
30	Bedrock, ice surface and steady-state ice surface of Langjökull and Hofsjökull ice caps. . . . .	44
31	Observed and modelled mass balance of Langjökull. . . . .	45
32	Response of Langjökull, Hofsjökull and southern Vatnajökull to the CE/VO-climate change scenario. . . . .	47
33	Volume and area reduction, and area-averaged runoff change for Langjökull, Hofsjökull and southern Vatnajökull. . . . .	47
34	Measured and simulated (WaSiM/MM5) discharge. . . . .	51
35	Classification of catchment types in Iceland. . . . .	52
36	Simulated total annual runoff for all of Iceland for the period 1961–1990. . . . .	53
37	Modelled mean annual and seasonal runoff in Iceland for the water years 1961–1990. . . . .	55
38	Projected change in mean annual and seasonal runoff from 1961–1990 to 2071–2100. . . . .	56
39	Projected change in mean annual number of days with snow covered ground from 1961–1990 to 2071–2100. . . . .	57
40	Mean seasonal variation in reference and future total runoff for all of Iceland, glacier-free areas and glaciers. . . . .	57
41	Key components of the Icelandic power system. . . . .	59
42	Different flow regimes: Þórisvatn and Háslón reservoirs. . . . .	60
43	Statistical distribution of temperature trends in Iceland. . . . .	61
44	Possible energy supply in the runoff to power stations in Iceland. . . . .	62
45	Generation costs for three possible climate trends from 1950 to 2010. . . . .	63
46	Power production capability as function of climatic trend. . . . .	63
D1	Projected mean annual and seasonal runoff in Iceland 2071–2100. . . . .	90
D2	Projected change in mean annual evaporation from 1961–1990 to 2071–2100. . . . .	91
D3	Modelled and projected mean annual number of days with snow covered ground in the periods 1961–1990 and 2071–2100. . . . .	91

# 1 Introduction

Global warming during the next decades due to increasing concentrations of CO<sub>2</sub> and other trace gases in the atmosphere (IPCC, 1990, 1996, 2001, 2007) is expected to have pronounced effects on the climate and hydrology of the Earth. The implications are far-reaching and affect many sectors of society. For Iceland, projected hydrological and glaciological changes are particularly important because of the large proportion of hydropower in the energy system of the country. Many glaciers and ice caps are projected to almost disappear during the next 100–200 years. These changes also have global implications such as changes in the vertical stratification in the upper layers of the Arctic Ocean (Curry *et al.*, 2003) and a rise in global sea level (Meehl *et al.*, 2007; Meier *et al.*, 2007).

Energy production in Iceland is primarily from renewable sources. In 2004, the primary energy supply was made up of 54% geothermal, 17% hydropower and 29% fossil fuels<sup>1</sup>. Approximately 80% of the production of electricity was from hydropower in 2005 and this proportion will rise to 85–90% at the end of 2007 when the Kárahnjúkar hydropower plant becomes operational. Hydropower in Iceland is highly dependent on runoff from ice caps and glaciers, which cover about 11% of Iceland and receive about 20% of the precipitation that falls on the country. They store, in the form of ice, the equivalent of 15–20 years of annual average precipitation over the whole country. Substantial changes in the volume of glacier ice may, therefore, lead to large changes in the hydrology of glacial rivers, with important implications for the hydropower industry and other water users. Runoff from glaciers is particularly important for the hydropower industry because hydropower plants use runoff from highland areas, where glaciers tend to be located.

The effect of climate change on hydrology and renewable energy production, especially hydro-power production, in the Nordic countries has been investigated in a series of Nordic research projects complemented by national projects in the respective countries (the name of the Icelandic national project is given after the slash in each case where appropriate): “Climate Change and Energy Production” (CCEP) (1991–1996) (Sælthun *et al.*, 1998), “Climate, Water and Energy / Veðurfar, vatn og orka” (CWE/VVO) (2002–2003) (Kuusisto, 2003), “Climate and Energy / Veður og orka” (CE/VO) (2003–2006/2003–2007) (Fenger *et al.*, 2007), and “Climate and Energy Systems” (CES) (2007–2010). These projects have adapted climate change scenarios for use in hydrological and glaciological simulations and provided quantitative estimates of potential changes in average runoff and seasonal runoff variations that may be caused by future climate change. The results have demonstrated the importance of future climate change for the energy sector of the Nordic countries, especially for hydro-power plants located in partly glaciated watersheds, which is common in Norway and Iceland. This report summarises the results of the project “Veður og orka” (VO), which is the Icelandic counterpart of the Nordic project “Climate and Energy” (CE).

---

<sup>1</sup><http://www.orkutolur.is/mm/frumorka/uppruni.html>”.



## 2 Recent variations in climate and runoff in Iceland

### 2.1 The climate of Iceland

Relatively mild Atlantic Ocean currents and the huge land/ice mass of Greenland are two of the most important factors in determining the climate of Iceland. Icelandic climate is characterised by large decadal variations associated with the location of storm tracks across the North Atlantic Ocean, the position of the sea ice margin to the north of the country and the phase of the North Atlantic Oscillation (NAO). The main characteristics of the climate of Iceland are described by Einarsson (1984).

The Icelandic Low (IL) is a semi-permanent centre of low pressure over the North Atlantic Ocean, typically situated between Greenland and Iceland, and between 60° N and 65° N (Serreze *et al.*, 1997). It represents one of the centers of action in the atmosphere of the Northern Hemisphere; it also has a strong influence on the climate of Iceland, by affecting predominant wind directions and variability through its cyclonic activity. The North Atlantic Oscillation Index (NAOI) is defined as the difference of the intensity of the Icelandic Low and the North Atlantic subtropical high, also known as the Azores High (Hurrell *et al.*, 2003). Although the number and intensity of cyclone events tends to increase during periods of positive NAOI (Serreze *et al.*, 1997), the NAOI is only weakly correlated with many climate variables at individual meteorological stations in Iceland (Björnsson and Jónsson, 2003), probably because the island is close to one of the dipole centers of the NAO (Hanna *et al.*, 2004). However, a recent study by Crochet (2007) shows that there is relatively high correlation between the NAOI and area-averaged winter precipitation characteristics in Iceland.

The sea level pressure (SLP) in Iceland is highly variable, but generally tends to be low in mid-winter and reach a maximum in May. In recent decades, the low pressure period, which usually ends around mid-February, has extended into March (Jónsson and Miles, 2001). Long time-series of sea level pressure in Iceland, from 1820–2002, show no significant overall trends (Hanna *et al.*, 2004).

The air temperature in Iceland is strongly influenced by the sea surface temperature (SST) of the surrounding ocean. The SST depends on the proportions and the origin of water masses around the country. South of Iceland, relatively warm and saline Atlantic waters are predominant. In the North, varying proportions of Atlantic and Polar or Arctic water create a large variability in the SST (Ólafsson, 1999). The air temperature is negatively correlated with sea ice cover, especially in the northern part of the country, but sea ice around Iceland has been less frequent in the 20<sup>th</sup> century than it was on average in the period 1600–1900 (Ogilvie and Jónsson, 2001).

Because of the importance of local SST in determining climate, air temperatures in Iceland tend to be relatively mild, with low seasonal variations. The amplitude of the seasonal cycle in temperature is typically less than 15° C with a maximum in late July or August and a minimum in late December/early January or, at some locations, in March (Björnsson *et al.*, 2007b). The temperature is generally higher in southern Iceland than in the northern part of the country and the amplitude of the seasonal cycle is larger inland.

Precipitation in Iceland is also correlated with SST in the North Atlantic. Phillips and Thorpe (2006) found significant concurrent relationships between SST and precipitation, particularly in western Iceland, and weaker lagged relationships between SST and February and December precipitation in North Iceland with up to two-monthly lead-times. They concluded, however, that the predictive skills of the SST are weak and confined to certain times of the year.

There are considerable variations of precipitation in Iceland depending on the cyclonic activity and track. Precipitation is generally higher in the South than in the North and highest on the glaciers and the highest mountains. The seasonal cycle of precipitation reflects, to some extent, the seasonal cycle of SLP. In most areas, measured precipitation is low in the summer, highest in the autumn and stays high until the early spring. Recent model studies (Rögnvaldsson *et al.*, 2007) and studies of gauge-corrected precipitation (Crochet, 2007) indicate, however, that precipitation may be as high or even higher during

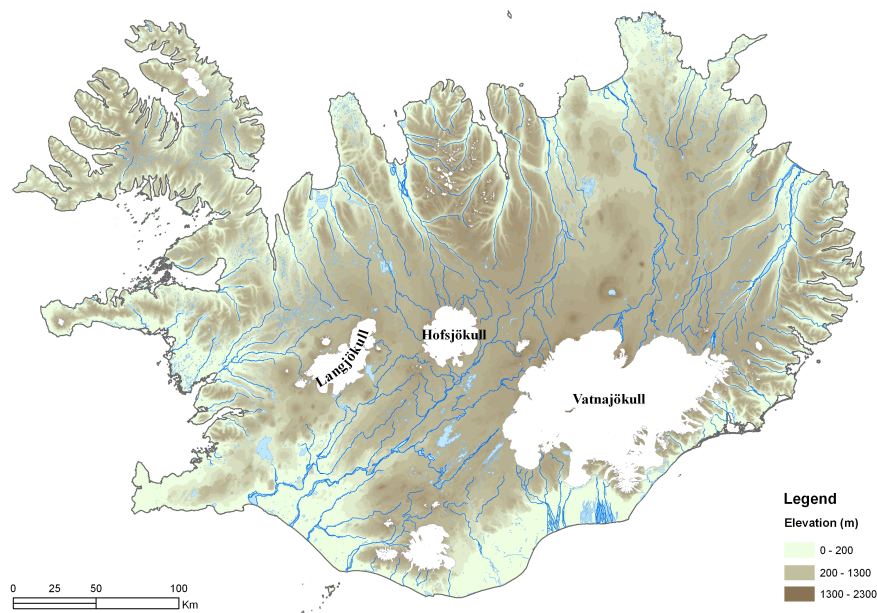


Figure 1: Main rivers and glaciers in Iceland.

winter (*cf.* Fig. 27 in Section 4 about precipitation modelling). High winds result in an undercatch of precipitation, especially during snowfall. The undercatch is therefore highest during the winter when temperature is often below  $0^{\circ}\text{C}$  and winds are comparatively high. This roughly coincides with the seasonal cycle of IL cyclonic intensities, which produces deeper IL cyclones during the cold season (October–March) than during the warm season.

## 2.2 The hydrology of Iceland

Rivers in Iceland (Fig. 1) are often divided into three categories according to their origin (Kjartansson, 1945; Rist, 1990): groundwater-fed rivers, direct-runoff rivers, and glacial rivers. Figure 2 shows average seasonal discharge profiles of three rivers, representing these principal types.

The largest contribution to Icelandic runoff is from rivers fed directly by rain and snowmelt but glacial and groundwater contribution is substantial. In terms of the geological context, the bedrock in Iceland is largely comprised of Tertiary plateau basalts, but large areas in the central parts of the country are covered with hyaloclastites formed by subglacial volcanism during the Pleistocene and postglacial lava formations. Precipitation infiltrates through these porous lavas into groundwater aquifers, which sometimes extend to the ocean. The hydrological conductivity of the bedrock determines the storage capacity and the response time of the aquifers. Most floods in Iceland, as in other cold regions, involve snow and ice (Snorrason *et al.*, 2000). They fall into three categories: floods caused by the interplay of rain and melting of snow and ice, floods caused by ice jamming and jam-breaking, and floods originating from subglacial or glacier-margin lakes.

The total runoff from Iceland had been evaluated twice prior to the work presented in this report. According to Rist (1956), the average runoff from all of Iceland, for the water years 1948–1955 was  $5500\text{ m}^3\text{ s}^{-1}$  or  $1690\text{ mm y}^{-1}$ . Tómasson (1981, 1982) later estimated an average runoff of  $5150\text{ m}^3\text{ s}^{-1}$  or  $1586\text{ mm y}^{-1}$  for the water years 1950–1975 and an average evaporation of  $310\text{--}414\text{ mm y}^{-1}$ . Sub-surface groundwater flow to the ocean was estimated at  $33\text{--}62\text{ mm y}^{-1}$ . From a runoff map and an elevation map, potential hydropower in Iceland was estimated to be  $\sim 187\text{ TW h y}^{-1}$ . A new runoff estimate for the period 1961–1990 is presented in Section 6.

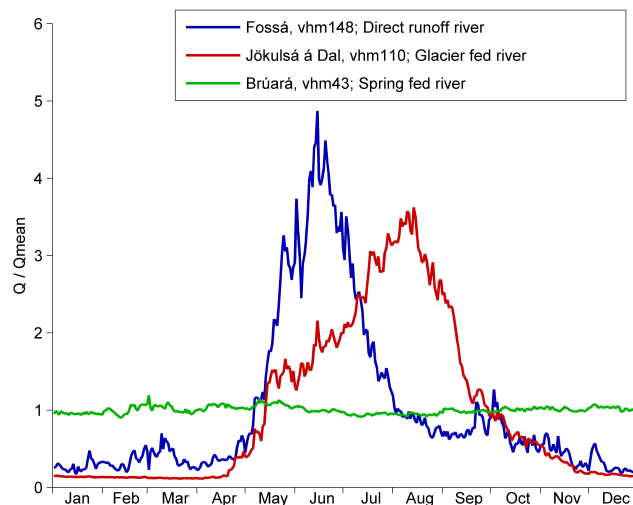


Figure 2: Seasonal discharge variations of three representative Icelandic rivers. *Fossá* is a direct-runoff river in E-Iceland. Note the large spring/early summer peak due to snowmelt within the drainage basin. *Jökulsá á Dal* is a glacial river in E-Iceland originating in the Vatnajökull ice cap. Note the strong effect of summertime glacier melt on the discharge. *Brúará* is a groundwater-fed river in SW-Iceland, showing very little seasonal variation.

### 2.3 Snow and glaciers

Precipitation in Iceland may fall as snow in all seasons but fresh snow is rare in July and August (Jónsson, 2002). The snow cover largely melts away during April, May and June, but in the high mountains the melt season may extend into July and August. Jónsson and Jónsson (1997) give an analysis of maximum snow depth in Iceland and classify the country into regions according to the magnitude of the 50-year snow depth.

Glaciers cover almost 11% of Iceland and they receive about 20% of the precipitation that falls on the country as mentioned in the introduction. They store, in the form of ice, the equivalent of 15–20 years of annual average precipitation over the whole country and they release meltwater from this storage on time-scales ranging from seasons to centuries. They are vulnerable to climate variability and change and several studies have dealt with their response to climate change, as summarised in Section 5 of this report.

### 2.4 Recent variations in temperature and precipitation

Figure 3 shows annual average temperature of the northern hemisphere since 1850 and annual mean temperature at Stykkishólmur, western Iceland, since 1831. The figure shows a generally warming trend since the latter part of the 19<sup>th</sup> century, both for Stykkishólmur and for the northern hemisphere as a whole, with the largest rate of warming in the two periods 1920–1940 and 1980–2006. The total warming in Stykkishólmur since the 1880s is approximately 1.5° C according to the 10-year running average curve, and approximately 1° C for the northern hemisphere. The amplitude of temperature fluctuations from a simple linear warming trend are, as expected, larger for Stykkishólmur compared with the northern hemisphere average. Time periods with the most rapid warming and cooling are shorter and have larger warming or cooling rates in Stykkishólmur than for the northern hemisphere.

Figure 4 shows annual precipitation at five weather stations in Iceland since the late 19<sup>th</sup> century or early 20<sup>th</sup> century. The precipitation records show considerable annual scatter (14–21% of mean values) and substantial decadal variations but they do not exhibit a consistent long-term trend as op-

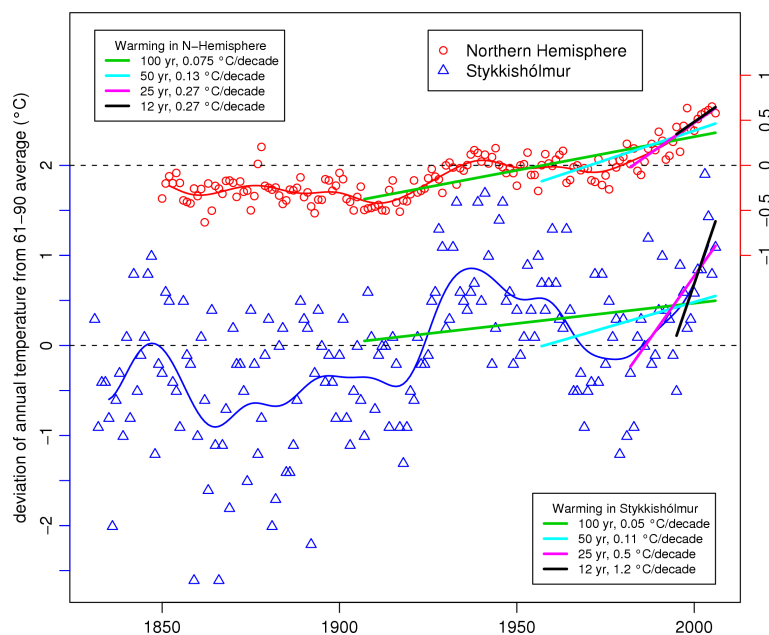


Figure 3: Annual average temperature of the northern hemisphere (1850–2006, data from CRU/Hadley) and annual mean temperature at Stykkishólmur, western Iceland, (1831–2006, data from IMO), plotted as deviations from the average of the period 1961–1990. The thin solid curves show an exponentially weighted running average with a 10-year time window. The thicker straight line segments show linear least squares fits to the annual data for 100, 50, 25 and 12 year periods preceding the year 2006 and the corresponding warming rates in degrees per decade for each period are given in the legend boxes.

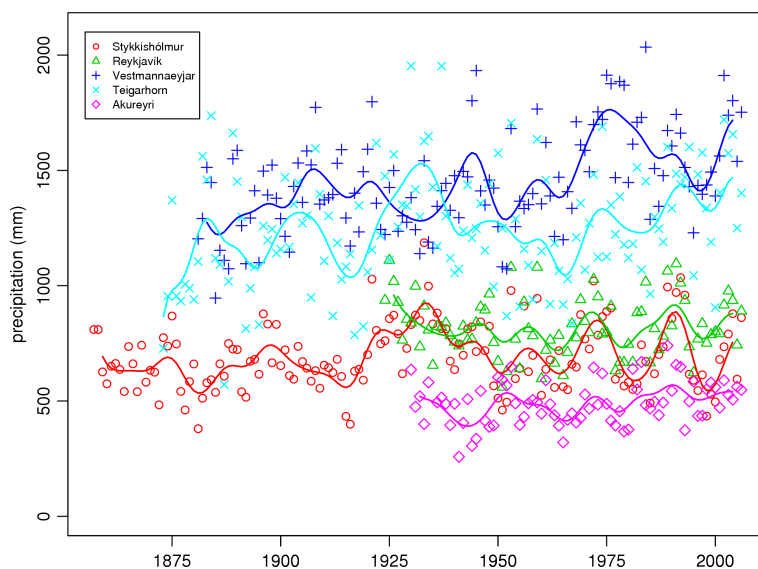


Figure 4: Annual precipitation at the weather stations Stykkishólmur, western Iceland, Reykjavík, southwestern Iceland, Vestmannaeyjar (partly Stórhöfði, partly Vestmannaeyjar village), southern Iceland, Teigarhorn, south-eastern Iceland, and Akureyri, northern Iceland since the late 19<sup>th</sup> century or early 20<sup>th</sup> century (data from IMO). The solid curves show an exponentially weighted running average with a 5-year time window. Information about the history of precipitation measurements in Iceland is provided by Jónsson (1994, 2003).

posed to the temperature time-series shown in Figure 3. Annual and decadal precipitation variations at different stations tend to be less coherent than for temperature.

Climatic variability of precipitation over the second half of the 20<sup>th</sup> century has recently been



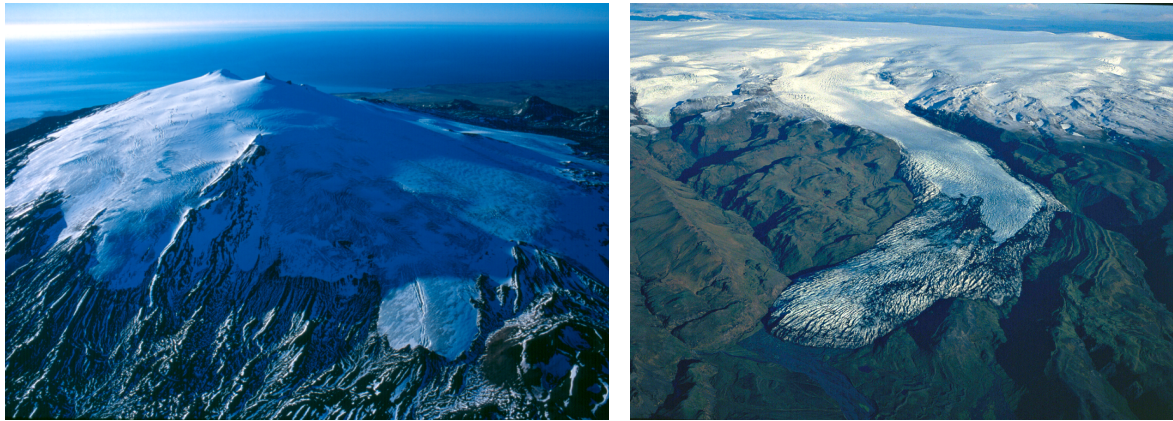


Figure 5: Oblique aerial photographs of Hyrningsjökull during retreat (view to NW on 18 October 2001) and Sólheimajökull during advance (view to NE on 30 October 1985). Photographs Oddur Sigurðsson.

studied by Crochet (2007), who used both bias-corrected raingauge measurements and precipitation forecasts from ECMWF Re-Analysis (ERA-40). That study emphasised a decadal variability especially during the winter season and indicated that intra- and inter-annual variations of accumulated precipitation amounts are driven by variations in the statistical characteristics of the precipitation rate, such as intensity and occurrence. These variations are in turn modulated by differences in size and relative location of the precipitation systems crossing Iceland caused by changes in atmospheric circulation patterns over the North Atlantic sector, especially in wintertime, in relation to variations in the strength and phase of the NAO. For instance, measurements from the comparatively recent 1991–2000 period show a decrease of annual precipitation.

Trends and long-term variability in river discharge, temperature and precipitation have been investigated in several studies dealing with the periods 1941–2002 and 1961–2000. Main results from these studies are outlined in a separate subsection below.

## 2.5 Recent glacier variations

During historical times, glaciers and ice caps in Iceland have retreated and advanced in response to climate changes that are believed to have been much smaller than the greenhouse-induced climate changes expected during the next 100–200 years. In many cases, these changes have left clear marks on the landscape in the neighbourhood of the glaciers as shown in Figure 5.

Most glaciers in Iceland reached their maximum postglacial extent around 1890 (Sigurðsson, 2005). During the first quarter of the 20<sup>th</sup> century, retreat was notable but not rapid (Björnsson, 1998). The abrupt increase in temperature that occurred about 1925 (Fig. 3) was accompanied by a rapid retreat of glacier fronts all over Iceland (Fig. 6) (Eythorsson 1931, 1963 and Sigurðsson 1998). By 1960, all monitored glaciers had retreated from their 1930 position, although, typically, 10–30% of the glacier termini were advancing each year (Fig. 7) (Jóhannesson and Sigurðsson, 1998). The rate of retreat slowed down as the climate cooled gradually during the 1940s and 1950s. Almost all non-surging glaciers advanced to a varying degree for 2–3 decades following the 1960s and then returned to retreating during the 1990s, particularly after 1995 as temperatures began rising rapidly (Fig. 3), with 2002–2004 the warmest 3-year period on the almost 200-year-long instrumental record. By the year 2000, all monitored non-surging glaciers were retreating (Sigurðsson *et al.*, 2007).

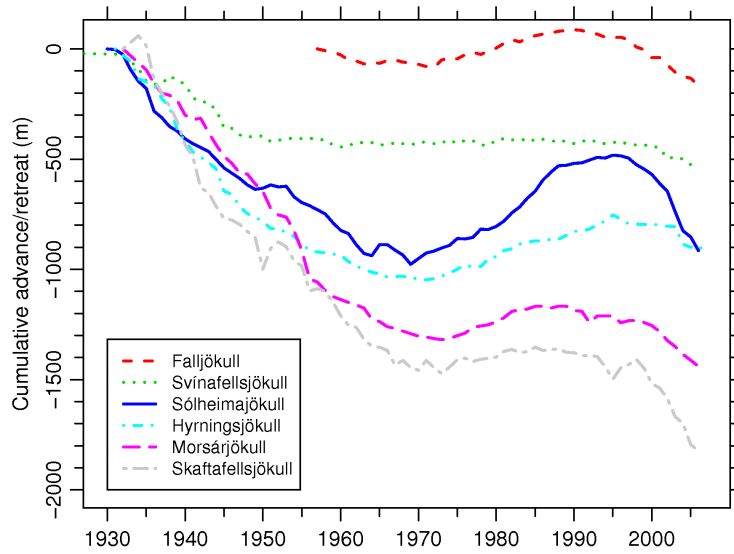


Figure 6: Cumulative variations of the termini of six non-surge-type glaciers in Iceland during the period 1930–2007.

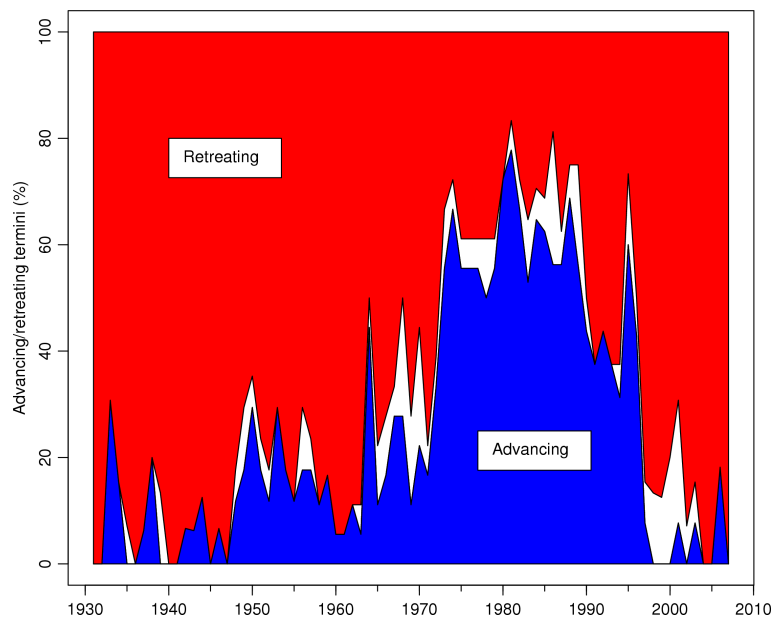


Figure 7: Percentage of advancing and retreating termini of non-surging glaciers in Iceland from 1930/1931 to 2006/2007. Over most of the time period shown, the figure is based on measurements at 15 to 19 locations (somewhat fewer termini in the years 1931 to 1935).

## 2.6 Quantitative analysis of precipitation and discharge variations

Jónsdóttir and Uvo (2007) aimed at explaining how atmospheric circulation and sea surface temperature influences seasonal and annual precipitation, and, consequently, runoff in Iceland. They applied an empirical orthogonal function (EOF) analysis on annual and seasonal time-series of precipitation and discharge to identify their key modes of variability during the period 1966–2004. The correlation between the time-series of each EOF mode with individual time-series of sea level pressure (SLP), air temperature and sea surface temperature (SST) was then evaluated.

The analysis evidenced how large-scale climate variables are connected to the regional rainfall and runoff in Iceland. They showed that the strength of the polar vortex may be, at least, as important for the precipitation in some areas of Iceland as the strength of the Icelandic Low (IL). Moreover, the location of the semi-permanent IL often defines the predominant wind direction over the country and, as such, the regions of preferred precipitation.

Since the watersheds act as large precipitation gauges with response patterns depending on the geology and glaciers, the variability of the annual discharge closely resembles the variability of precipitation, except for the glacial rivers. Glacial melt is highly correlated to air temperature and SST, and the spring discharge is affected by winter and spring temperatures.

The results also revealed that Icelandic hydrological conditions in the spring can be forecast by precipitation and temperature of the autumn and winter seasons as well as by the general prevalent circulation patterns. Additionally, a potential for seasonal forecast of precipitation, and river discharge in other seasons was identified, particularly if seasonal forecast of SLP is available.

## 2.7 Trend analysis by non-parametric methods

The Mann-Kendall trend test (Salas, 1993) was applied to time-series of temperature, precipitation and discharge, with the aim of identifying whether long-term changes in discharge have occurred in Iceland (Jónsdóttir *et al.*, 2006). The relatively short length of most of the discharge records poses limitations to this study, and trends are in addition highly dependent on the period analysed due to relatively large decadal variability. Such variability is clearly seen in the annual time-series of discharge in the river Hvítá at Kljáfoss (Fig. 8). It is helpful to distinguish between three types of time-series variability in this connection. Firstly, there are interannual fluctuations that are uncorrelated from year-to-year. Secondly, there is “natural variability” on longer time-scales that has a certain persistency over several years, decades or even longer periods, but which may be considered without a long-term trend on time-scales longer than corresponding to the autocorrelation of the series. This kind of variability may lead to statistically significant, alternating trends that are completely dependent on the study period. Thirdly, there are variations that are typically not considered “natural fluctuations” and involve a long-term change in the expected value of the time-series. Such trends may be expected to have the same sign over time periods longer than corresponding to the autocorrelation of the time-series. This distinction is not rigorous as it involves a non-unique conceptual model of the statistics of the time-series under consideration. For example, Ice Ages and the Little Ice Age may perhaps either be considered to represent “natural variations” or “long-term trends” depending on the context. In studies of global climate change it is often implicitly assumed that statistically significant trends are a sign of human-induced changes in climate. This is not a valid viewpoint. It is of course clear that statistically insignificant trends cannot be used to detect signs of human-induced climate change. Statistically significant trends can, on the other hand, both arise due to human activity or due to “natural variations” with several-year, decadal or longer time-scales that are related to the autocorrelation of the time-series in question. This has to be kept in mind in the interpretation of the results described below.

Series of monthly temperature, precipitation (uncorrected gauge values) and discharge were analysed and compared (Jónsdóttir *et al.*, 2006). In accordance with the study by Hisdal *et al.* (2006), data from two periods of different lengths were analysed separately. The first period, 1941–2002, goes back to the start of streamflow measurements in Iceland, but includes only 2 discharge records. The other period 1961–2000, includes 10 discharge records from S-, W- and N-Iceland. Seasonal values of meteorological variables and discharge were classified according to the four season division: autumn, Sep–Nov (SON), winter, Dec–Feb (DJF), spring, March–May (MAM) and summer, June–Aug (JJA). For discharge, the spring season was defined as April–June (AMJ). For flood analysis, floods in the period 1 March to 16 July are considered spring periods, and floods in the period 17 July to 30 November

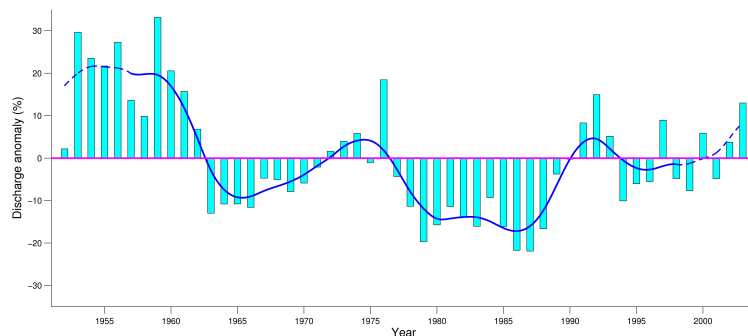


Figure 8: Annual deviations from mean discharge in the Hvítá river at Kljáfoss, W-Iceland. Columns show annual values while the line represents Gauss filtered values ( $\sigma^2 = 3$ ).

are considered autumn floods.

### 2.7.1 Temperature

Warming trends for 100 yr, 50 yr, 25 yr and 12 yr periods preceding the year 2006 are indicated by the linear least squares fits shown in Figure 3. Decadal variations in temperature during the last century have been large. A part of these variations, for example the overall warming between the late 19<sup>th</sup> century and the present, is generally believed to be related to human-induced climate change. Other aspects of the temperature variations, for example the warm 1930s and 1940s and the cooler period that followed, are more often interpreted as a random variation caused by the internal dynamics of the atmosphere–ocean system. Because of the large amplitude of natural, decadal fluctuations, results from the Mann-Kendall trend analysis may be expected to be strongly dependent on the period studied as discussed above. For example, the Stykkishólmur data in Figure 3 indicate a positive linear trend of 0.11 °C per decade in the period 1957–2006. Mann-Kendall analysis of annual temperature data from 16 stations for the period 1941–2002, on the other hand, showed a negative trend at 9 stations and the negative trend was significant (0.1–0.2 °C per decade) for three stations. This illustrates the effect of the warm period in the 1920s to the 1950s on the results. For the period 1961–2000, however, a positive trend in mean temperature was found in 9 out of 18 series and the trend was significant (0.2–0.3 °C per decade) in two series, whereas none of the series yielded a significant negative trend. Significant warming trends during summer and/or autumn were found for 13 of these 18 series, but a consistent cooling trend was found for the spring season (MAM) during both periods studied (1941–2002 and 1961–2000). The spring cooling coincides with a trend towards lengthening of the winter low pressure period discussed by Jónsson and Miles (2001), who showed that this period, that previously ended around mid-February, has in recent decades extended into March. This lengthening of the low-pressure season can be linked to the contribution of the Icelandic Low to the positive trend in the NAOI since the 1960s (Jónsson and Miles 2001).

### 2.7.2 Precipitation

For the period 1941–2002, significant positive trends of 4–8% per decade in annual precipitation were found for 5 out of 12 stations, located in E-, N- and SW-Iceland. For the period 1961–2000, 5 out of 28 stations had a significant positive trend. Four of these stations, with a 4–15% increase in precipitation per decade, are located in E-Iceland. Stronger positive trends were found for the autumn and winter months than for other seasons. None of the stations had a significant negative trend in annual precipitation.

It is not certain that these positive trends reflect actual precipitation changes. During autumn and

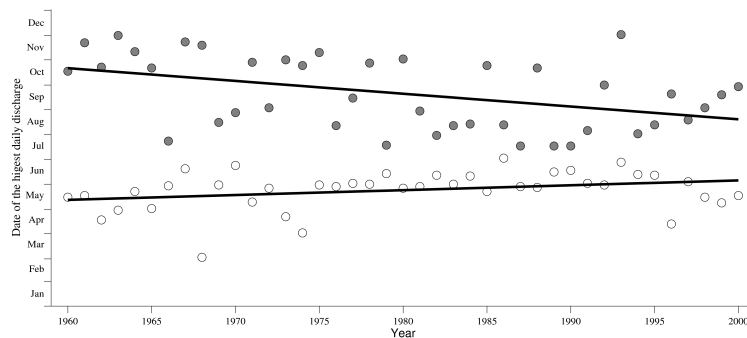


Figure 9: Time of spring and autumn maximum daily discharge at stream gauge V96, Maríufoss, Tungnaá river. Floods occurring in the period March 1 to July 16 are classified as spring floods, and those occurring between July 17 and November 30 as autumn floods.

winter, the trend in precipitation was strongest in the northern and eastern part of the country, where much of the precipitation falls as snow during autumn and winter and may be underestimated by gauges in wind and for temperatures below 0° C. Consequently, a positive precipitation trend in the period 1961–2000 may to some extent be attributable to a positive temperature trend during the same period. Higher temperatures are presumably accompanied by a higher ratio of rain to snow, leading to a better catch of precipitation at the stations. Moreover, the installation of wind shields on gauges during the 1950–1960 period, which reduces the undercatch of precipitation (Jónsson, 2003), may explain some of the trends seen in precipitation during 1941–2002. This is supported by an analysis of gauge-corrected station precipitation and ERA-40 precipitation by Crochet (2007) (*cf.* Fig. 28) who found that area-averaged precipitation in Iceland did not show any significant linear trend in the period 1961–2000 (*cf.* also Fig. 4).

### 2.7.3 Discharge

Only two discharge series are available during the longer period (1941–2002). One of these, from the Svartá river in Skagafjörður (N-Iceland), showed a positive trend of 4% per decade. For the period 1961–2000, data from 10 stations were studied. None of them showed a significant trend in mean annual discharge. Trends for the summer season (JJA) are, evident, however, a 6–7% increase per decade was obtained for the summer discharge from two stations (Tungnaá, S-Iceland, and Dynjandisá, NW-Iceland). The reason for the increased summer runoff can be attributed to cooler spring temperatures (*cf.* the above section about temperature); the snow melt in watersheds at high elevations becoming increasingly delayed from spring into summer.

The effect of cooling in the spring also appears in the trend analysis of timing and volume of spring floods, which are delayed by 5 days per decade for some stations. The spring maximum daily discharge has also increased in some of the series in relation to the delay of the spring flood. No clear trends appear in autumn floods, except for two watersheds where the melting of snowpack and glacier ice extends into the period of autumn floods (defined here as the period from July 17 to November 30 as described above). The river Tungnaá, flowing westwards from the Vatnajökull ice cap, collects water from one of these watersheds. The timing of spring and autumn floods from a station at Maríufoss in Tungnaá is shown in Figure 9, there the delay of the spring flood is evident.

### 2.7.4 Conclusions

The main conclusions from the trend analysis are that, although a statistically significant increase in measured (uncorrected) precipitation is found at a few stations, precipitation variations in Iceland in the

latter part of the 20<sup>th</sup> century seem to be dominated by decadal variations and discharge in non-glacial rivers has not increased. In spite of a long-term warming trend during the last 100–200 years (*cf.* Fig. 3), spring temperatures were found to have an overall negative trend during the study periods and, as a result, spring floods occur later than before and have in some cases become larger during these periods.

## **2.8 Trend analysis by parametric methods**

In order to extend the analysis of trends to extreme events, Jónsdóttir (2007) used a parametric trend test to analyse temperature, precipitation and discharge data from the period 1961–2000 from 17, 28 and 10 stations, respectively. For the rivers studied, drainage basin areas vary in size between  $\sim 40 \text{ km}^2$  and  $\sim 5700 \text{ km}^2$ . Gaps in the discharge records were filled using routine methods employed by the Hydrological Service. Some of the rivers have high groundwater components, which smooth out variations in the discharge between seasons and years. The parametric trend study yielded results that are in good agreement with those already described from the Mann-Kendall (non-parametric) test with respect to the sign and magnitude of trends.

### 3 Climate change scenarios

Dynamic downscaling of global atmospheric simulations from the Hadley center model (HadAM3H, Johns *et al.*, 2003) was used to assess a plausible regional temperature and precipitation change for Iceland. Similar downscaling was carried out within the CE project for the other Nordic countries (Rummukainen, 2006; Fenger, 2007). The model represents a coupled ocean-ice-atmosphere system with a horizontal resolution of T106 which corresponds roughly to 125 km. The dynamic downscaling was carried out with the HIRHAM regional climate model (Bjørge *et al.*, 2000) for a limited area (Fig. 10) over the N-Atlantic and NW-Europe (Haugen and Iversen, 2005). The HIRHAM simulations have a horizontal resolution of about 55 km and 19 vertical levels. Most weather systems approach Iceland from the south and the west. The outer boundaries of the simulation domain, southwest of Iceland, are only about 1200 km away. This may have an impact on the development of extratropical cyclones arriving from this direction. It is not clear how important this effect may be and should be investigated in connection with future simulations. Some numerical noise is found at the outermost gridpoints of the HIRHAM domain, but this noise fades out within 5 grid points or even less. Global simulations corresponding to two emission scenarios were downscaled, *i.e.* the IPCC SRES A2 and IPCC SRES B2 (Nakicenovic and Swart, 2000).

#### 3.1 Precipitation

Figure 11 shows the projected change in mean annual precipitation in Iceland from 1961–1990 to 2071–2100 as simulated with the HIRHAM model and Figure 12 shows the projected seasonal changes (Pálsson *et al.*, 2005; Rögnvaldsson and Ólafsson, 2005). The change in the mean annual precipitation is moderate. In most regions there is an increase of 0–10%, but in the central highlands there is a small decrease. In general, the predicted patterns of precipitation change are similar in both scenarios, A2 and B2.

While there is only a little average increase in mean annual precipitation in the lowland, there is relatively large change in the seasonal cycle. The autumn is expected to be considerably wetter in S-Iceland and W-Iceland, while the projections for N-Iceland and E-Iceland are more ambiguous. The spring becomes slightly drier everywhere and the winter is expected to be drier in SW-Iceland

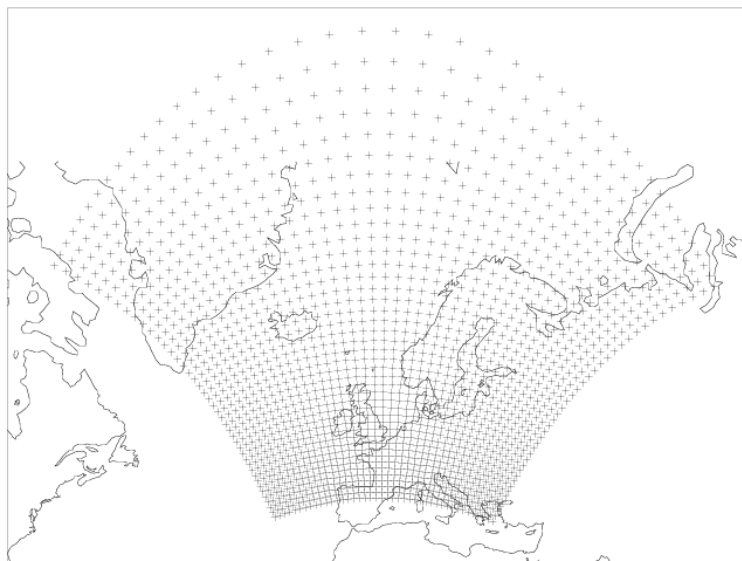


Figure 10: The simulation domain and gridpoints of the HIRHAM dynamic downscaling.

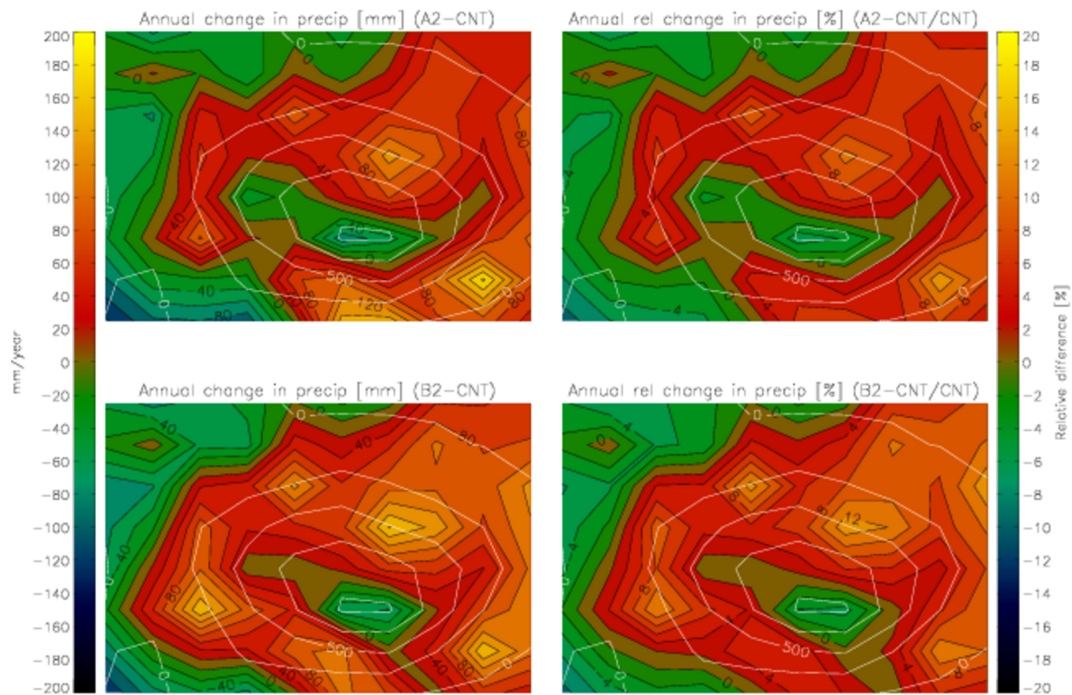


Figure 11: Change in annual precipitation in Iceland according to the HIRHAM A2 and B2 downscaling of HadAm3 GCM simulations. The left hand panels show changes in mm and right hand panels show relative changes (difference of the mean precipitation in the periods 2071–2100 and 1961–1990 relative to the mean precipitation of 1961–1990). The top panels show scenario A2 and the bottom panels scenario B2. White contours indicate the model topography of Iceland with 250 m spacing.

and much wetter in NE-Iceland. The summer predictions are rather noisy. As for most other aspects of projected changes in precipitation, it is unclear to what degree these local and seasonal changes are due to “natural” fluctuations in the climate simulations or to what extent they represent a true deterministic signal caused by greenhouse warming.

There is a clear slope-signal in the predicted precipitation change, particularly in the autumn precipitation increase in the south and in the winter precipitation increase in the NE. The maximum increase coincides with the maximum slope of the topography, indicating that the orographic enhancement of precipitation will increase. This raises concerns: Firstly, the complexity of the connection on climatic time-scales between precipitation in the highlands and in the lowlands may be even greater than previously considered. This has implications for numerical simulations that do not resolve the topography and interpretation of observational data retrieved in the lowlands. Figure 13 shows time-series of the ratio of precipitation observed at locations where orographic enhancement is great to precipitation observed away from the mountains. The figure reveals not only a substantial interannual, but also a decadal variability in the orographic enhancement of precipitation. Secondly, the true orography is far more complex and steeper than represented in the HIRHAM simulations. Consequently, a weak slope signal in the simulations may be interpreted as an indicator of a much greater change.

### 3.2 Winds

Figure 14 shows the frequency of geostrophic wind directions over Iceland in the control simulation (1961–1990) and in the two future simulations for 2071–2100. Hardly any changes are predicted in the frequency of easterly and westerly winds, while northerly winds are predicted to become more frequent and southerly winds less frequent. The simulations indicate a small reduction in the mean wind speed.



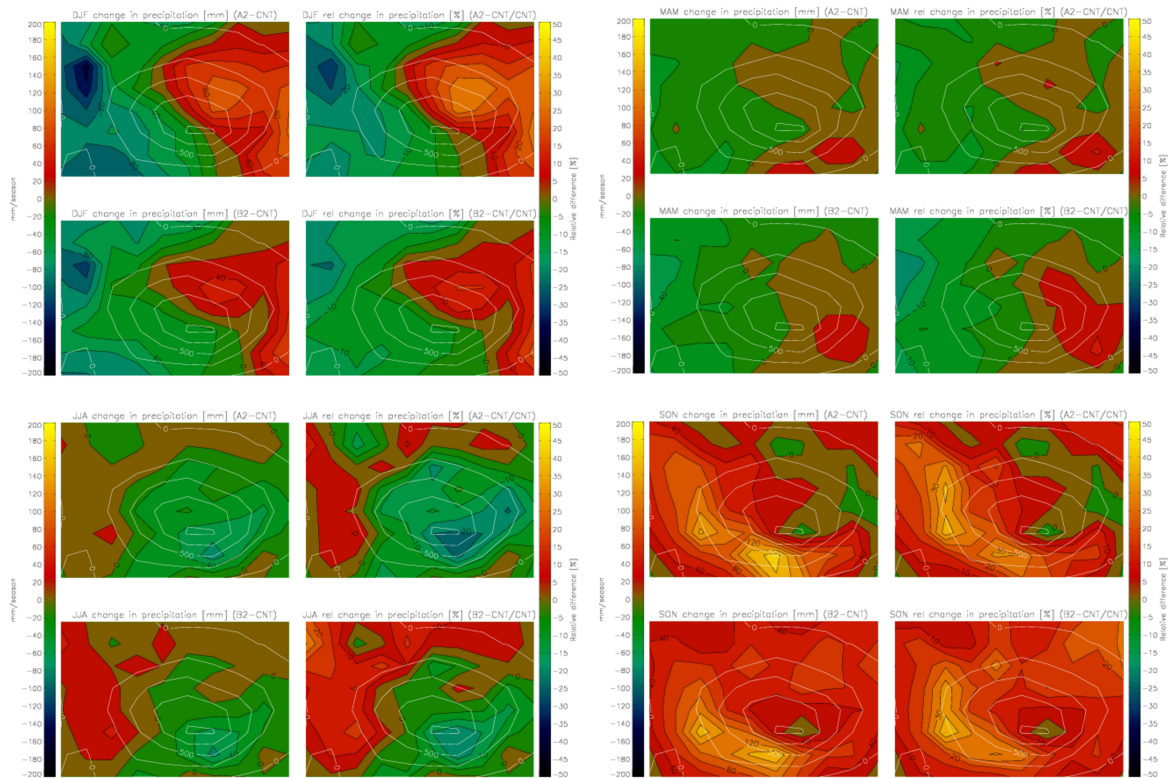


Figure 12: Change in seasonal (DJF: top left, MAM: top right, JJA: bottom left, and SON: bottom right) precipitation in Iceland according to the HIRHAM A2 and B2 downscaling of HadAm3 GCM simulations (see explanation in the caption of Figure 11).

### 3.3 Temperature

As for precipitation, the projected patterns of temperature change are similar in both scenarios, A2 and B2. The seasonal cycle of temperature is projected to be different in a future climate in Iceland (Fig. 15). Very little warming is projected for mid-winter and relatively little warming for mid-summer. A substantially greater warming is expected in the spring and in the autumn. The absence of warming in mid-winter is attributed to a reduction in the number of southerly windstorms. The relatively large projected warming in the spring and fall may partly be attributed to a shortening of the season with snow cover. A substantial reduction is predicted in the intensity and frequency of cold spells in winter and spring and some increase is predicted in the frequency and intensity of heat waves. The projection in Figure 15 is not in complete harmony with the observed changes in recent decades (Fig. 16). Late summer and most of the autumn have indeed received greater warming than spring and early summer, but the mid-winter warming in the observations and lack of warming in late-winter are not as expected from the scenario. These deviations cannot be easily explained. There are indications that oscillations in mean temperatures in late winter/early spring and in the autumn are to some extent associated with variability in the meridional advection of warm airmasses towards Iceland. This advection is closely linked to the general circulation pattern in the N-Hemisphere, including the intensity of the Canadian upper trough, which in turn is associated with the cold continental winter. A large temperature increase is projected over the Canadian Arctic in the future and it must not be considered unexpected if this leads to changes in the general circulation that are well beyond what has been observed in the oscillations of recent decades.

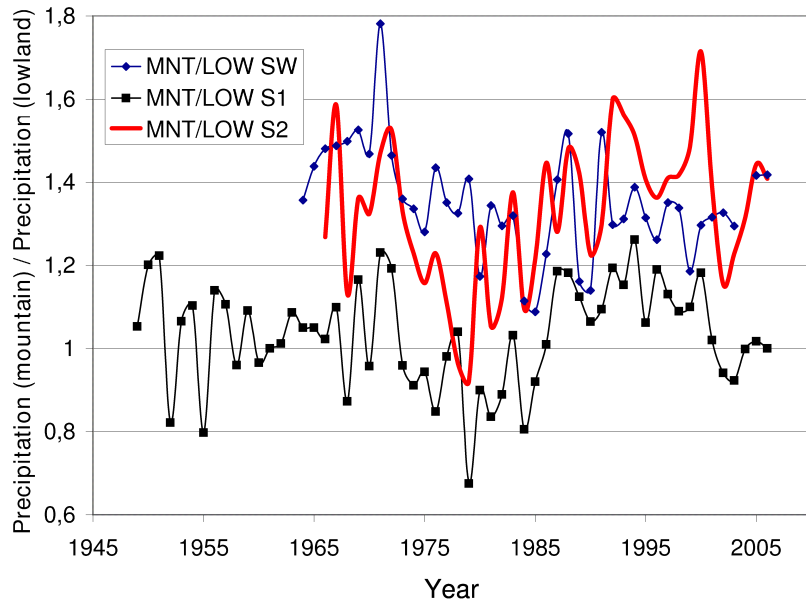


Figure 13: Ratio of observed precipitation at locations where there is significant orographic enhancement of precipitation (mountain) to precipitation observed in the same region, but farther away from the mountains (lowland). The weather stations are Stardalur and Keflavíkurlugvöllur (SW), Vatnsskarðshólar and Stórhöfði (S1) and Skógar and Stórhöfði (S2).

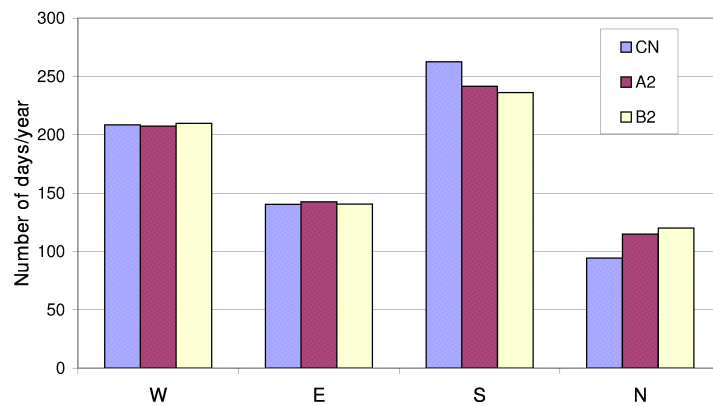


Figure 14: Frequency of geostrophic wind directions over Iceland in the control simulation of the HIRHAM downscaling of HadAm3H (1961–1990) and in the two future simulations A2 and B2 for 2071–2100.

### 3.4 Scenarios for glaciological and hydrological simulations

On the basis of the above simulations, scenarios were prepared for the glaciological and hydrological modelling described in Sections 5 and 6. For temperature, an average was estimated for the whole country, while, for precipitation, four different sets of values were estimated for four different parts of the country. Differences in monthly averages were negligible between the A2 and B2 emission scenarios. Therefore, an average of the projections corresponding to the two emission scenarios was computed and applied in the glaciological and hydrological simulations.<sup>2</sup> The precipitation scenarios

<sup>2</sup>This averaged scenario for Iceland is denoted with “Mean of RegClim H/A2 and H/B2 scenarios” in reports from the hydrological modelling group of the CE project (*i.e.* Bergström *et al.*, 2007). For other Nordic countries, separate scenarios corresponding to the A2 and B2 emission scenarios were employed in hydrological simulations.

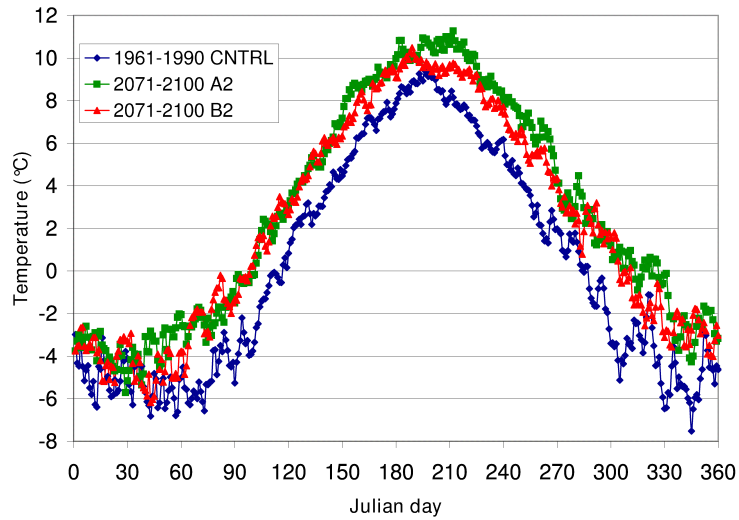


Figure 15: Seasonal cycle of temperature 1961–1990 (control) and 2071–2100 in an inland area in SW-Iceland according to a HIRHAM downscaling of HadAm3 GCM (Scenarios A2 and B2).

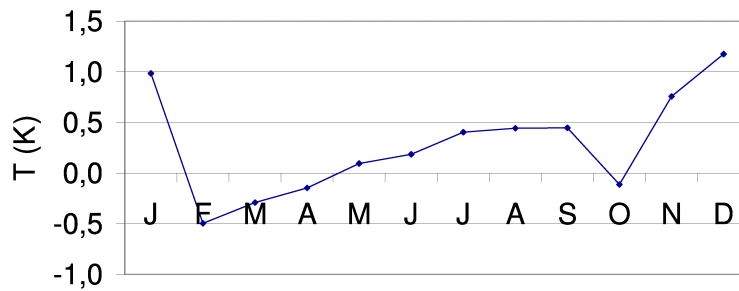


Figure 16: Observed seasonal change in temperature in Reykjavík from the 40 year period 1947–1986 to the 20 year period 1987–2000.

were further smoothed with a three-month running mean. Figure 17 shows the seasonality of the temperature and precipitation change, averaged over the whole of Iceland, and Figure 18 shows the precipitation change for SW-, NW-, NE- and SE-Iceland. According to the CE/VO scenario, average annual temperature will increase by 2.8°C from 1961–1990 to 2071–2100. Average increase in annual precipitation for the whole country is about 6% over this period but the change in precipitation varies from one part of the country to another and between seasons. As already noted, the highest warming is projected in the spring and fall, in particular in the fall, with lower warming during the summer and the lowest warming during the winter. This variation is different from the scenario, which was used for Iceland in the previous CWE project (Jóhannesson *et al.*, 2004), where the specified warming was highest in mid-winter and lowest in mid-summer with a sinusoidal variation in between.

The precipitation scenario for the glaciological simulations was created by taking the average of precipitation changes in the four parts of the country because the modelled ice caps are located in the central highlands where separate scenarios for SW-, NW-, NE- and SE-Iceland are not appropriate (Fig. 17).

The glaciological modelling presents a special problem in that it requires a continuous temperature and precipitation variation because the dynamic glacier model must be run as a transient simulation for the whole period from the present to the future period under consideration. It is nontrivial to continue the observed temperature and precipitation records, which were used in the glacier simulations

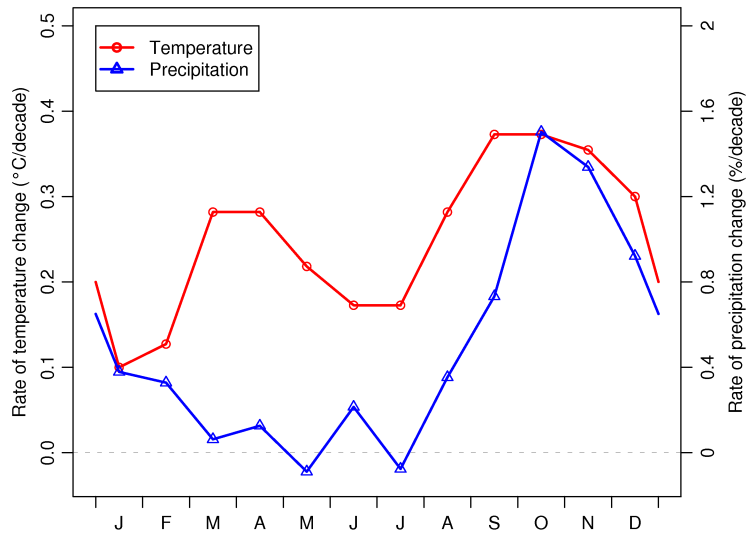


Figure 17: A scenario for seasonal changes in temperature and precipitation for the 21<sup>st</sup> century averaged over Iceland. The precipitation has been smoothed with a three-month running average. In the glaciological simulations, the precipitation in the Icelandic highland was assumed to vary in accordance with the average for the whole of Iceland shown in this figure.

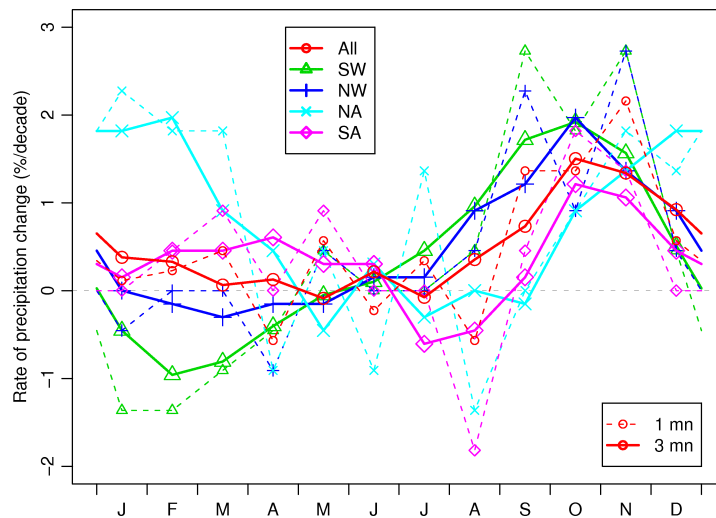


Figure 18: A scenario for seasonal precipitation change for the 21<sup>st</sup> century for SW-, NW-, NE- and SE-Iceland. Dashed curves show monthly values and solid curves show three-month running averages which were used in the hydrological simulations.

until the year 2005, with the climate change projections, which specify differences between the periods 1961–1990 and 2071–2100. The temperature time-series were continued into the future from 2006 and onward based on a study of temperature observations in Reykjavík since 1867 by Jónasson (2004). Expected values for the temperature of the first years after 2005 were estimated based on an autoregressive time-series model, which takes into account the interannual persistency of the temperature record. The temperature was then extrapolated from this level into the future with the warming rate needed to obtain the climate projected by the CE/VO scenario for 2071–2100. Precipitation was interpolated linearly between the midpoints of the 1961–1990 and 2071–2100 periods, but observed precipitation was used until 2005, as for the temperature. In this manner, the observed, comparatively

rapid warming in Iceland since the 1980s is correctly reflected in the input of the glacier models, and at the same time the projected warming from 1961–1990 to 2071–2100 is consistent with the general CE/VO scenario.

## 4 Precipitation modelling

### 4.1 Introduction

The geographical distribution of precipitation in Iceland is poorly known but very important for hydrological applications, both in general and particularly in the context of climate change. Therefore, an extensive task carried out in the VO project was concerned with modelling of precipitation and a compilation of precipitation data sets on a regular grid covering the whole country. These data sets provide the opportunity to model river runoff and glacier mass balance both in the current climate and also in a hypothetical future climate based on the CE/VO climate change scenarios.

Statistical methods with a varying degree of complexity are commonly used to produce gridded precipitation data sets from raingauge data. In Iceland, the use of such methods is questionable because of exceptionally high spatial variability of the precipitation. The raingauge network is also sparse and largely limited to lowland areas and the measurement quality is affected by wind-induced under-catch, especially in wintertime when much of the precipitation falls in the form of snow. Due to the high variability of the precipitation and relative sparseness and low reliability of precipitation observations in Iceland, efforts have recently been made to simulate precipitation in the current climate with meteorological models. Two approaches based on physical modelling of orographic precipitation have been considered and compared. The first one is provided by the mesoscale MM5 model (Grell *et al.*, 1995), and the second one by the diagnostic model of Smith and Barstad (2004), which is based on linear mountain wave theory. Both are in this study based on dynamic downscaling of large-scale meteorological fields provided by the ERA40 reanalysis (Uppala *et al.*, 2005).

The climate of Iceland is largely governed by the interaction of orography and extra-tropical cyclones, both of which can be described quite accurately by present day atmospheric models. As a result, dynamical downscaling of the climate, using physical models, gives valuable information about precipitation distribution, especially in the data-sparse highlands.

The downscaled precipitation was validated based on corrected precipitation at meteorological stations and on precipitation estimates derived from mass balance measurements on the Icelandic ice caps. Thirdly, output from the MM5 model was used as input to the WaSiM hydrological model (Jasper *et al.*, 2002) for the same six watersheds as used for validation purposes by Rögnvaldsson *et al.* (2007) and the simulated discharge compared with observed discharge.

This section begins with a description of the precipitation data set before the two model approaches are described in separate subsections. The section is then concluded with a comparison of the model results.

### 4.2 Precipitation observations at meteorological stations

Precipitation is measured over 24 hours periods ending at 09:00 UTC each day, using gauges of Hellman type equipped with a Nipher type shield. In order to deal with measurement biases, the dynamic correction method proposed for Nordic gauges by Førland *et al.* (1996) was adopted. The method requires temperature and wind information at each site. For the stations measuring precipitation only, the closest wind and temperature measurements were used. The correction procedure is formulated as follows:

$$P_c = k \cdot (P_g + \Delta P_w + \Delta P_e) . \quad (1)$$

In (1),  $P_c$  is the corrected daily precipitation,  $k$  is a correction factor due to aerodynamic effects and depending on wind speed, temperature and the phase (liquid, solid, mixed) of the precipitation,  $P_g$  the measured daily precipitation,  $\Delta P_w$  the wetting loss (set to  $0.14 \text{ mm d}^{-1}$  for rain and  $0.10 \text{ mm d}^{-1}$  for snow),  $\Delta P_e$  the evaporation loss (set here to 0). When trace precipitation is recorded ( $P_g = 0$ ), the

corrected precipitation is calculated as follows:

$$P_c = k \cdot (\Delta P_t), \quad (2)$$

where  $\Delta P_t$  (set to  $0.10 \text{ mm d}^{-1}$ ) represents the sum of evaporation and wetting losses for trace precipitation.

Only the stations operational during 11 years or longer over the period 1958–2006 were selected and corrected. The details of the equations used in the correction procedure and a comparison between corrected and measured precipitation can be found in Crochet (2007) and Crochet *et al.* (2007).

### 4.3 Modelling with the MM5 model

The idea of using limited area models (LAMs) for regional climate simulations was introduced by Dickinson *et al.* (1989) and refined by Giorgi (1990). One of the benefits of such an approach is that it is relatively inexpensive in terms of computer resources used for simulations of the atmospheric flow at relatively high spatial and temporal resolutions. As resolution is increased, processes governed by the interaction of the large scale flow and topography become better resolved by the models. One drawback of this approach which is not present in global climate models is that the simulations are dependent on the lateral boundary conditions. These can constrain the model dynamics and hence affect the results (*e.g.* Warner *et al.*, 1997). To minimise the constraining effects of the boundary conditions, Qian *et al.* (2003) suggested consecutive short term integration, overlapping in time as to minimise the effects of spin-up, instead of a single long term integration. Other investigators (*e.g.* Giorgi and Mearns, 1999) opt for longer integration times, emphasising the importance of the model to be free to develop its own internal circulations. Liang *et al.* (2004) used this approach when simulating precipitation over the U.S. during 1982–2002 using the MM5-based regional climate model CMM5.

Several case studies investigating orographic forcing of precipitation have been made in recent years. Chiao *et al.* (2004) used the MM5 model at a 5 km horizontal resolution to simulate a heavy precipitation event during MAP IOP–2B. The precipitation was satisfactorily reproduced by the model although the total amount of precipitation was slightly higher than measured by rain-gauges. Buzzi *et al.* (1998) simulated a 1994 flooding event in northwestern Italy. The role of orography was found to be crucial in determining the precipitation distribution and amount.

Atmospheric flow over Iceland was simulated for the period January 1961 through June 2006 using version 3–7–3 of the PSU/NCAR MM5 mesoscale model (Grell *et al.*, 1995). The domain used is  $123 \times 95$  points, centered at  $64^\circ \text{ N}$  and  $19.5^\circ \text{ W}$ , with a horizontal resolution of 8 km. There are 23 vertical levels with the model top at 100 hPa and model output is every 6 hours. The domain setup is shown in Figure 19. The MM5 model was used with initial and lateral boundaries from the ERA40 re-analysis project to 1999. After that date, operational analysis, from the ECMWF were used. The ERA40 data were interpolated from a horizontal grid of  $1.125^\circ$  to  $0.5^\circ$  prior to being applied to the MM5 modelling system. The modelling approach differs from that used by Bromwich *et al.* (2005). Instead of applying many short term (*i.e.* on the order of days) simulations and frequently updating the initial conditions, the model was run over a period of approximately six months with only lateral boundary conditions updated every six hours. This was made possible by taking advantage of the OSU land surface model (Chen and Dudhia, 2001).

#### 4.3.1 Verification of simulated precipitation

<sup>3</sup> Several authors have used runoff measurements for validation of precipitation simulated by atmospheric models. Benoit *et al.* (2000) reported some of the advantages of using one-way coupling of

---

<sup>3</sup>This section on model comparison with hydrological data is to a large extent based on work by Jóna Finndís Jónsdóttir, in particular on the paper Jónsdóttir (in press).

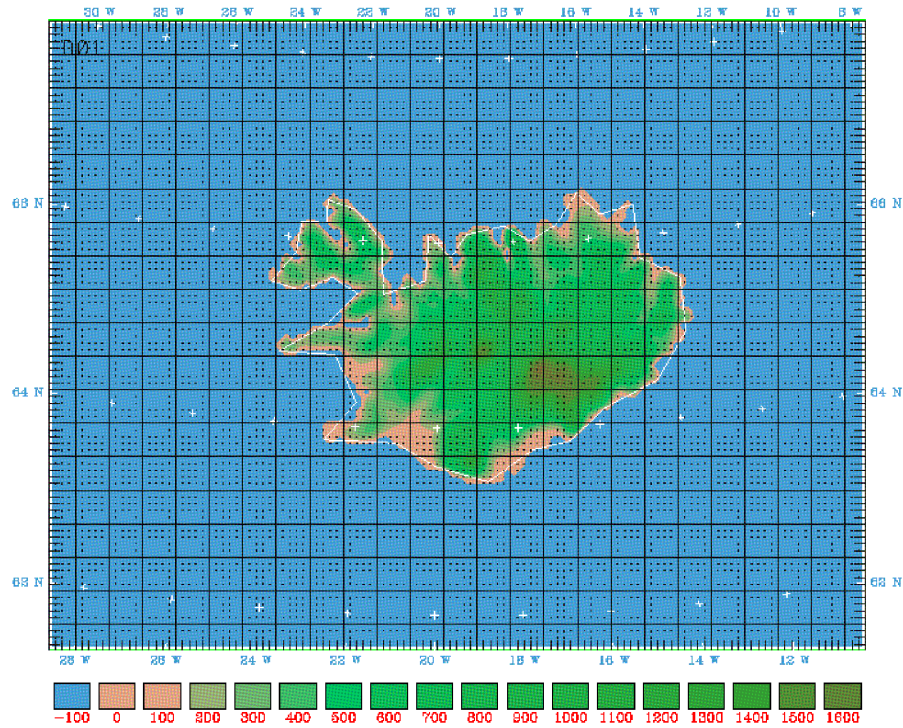


Figure 19: Domain setup of the MM5 model, horizontal grid size is 8 km.

atmospheric and hydrological models, calibrated with observed discharge data, for validation of precipitation calculated by the atmospheric models. They concluded that stream flow records give a better estimate of the precipitation that has fallen over a region than point precipitation measurements, and even though there were uncertainties related to their hydrological model (WATFLOOD), it was sufficiently sensitive to help improve atmospheric models. Jasper and Kaufmann (2003) compared results from WaSiM watershed models that were on one hand driven by meteorological observations and on the other hand driven by data from atmospheric models. They concluded that the hydrological model was sufficiently sensitive to provide substantial information for the validation of atmospheric models.

Rögnvaldsson *et al.* (2007) simulated atmospheric flow over Iceland for the period September 1987 through June 2003 using version 3–5–3 of MM5 driven by initial and boundary data from the ECMWF. The simulated precipitation was compared with two types of indirect precipitation observations. Firstly, winter balance on two large outlet glaciers in SE-Iceland and on two large ice caps in central Iceland. Secondly, model output was used as input to the WaSiM hydrological model to calculate and compare the simulated runoff with observed runoff from six watersheds in Iceland for the water years 1987–2002. Model precipitation compared favourably with both types of validation data.

**Comparison with hydrological data** As described in Section 6, Jónsdóttir (in press) used the latest output from version 3–7–3 of the MM5 model as input to the WaSiM model for the period 1961–1990 to create a runoff map of Iceland. The difference between measured and modelled discharge was in general found to be less than 5% although larger discrepancies were observed (see Table C1 in Appendix C). The WaSiM model was not run with a groundwater module. Instead precipitation simulated by MM5 was scaled in order to make the simulated water balance fit the measured water balance for individual watersheds as described in Section 6. Therefore, comparison of measured and simulated water balance cannot be directly used for validation of the model-generated precipitation. According to the non-scaled MM5 output for the period 1961–1990, mean precipitation for the whole of Iceland



was  $1790 \text{ mm y}^{-1}$ . After scaling the precipitation, this value was reduced to  $1750 \text{ mm y}^{-1}$ , *i.e.* by approximately 2%. This difference can, to some extent, be explained by the fact that precipitation falls on porous post-glacial lava in some areas and flows through groundwater aquifers to the ocean without participating in surface runoff. Earlier research (Tómasson, 1982) have estimated this flow to be on the order of  $33\text{--}62 \text{ mm y}^{-1}$ . This comparison of total accumulated scaled and non-scaled precipitation indicates that MM5 produces comparatively unbiased precipitation estimates when integrated over the whole of Iceland.

Table 1 compares observed and modelled discharge from six watersheds that are not much affected by groundwater flow (the same discharge stations as used for validation of an earlier MM5 model version by Rögnvaldsson *et al.*, 2007; *cf.* Table 1 and Fig. 2). Here, un-scaled precipitation is used in the hydrological modelling in order to obtain an independent validation of the precipitation generated by MM5. For four out of six watersheds, the difference in the water balance is reduced when the newer version of the MM5 model is used compared with the results obtained with the earlier model version. The relative difference between the simulated and observed water balance is in the range  $-8$  to  $13\%$ , with four of the six values in the range  $-4$  to  $5\%$ , indicating a satisfactory performance of the model.

Table 1: Comparison of observed and simulated discharge [ $\text{m}^3 \text{ s}^{-1}$ ] at six discharge stations using unscaled modelled precipitation from versions 3-5 and 3-7 of the MM5 model. Note that the simulation periods are not the same for the two model versions. Hence, the measured discharge can differ somewhat between the columns corresponding to the two versions.

Station #	MM5 V3-5			MM5 V3-7		
	$Q_{\text{meas}}$	$Q_{\text{calc}}$	Difference	$Q_{\text{meas}}$	$Q_{\text{calc}}$	Difference
45	12.3	13.4	8.9%	10.3	10.8	5.0%
128	29.4	32.2	9.7%	22.4	25.3	13.0%
148	9.1	10.4	14.3%	8.2	7.9	$-4.0\%$
198	26.8	25.4	$-5.2\%$	15.5	15.3	$-1.0\%$
200	48.4	53.9	11.4%	39.6	40.3	2.0%
265	19.6	20.8	6.1%	19.9	18.4	$-8.0\%$

**Observed and modelled surface temperature** In addition to simulated precipitation, the WaSiM model used simulated two-metre temperature, surface winds and shortwave radiation as input fields. The simulated temperature field is particularly important in the hydrological simulations because of its effect on the melting of snow and ice. Therefore, a validation of the simulated temperature is important as a part of the validation of the hydrological simulations although it is only indirectly related to the modelled runoff.

Gylfadóttir (2003) produced mean temperature maps for Iceland using spatial interpolation of observed temperature. Figure 20 (top) shows the mean annual temperature for the period 1961–1990 based on the data from Gylfadóttir (2003). The bottom figure shows the simulated mean annual temperature from MM5 for the period 1961–1990. Both data sets have been re-gridded to the same  $0.075^\circ \times 0.075^\circ$  latitude/longitude grid. For the sake of clarity, the map of observed temperature has been masked with data from the MM5 simulation at points over the ocean (*i.e.* at locations where there were no observational values). The temperature map of Björnsson *et al.* (2007a) was on a  $1 \times 1 \text{ km}$  horizontal grid. Even after a re-gridding to a coarser grid with a similar horizontal resolution as the original MM5 grid, the map still shows signs of greater orographical influences (Fig. 20 – top) than the MM5 simulated temperature map (Fig. 20 – bottom). This can, for example, be seen on temperature values over the Snæfellsnes peninsula in W-Iceland and at Tröllaskagi peninsula in N-Iceland. Both maps show a similar temperature pattern, the ice caps and the high altitude interior being coldest

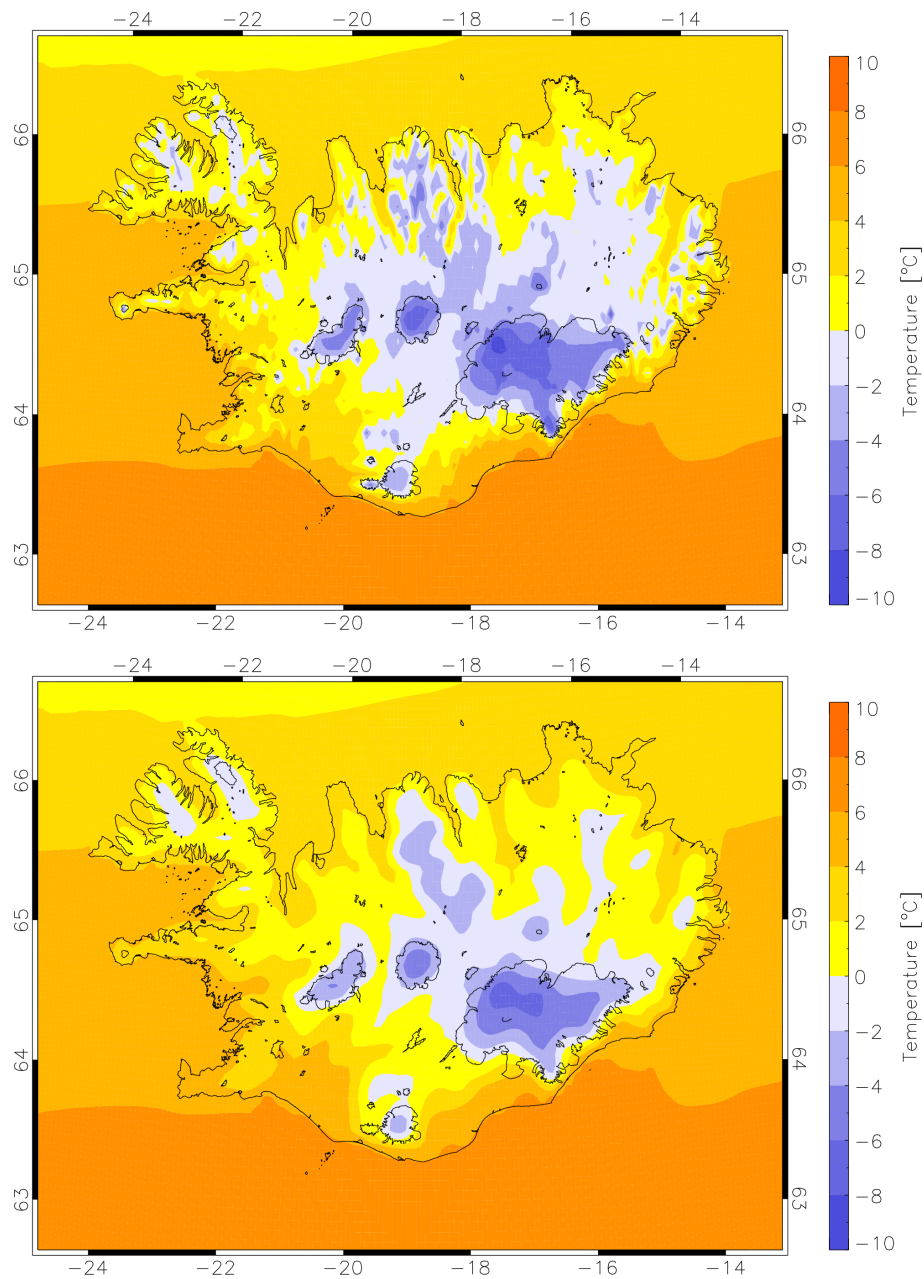


Figure 20: Observed (top) and MM5 simulated (bottom) mean annual two-metre temperature [ $^{\circ}\text{C}$ ], re-gridded on a  $0.075^{\circ} \times 0.075^{\circ}$  latitude/longitude grid.

whilst the coastal areas in the south and the south Iceland lowland are warmer. The difference of the two maps is depicted in Figure 21. On average, the MM5 map is approximately  $0.9^{\circ}\text{C}$  warmer than the map derived from observations. The reason for this difference is not clear as the mean elevation of the orography corresponding to the two maps is approximately the same (509 m a.s.l.).

**Comparison with glaciological data** The spatial variability of the mass balance on large ice masses, such as Vatnajökull and Langjökull ice caps, can be mapped given data along several profiles extending over the elevation range of the ice caps. Mass balance has been observed on parts of Vatnajökull ice cap in SE-Iceland since 1991 (Björnsson *et al.*, 1998) and from 1996 on Langjökull ice cap, central Iceland (Björnsson *et al.*, 2002) (see location map on Fig. 22). Here, we use measurements of (accumulated)

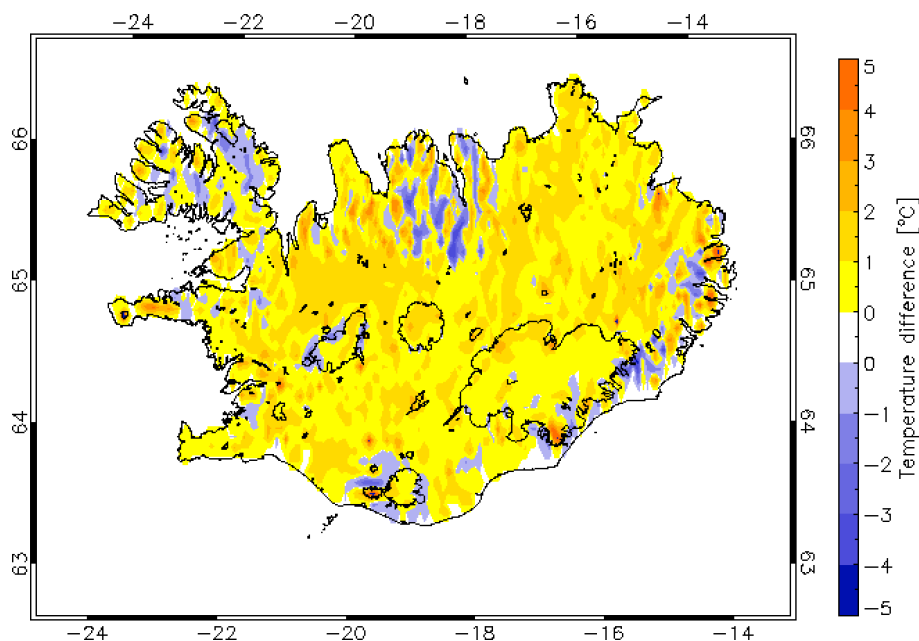


Figure 21: Temperature difference (MM5 – Obs) between the two maps shown in Figure 20. The simulated mean annual temperature by MM5 is on average approximately 0.9°C higher than the mean observed annual temperature. White colour indicates absolute temperature difference less than 0.02°C.

winter mass balance, expressed in terms of liquid water equivalents. Björnsson *et al.* (1998) estimated the uncertainty of the areal integrals of the mass balance to be a minimum of 15%. Due to surging of the Dyngjufjökull glacier in 1998–2000, the uncertainty is considerably greater for this period and the following winter (Pálsson *et al.*, 2002a). As yet unpublished data for the past few winters are from Björnsson and Pálsson<sup>4</sup>. The ice caps and typical locations of the mass balance stakes are depicted in Figure 22.

Mass balance on Hofsjökull ice cap has been observed at sites along profile HN (*cf.* Fig. 22) since 1987 and along profiles HSV and HSA since 1988 (Sigurðsson *et al.*, 2004). In our model configuration the maximum elevation of the Hofsjökull ice cap is approximately 1540 metres, *i.e.* more than 250 metres lower than in reality. Hence, we use area-integrated data from an elevation range of approximately 1450–1650 metres along the three profiles HN, HSV and HSA (Jóhannesson *et al.*, 2006). The winter balance on Hofsjökull has been modelled to estimate the amount of precipitation that falls as rain and ablation that may take place during the winter season. These estimates have been added to the measured winter balance to produce estimates of total precipitation at the measurement sites. This correction has not been carried out for Vatnajökull and Langjökull. The amount of liquid precipitation and winter ablation, therefore, has to be implicitly considered when comparison is made between precipitation simulated by MM5 and the glaciological measurements for Vatnajökull and Langjökull as discussed below.

The simulated winter precipitation at Hofsjökull ice cap is in good agreement with observations (*cf.* Fig. 23) over the northern part of the ice cap (HN, red dots, *cf.* Fig. 22), the SE-part (HSA, green dots, *cf.* Fig. 22) and the SW-part (HSV, blue dots, *cf.* Fig. 22). The solid line in Figure 22 shows the average of the observed winter precipitation, corrected to take liquid precipitation and/or winter ablation into account, at altitudes between 1450 and 1650 metres at locations HN, HSA and HSV. The dashed line represents precipitation simulated by MM5 (nine point average) at the location of the

<sup>4</sup>Helgi Björnsson and Finnur Pálsson, Institute of Earth Sciences and Science Institute, University of Iceland, personal communication.

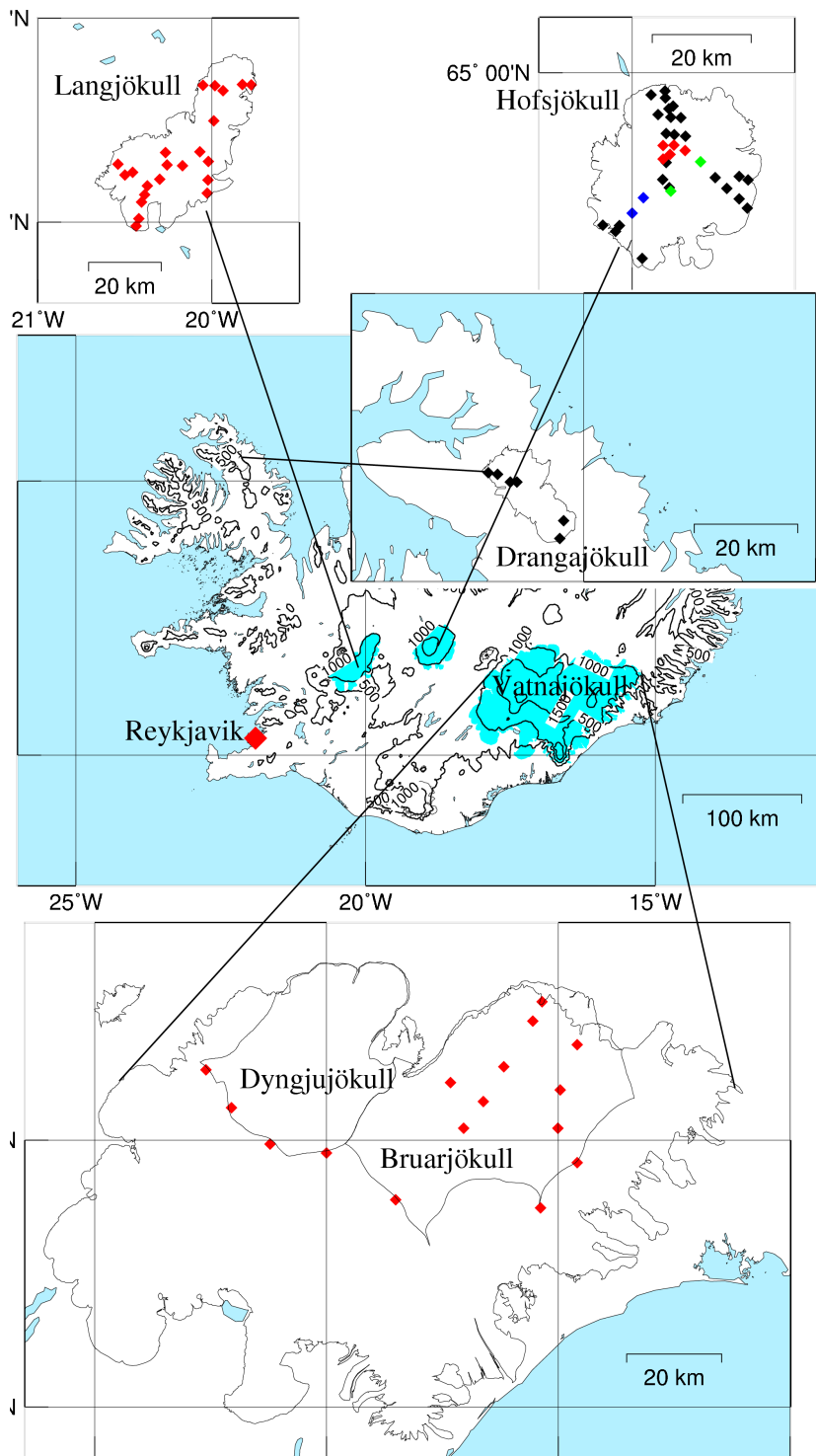


Figure 22: Overview of the six ice caps and glaciers used for validation purposes, dots indicate a typical location of observation sites. Red dots on Hofsjökull glacier are along profiles HN (N-part), blue dots along profile HSV (SW-part) and green dots along profile HSA (SE-part), observations at locations shown in black at Hofsjökull have not been used in this study. Drangajökull is split up in two regions, NW- and SE-part (*cf.* Table 2).

ice cap. The simulated precipitation is within one standard deviation of the average observed winter precipitation within this altitude range for sixteen out of nineteen winters during the period (1987–

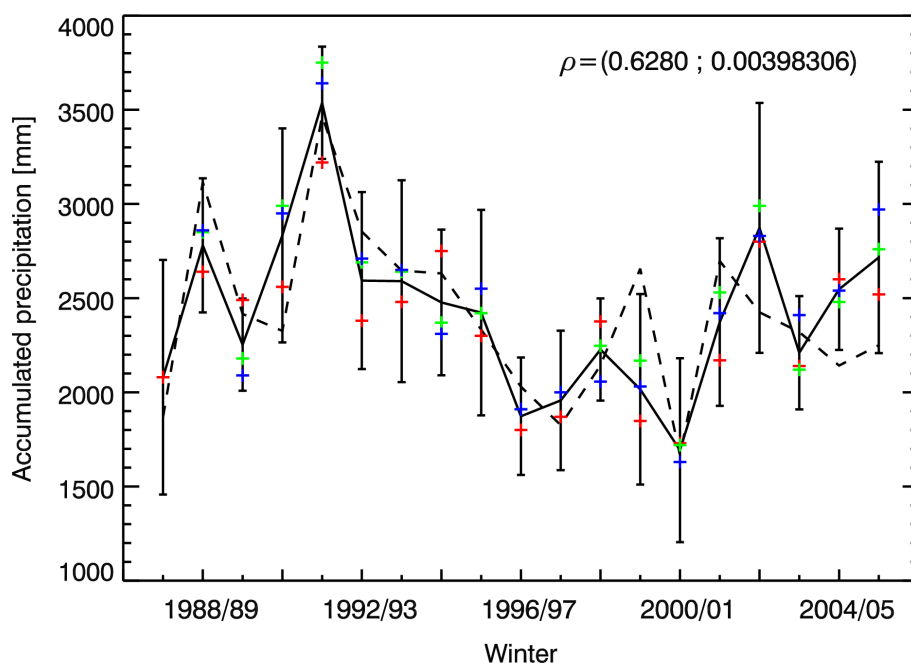


Figure 23: Estimated mean accumulated winter precipitation [mm] along profiles HN (N-part), HSA (SE-part) and HSV (SW-part) at altitudes between 1450 and 1650 metres (solid line, Jóhannesson *et al.*, 2006). Dashed line represents simulated precipitation by MM5 (nine point average) at Hofsjökull ice cap. Red, green and blue crosses represent mean winter balance values at stakes along profiles HN, HSA and HSV respectively within the altitude interval 1440–1680 metres (*cf.* Fig. 22). Error bars indicate the standard deviation of the observations. Observed values from individual snow stakes are from Sigurðsson *et al.* (2004), Sigurðsson and Sigurðsson (1998) and Sigurðsson and Thorsteinsson (personal communication).

2006). The Spearman's rank correlation is 0.63 with a significance value of 0.004 and the *RMS* error is 49 mm y<sup>-1</sup>.

Areal integrals of winter balance over the Vatnajökull ice cap as a whole (8100 km<sup>2</sup>), the Dyngjujökull (1040 km<sup>2</sup>) and Brúarjökull (1695 km<sup>2</sup>) outlet glaciers on the north side of the ice cap, and the Langjökull ice cap (925 km<sup>2</sup>) are compared with simulated wintertime precipitation by the MM5 model in Figure 24. The winter balance is not corrected for to take liquid precipitation and/or winter ablation into account as mentioned above. The model shows least skill on Langjökull ice cap ( $\rho = 0.50$ ; 0.14) where it has an *RMS* error equal to 372 mm y<sup>-1</sup>, and the greatest skill on Brúarjökull ( $\rho = 0.83$ ; 0.0002) where the *RMS* error is equal to 171 mm y<sup>-1</sup>. The correlation for Dyngjujökull is 0.61 with a significance value of 0.06 and the *RMS* error is equal to 286 mm y<sup>-1</sup>. The simulated precipitation is within estimated observational error-margins for 10 out of 12 winters for Dyngjujökull, 13 out of 14 for Brúarjökull and 5 out of 10 for Langjökull ice cap. The correlation for Vatnajökull ice cap is 0.89, with a significant value of 0.06 and the *RMS* error is equal to 388 mm y<sup>-1</sup>. The relative importance of liquid precipitation and/or winter ablation is greatest for Vatnajökull as a whole because the southern margin of the ice cap reaches near sea level where rain may fall and ablation may take place at any time of the year. The north flowing outlet glaciers from Vatnajökull and Langjökull ice cap do not reach as far down so this problem is less important there. This is presumably the reason why the simulated winter precipitation is approximately 500 mm more than the observed winter balance for the Vatnajökull ice cap as a whole.

Mass-balance measurements at Drangajökull ice cap in NW-Iceland have only been carried out since 2004. Table 2 shows a comparison between simulated and observed winter balance for the mass-balance years 2004–2005 and 2005–2006 (Oddur Sigurðsson, personal communication). The model

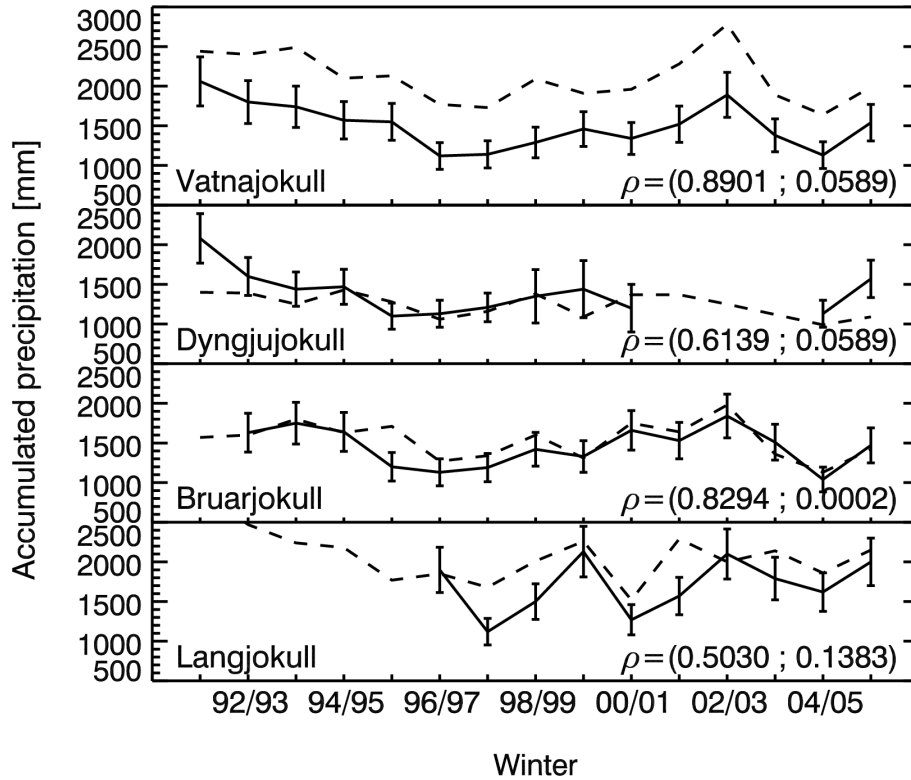


Figure 24: Observed accumulated winter balance (solid) and precipitation simulated by MM5 (dashed) for Vatnajökull ice cap as a whole (top), Dyngjujökull (second from top) and Brúarjökull (second from bottom) outlet glaciers and Langjökull ice cap (bottom). Error bars indicate 15% uncertainty of the observations, except for 1998–2001 at Dyngjujökull where it is 25%. Glaciological data for Vatnajökull, Dyngjujökull and Brúarjökull are from Björnsson *et al.* (1998, 2002) and Pálsson *et al.* (2002a,b, 2004b,c,d) Data for Langjökull ice cap are from Björnsson *et al.* (2002) and Pálsson *et al.* (2004a). As yet unpublished data for the past few winters are from Björnsson and Pálsson.

does not appear to capture the strong observed NW–SE precipitation gradient. The single grid cell values for the SE-part are very close to the observed values but they are too high for the NW-part. The area-averaged values from MM5 are, however, close to mean observed values for the NW-region of the ice cap but too low for the SE-part.

Table 2: Accumulated winter balance and simulated wintertime precipitation at Drangajökull, NW-Iceland (*cf.* Fig. 22). Observed winter balance is taken as the mean of stakes above 400 metre altitude in the northwestern (NW) part of the ice cap and in the southeastern (SE) part. Simulated precipitation is both taken as a nine point mean value (lower values) for the nearest grid cells as well as the nearest grid cell value (higher values).

Winter	NW <sub>Obs</sub> [mm]	NW <sub>MM5</sub> [mm]	SE <sub>Obs</sub> [mm]	SE <sub>MM5</sub> [mm]
2004/05	1797 (3 pts.)	2090/2554	2675 (2 pts.)	2072/2603
2005/06	1833 (3 pts.)	2105/2524	2815 (2 pts.)	2127/2604

In general, the MM5 model results compare favourably with the observed winter balance, in particular for Hofsjökull, where corrections to take liquid precipitation and/or winter ablation into account have been made, and for the comparatively high altitude outlet glaciers Dyngjujökull and Brúarjökull, where such corrections are relatively unimportant. More extensive comparison of simulated precipitation with glaciological observations needs to be made with corrected mass balance data from all the

ice caps.

#### 4.4 Modelling with the LT model

The model used in this section is based on the linear theory (LT) of orographic precipitation proposed by Smith and Barstad (2004). The model includes the major orographic precipitation processes in a relatively simple and compact formulation, using a small set of equations and a limited number of parameters. The result is a model not computationally demanding and very fast to run even on a simple desktop computer, allowing the estimation of precipitation at fine temporal and horizontal scales, over long periods of time. Cloud physics is included in the model using steady-state advection equations of vertically integrated condensed water. Airflow dynamics is described using linear mountain wave theory. The model as applied to downscaling of precipitation in Iceland is described in Appendix A.

##### 4.4.1 Model calibration

The model parameters  $\tau_c$  (conversion time from cloud water to hydrometeors),  $\tau_f$  (fallout time of hydrometeors to the ground) and  $N_m$  (moist buoyancy frequency) were adjusted by comparing simulated precipitation with corrected precipitation observations (*cf.* Section 4.2) and precipitation derived from mass balance measurements made on Vatnajökull, Hofsjökull and Langjökull ice caps between 1995 and 2000 (*cf.* Section 5). A model setup allowing for the use of both ERA-40 data up to 2002 and higher resolution ECMWF analysis data after 2002 as large-scale input, led to re-adjustment of the parameters defined in Crochet *et al.* (2007). The new optimum values found were  $\tau = 1500$  s and  $N_m = 0.003$  s<sup>-1</sup>. This parameterisation was kept constant for the entire period 1958–2006.

##### 4.4.2 Model validation

The validation of simulated precipitation was made against the corrected raingauge data over the period 1958–2002, and against the precipitation derived from the mass balance measurements on the three ice caps over the period 1988–2002. The results are quite similar in quality to those obtained in Crochet *et al.* (2007), with some slight improvements over the northern slopes of Vatnajökull and over gentle terrain and regions of rain-shadow, indicating that the LT model simulates the spatial and temporal distribution and magnitude of precipitation in the mountainous regions of Iceland with remarkable skill. The use of a fixed parameterisation, however, leads to some variability in the simulation quality, that is not too noticeable for accumulation times of one month or longer. When very short accumulation periods are considered, such as the day, the use of a fixed parameterisation together with a wrong delineation of the large-scale background precipitation fields by ERA-40 may in some cases lead to a poor simulation performance. A variable parameterisation will be considered in a future development phase, together with the possibility to define a hybrid method by adjusting the simulated precipitation fields with raingauge observations. Also, the benefit of the new model setup with input information from the ECMWF analyses for the period 2002–2006 needs to be further verified.

#### 4.5 Comparison and interpretation of the two sets of model results

The dynamic and diagnostic downscaling results reveal several features of the precipitation pattern that have not been fully realised before. According to the simulations, the topographic precipitation gradient is greater in winter than in summer, in particularly for the MM5 model. Also, the MM5 simulations indicate that the precipitation maxima are shifted towards the upstream slopes in summer, while in winter they are closer to the mountain tops or even a little downstream. This effect is not noticeable in the LT model results.

The simulated precipitation fields were used to compute 30-year annual averages, 30-year mean monthly area-averages and area-averaged annual precipitation over Iceland. Some case studies of daily precipitation demonstrating the ability of the models to simulate precipitation were also investigated.

**30-year mean annual precipitation** The simulated precipitation from the LT and MM5 models was used to calculate 30-year mean annual precipitation fields for the reference period 1961–1990 (Fig. 25). For the MM5 model, the  $8 \times 8$  km data were interpolated on the  $1 \times 1$  km grid used in the LT model, using curvature splines in tension (Smith and Wessel, 1990). Both models produce similar patterns with a general precipitation decrease from the South to the North, corresponding to the dominating SE to SW moist flow, punctuated by large precipitation amounts on the ice caps and mountain ridges, featuring the strong control that orography exerts on the precipitation distribution. The LT model precipitation field is more detailed than the MM5 field, because the horizontal resolution of 1 km resolves smaller scale features than the nominal 8 km resolution of MM5. In some details, differences can be observed between the two fields that are not necessarily related to the difference in horizontal resolution. Figure 26 presents the difference map (LT – MM5) precipitation. One can see for instance that the LT model is drier than MM5 in the central highlands. Along Snæfellsness peninsula, MM5 simulates less precipitation than MM5 due to its cruder resolution. The LT model precipitation distribution and maxima on the Vatnajökull, Hofsjökull, Langsjökull and Mýrdalsjökull ice caps are more detailed due to the higher resolution of the underlying topography than for MM5. Usually, the LT model generates larger precipitation amounts on the ice caps and mountains than MM5, except on the Langsjökull ice cap, on Strandir and along the valleys of Tröllaskagi.

**30-year mean monthly area-averaged precipitation** The 30-year mean monthly precipitation for the standard period 1961–1990 was calculated and then averaged over Iceland. Figure 27 presents a histogram of the resulting seasonality of the simulated precipitation. Both models describe a similar seasonal distribution of precipitation but MM5 simulates consistently more precipitation except in the period June–September where the LT model produces more precipitation.

**Area-averaged annual precipitation time-series** Time-series of area-averaged annual precipitation over Iceland for the period 1958–2005 are presented in Figure 28. The results display similar interdecadal variations as described by Crochet (2007) for ERA-40 precipitation alone. This variability is in part related to atmospheric circulation patterns in the North Atlantic sector (NAO) as discussed in Section 2. The area-averaged, annual precipitation in Iceland in the reference period 1961–1990 is  $1660 \text{ mm y}^{-1}$  according to the LT model and  $1790 \text{ mm y}^{-1}$  according to the MM5 model, and  $1740 \text{ mm y}^{-1}$  in the more recent reference period 1971–2000 according to the LT model. The results indicate that MM5 produces systematically more precipitation (up to 20% more) than the LT model after 1972. For comparison, scaled time-series of ERA-40 and the scaled, (arithmetic) mean of gauge-corrected precipitation at 20 meteorological stations are also plotted. These two series are in good agreement with the variation of the LT model results with time and indicate that the MM5 model produces too much precipitation for some years. However, the hydrological validation of MM5 precipitation described in Section 4.3.1 indicates that the MM5 precipitation does not on average have much systematic bias for the whole period 1961–1990. It is possible that the LT model has some negative bias when averaged over the whole country and that the MM5 model overestimates the difference in precipitation between the early part and late parts of 1961–1990. This difference between the models needs to be investigated by further comparison with meteorological, hydrological and glaciological observations.



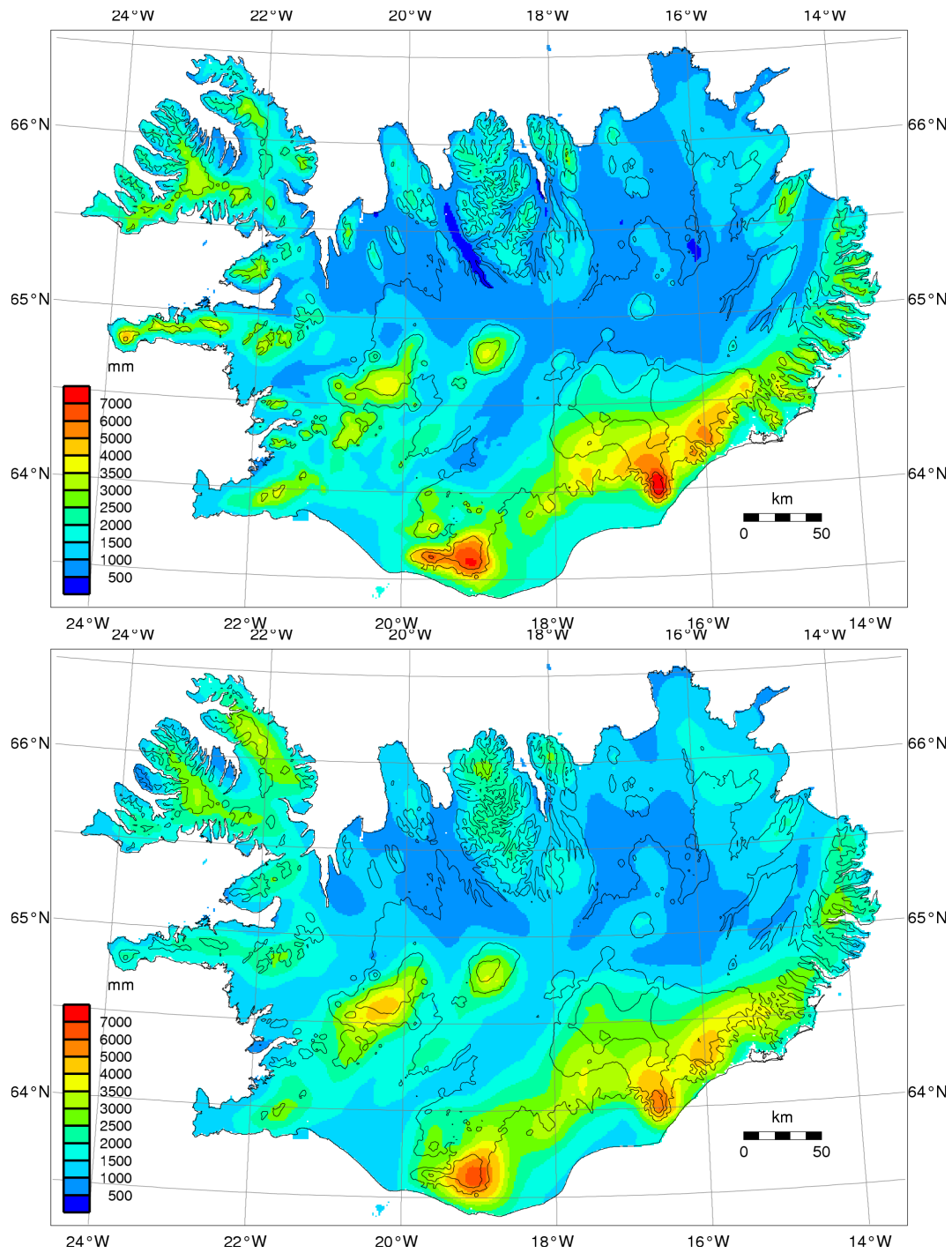


Figure 25: Simulated 30-year mean annual precipitation for the reference period 1961–1990 using the LT (top) and MM5 (bottom) models [mm].

**Daily precipitation** A comparison between LT and MM5 simulations was made on six separate days. The simulated precipitation is accumulated over 24 h ending a 1200 UTC, while the observation at meteorological stations are accumulated over 24 h ending at 0900 UTC. In three of these cases, extreme precipitation exceeding  $100 \text{ mm d}^{-1}$  was observed. The results are presented in Appendix B and include for each day LT and MM5 precipitation maps, a scatter plot of simulated precipitation versus observation and an estimation of the probability of detection (POD) and false alarm ratio (FAR) for

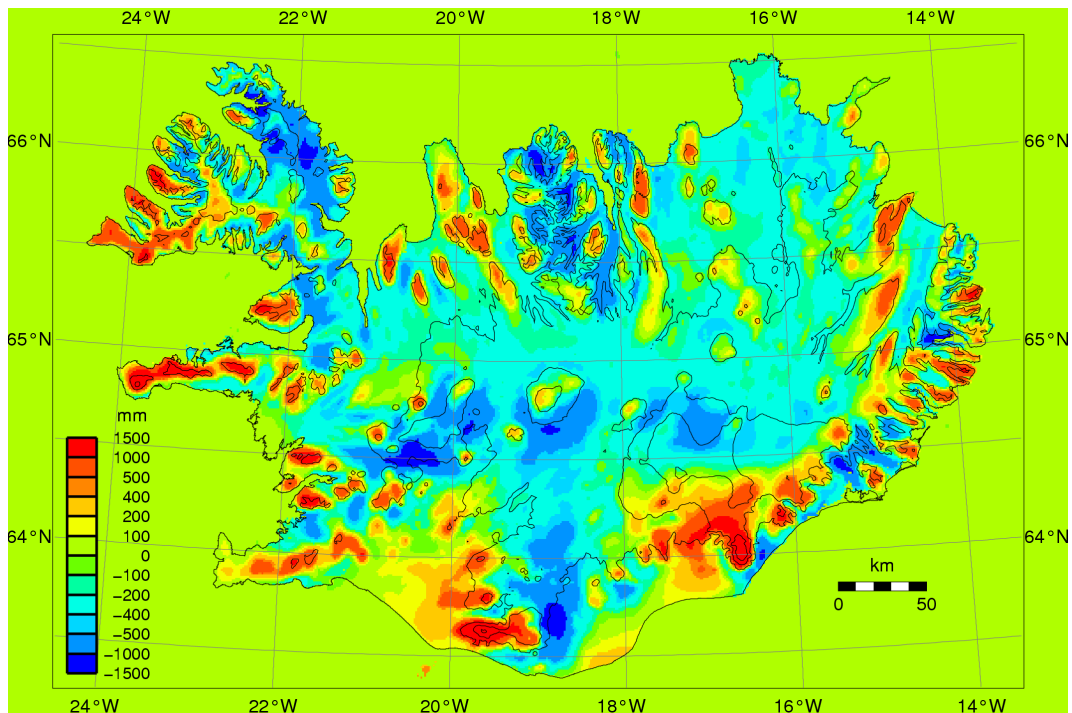


Figure 26: Difference in simulated 30-year mean annual precipitation by the LT and MM5 models for the reference period 1961–1990 (mm).

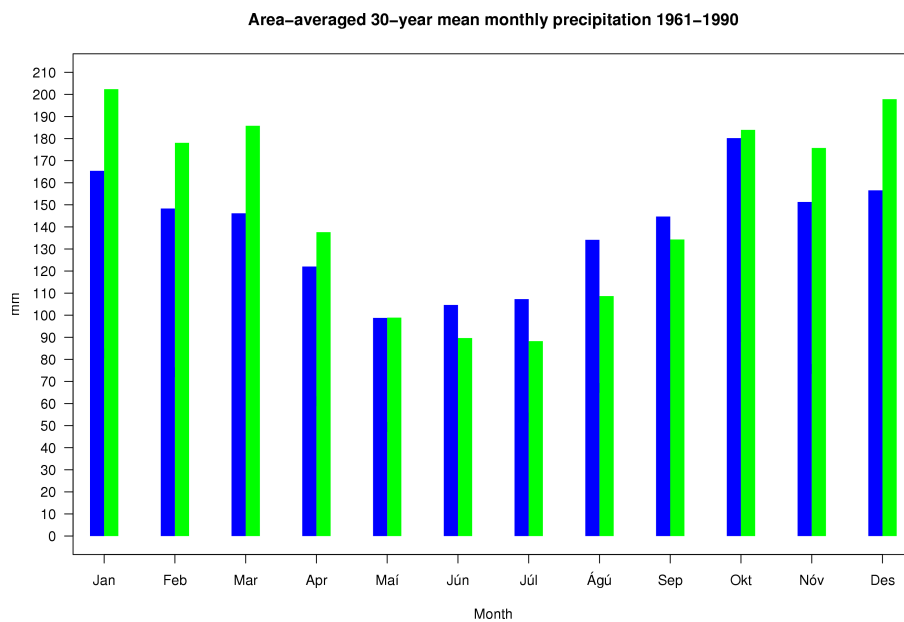


Figure 27: Simulated 30-year mean monthly precipitation by the LT (blue) and MM5 (green) models for the standard period 1961–1990 averaged over Iceland.

precipitation thresholds ranging from  $0.1 \text{ mm d}^{-1}$  to  $10 \text{ mm d}^{-1}$ . Both models are skillful in simulating individual precipitation fields, but systematic errors affecting both models over the entire range of values are sometimes observed, indicating possible errors in the background information used to run the models. Discrepancies between the accumulation period ending at 1200 UTC for the simulations and 0900 UTC for the observations may introduce further errors, especially when the precipitation field is

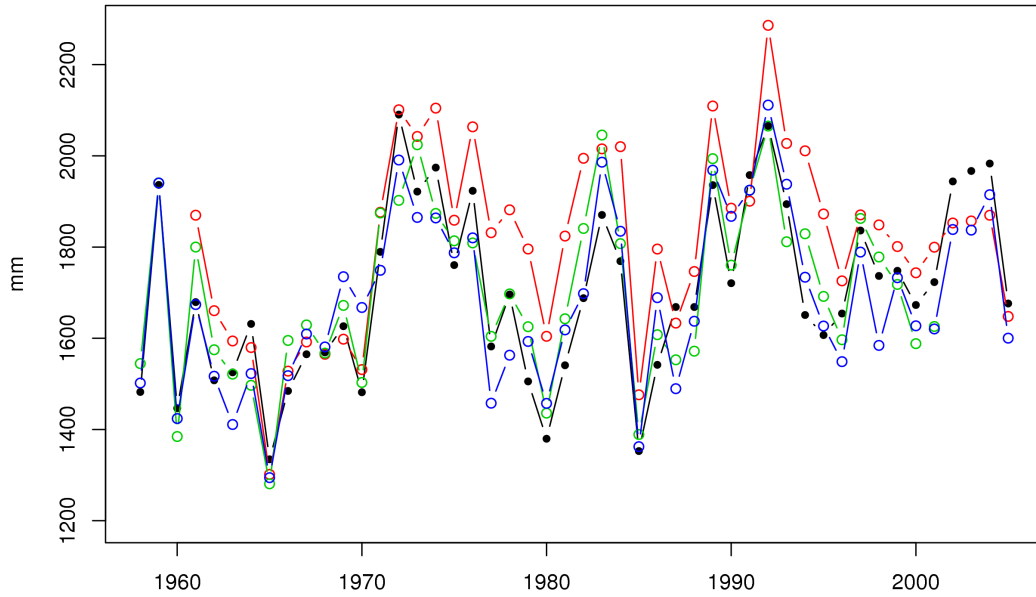


Figure 28: Area-averaged annual precipitation in Iceland for the period 1958–2005. In addition to precipitation simulated by the LT and MM5 models (black and red symbols and lines, respectively), the figure shows ERA40 precipitation, multiplied by 1.5 (green symbols and lines), and an average of 20 gauge-corrected precipitation series from meteorological stations, multiplied by 1.3 (blue symbols and lines).

intermittent and/or moves rapidly in time. The simulated precipitation maps by the two models are usually in agreement regarding the spatial pattern of precipitation, but discrepancies in the magnitude are sometimes observed. The lee drying is usually more pronounced for the LT model than for MM5. In cases where both models simulate the precipitation field well, the LT model validation plot appears less scattered than the MM5 scatter plot, maybe because its higher horizontal resolution resolves smaller scale features better than the nominal 8-km resolution of MM5. The MM5 model simulates the observed extreme precipitation on 30 July 1994 better than the LT model, but at the expense of a strong overestimation at several sites. For the other two extreme cases, *i.e.* 16 January 1995 and 26 October 1995, the largest precipitation observations are strongly underestimated by both models. For the LT model, this underestimation is partly related to the use of a fixed model parameterisation representing average conditions for the entire period, and not optimal parameters for these particular days. Special parameterisations better adapted to each case make it possible to improve these simulations (not shown). On the other hand, these last two extreme cases correspond to winter conditions where the gauge correction based on the use of average coefficients might be questionable. Also, these three extreme cases are rare by definition, and not representative of a typical performance of the models.



## 5 Glacier modelling

A coupled mass- and dynamic model was used to simulate the response of Langjökull, Hofsjökull and southern Vatnajökull (Fig. 29) to the CE/VO-climate change scenario described in Section 3. All three ice caps have extensive monitoring programmes which makes them suitable for glacier modelling. Surface and bed topographies have been constructed from GPS and radio-echo surveys (Fig. 30a,b; Björnsson, 1986, 1988; Björnsson *et al.*, 2006). Mass-balance measurements have been conducted over the last 10 to 15 years; at 22 stakes on Langjökull since 1996, 35 stakes on Hofsjökull since 1988 and at 23 stakes on southern Vatnajökull since 1993 (Figs. 29 and 31; Björnsson *et al.*, 1998, 2002, 2006; Sigurðsson *et al.*, 2004). Of the three glaciers, southern Vatnajökull is largest with 900 m maximum ice thickness and elevation ranging from the sea level up to 2100 m a.s.l. (Table 3). The

Table 3: Characteristics of the Langjökull, Hofsjökull and Vatnajökull ice caps.

Ice cap	Area (km <sup>2</sup> )	Volume (km <sup>3</sup> )	Maximum ice thickness (m)	Elevation range (m a.s.l.)
Langjökull	925	195	580	390–1290
Hofsjökull	880	200	760	600–1790
Vatnajökull	8100	3000	950	0–2100
Southern Vatnajökull	3710	1279	900	0–2100

area and volume of the Langjökull and Hofsjökull ice caps are similar (Table 3), but the elevation distributions differ: Hofsjökull covers a circular volcanic caldera, at 200–300 m higher elevation, and has 100–200 m larger maximum ice thickness than Langjökull, which covers mountain ridges (Fig. 30). As a consequence there is a considerable difference in the response of these two ice caps to climate warming.

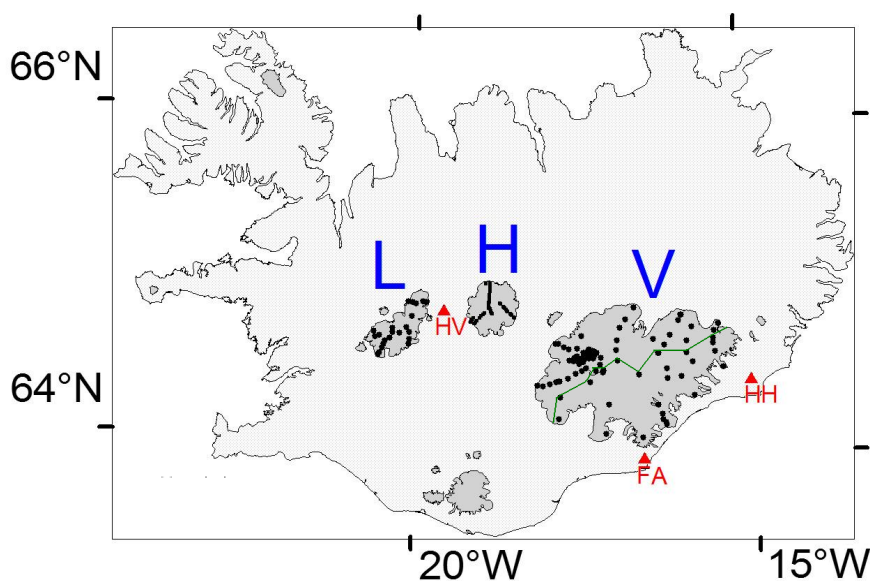


Figure 29: Langjökull (L), Hofsjökull (H) and Vatnajökull (V), sites of mass balance measurements (dots) and meteorological stations (triangles; HV: Hveravellir, FA: Fagurhólsmýri, HH: Hólar í Hornafirði). The green curve separates the southern and northern part of Vatnajökull.

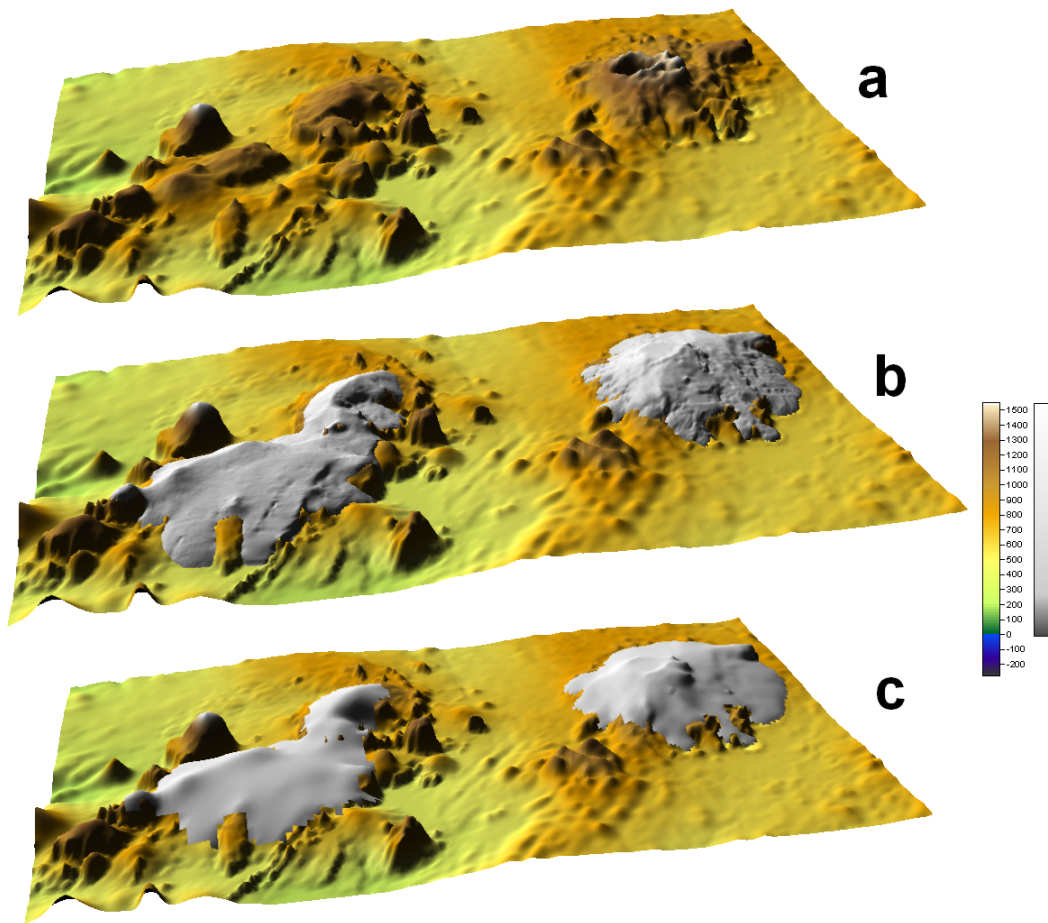


Figure 30: a) Measured bedrock of Langjökull and Hofsjökull ice caps. b) Measured 1997 and 1999 ice surfaces of Langjökull and Hofsjökull, respectively. c) Steady-state glacier geometries after a few hundred year spin-up with constant mass balance forcing.

## 5.1 Mass balance modelling

The mass balance was described with a degree-day model using temperature and precipitation measurements away from the glaciers and a constant temperature lapse-rate, separate degree-day scaling factors for snow and ice, and horizontal and vertical precipitation gradients assuming a constant snow/rain threshold of  $1^{\circ}\text{C}$  (Jóhannesson, 1995; Jóhannesson *et al.*, 1997). Daily temperature and precipitation at Hveravellir were used as an input to the mass balance models of Langjökull and Hofsjökull, and temperatures at Hólar í Hornafirði and precipitation at Fagurhólsmýri for the southern Vatnajökull (Fig. 29). The model parameters for the three ice caps are given in Tables 4 and 5. The mass balance models were calibrated to available mass balance observations up to the mass balance year 2004/2005, and evaluated by using full energy balance derived at several automatic weather stations on Langjökull and Vatnajökull (Guðmundsson *et al.*, 2003; Björnsson *et al.*, 2006). The model explains 86% of the variance in the summer balance of Langjökull but only 39% of the winter balance. Despite this, the model managed to describe 92% of the variation in the annual balance of Langjökull (Fig. 31). The results were much better for the other two ice caps; 80% and 92% of the annual variation in the winter balance of Hofsjökull and southern Vatnajökull respectively, were captured by the mass balance model and 95% of the summer balance on both the ice caps.

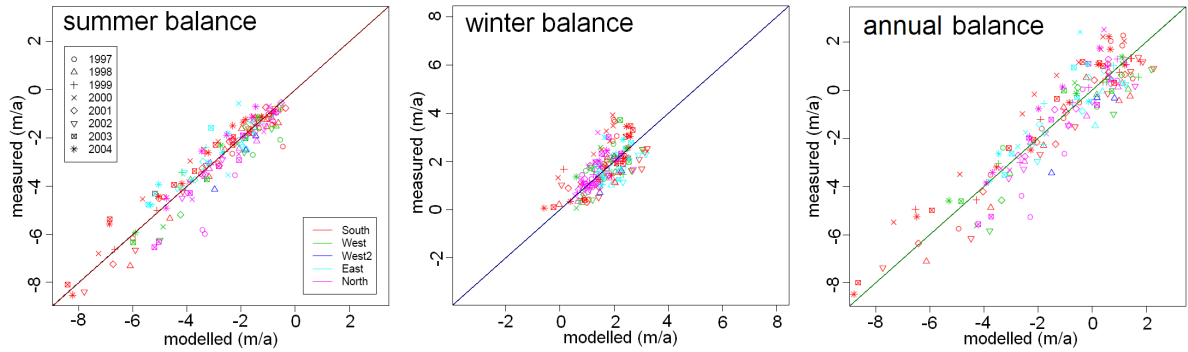


Figure 31: Linear regression between observed and modelled summer, winter and annual net balance of Langjökull.

Table 4: Common model parameters for degree-day mass balance modelling of Langjökull, Hofsjökull and Vatnajökull ice caps. See Jóhannesson (1995) and Aðalgeirsdóttir *et al.* (2006) for further explanations of the meaning of the parameters.

Parameter	Unit	Value
Snow/rain threshold ( $T_{s/r}$ )	$^{\circ}\text{C}$	1.0
Temperature standard deviation ( $\sigma$ )	$^{\circ}\text{C}$	3.0
Threshold snow thickness used in degree-day computations	$\text{m}_{\text{w.e.}}$	0.3

## 5.2 Dynamic modelling

The numerical ice flow model is the same as used by Aðalgeirsdóttir *et al.* (2006) for the southern Vatnajökull and Hofsjökull ice caps. The model is a vertically integrated finite-difference Shallow Ice Approximation model that neglects longitudinal stress gradients and surges, and excludes bed-isostatic adjustments and seasonal variations in sliding (Aðalgeirsdóttir, 2003; Aðalgeirsdóttir *et al.*, 2005). Glen’s flow law with an exponent  $n = 3$  is assumed (Paterson, 1994). Basal sliding is not parameterised separately, but implicitly included in the flow law parameter  $A$ . Series of model runs with a range of flow parameters were carried out to select a flow parameter that simulates the measured glacier geometry best. The resulting optimised flow parameter was equal to the flow parameter  $A$  suggested for temperate ice (Paterson, 1994) within the uncertainty of our analysis.

The coupled mass- and dynamic models were spun up using constant annual mass balance fields corresponding to the average climate of the period 1981–2000 when the ice caps are believed to have been close to a steady state on average. With the exception of the Breiðamerkurjökull outlet glacier of southern Vatnajökull, the shape, volume and area of the ice cap remained fairly constant during the spin-up in all three cases. Minor exceptions to this were encountered at the small surging outlets at southern Langjökull and south-eastern Hofsjökull and in areas not well covered by the mass balance stake network. The mass balance is probably slightly overestimated by the mass balance model at south-eastern Langjökull (Fig. 29) causing the simulated glacier to advance a little beyond its present southeastern margin. Surging is negligible in the dynamics of the southern parts of Vatnajökull and did not affect the spin-up. A 25 km long, 2–5 km wide trench, extending down to 300 m below sea level was created during the Little Ice Age advance of Breiðamerkurjökull outlet glacier (Björnsson 1996; Björnsson *et al.*, 2001; Nick *et al.*, 2007; location shown in Fig. 32). After reaching its maximum extent in the 1890s, Breiðamerkurjökull has retreated fast and is not near a steady state for the average climate of 1981–2000 (Aðalgeirsdóttir *et al.*, 2006). The observed ice surface geometry was therefore

Table 5: Model parameters for degree-day mass balance modelling of the Langjökull, Hofsjökull and Vatnajökull ice caps. See Jóhannesson (1995) and Aðalgeirsdóttir *et al.* (2006) for further explanations of the meaning of the parameters. The parameters for Hofsjökull are slightly different from the ones used by Aðalgeirsdóttir *et al.* (2006) because the Hofsjökull model has been recalibrated.

Parameter	Unit	Lang- jökull	Hofs- jökull	S-Vatna- jökull
Degree-day factor for ice ( $DDF_i$ )	mm <sub>w.e.</sub> d <sup>-1</sup> °C <sup>-1</sup>	7.01	7.44	5.30
Degree-day factor for snow ( $DDF_s$ )	mm <sub>w.e.</sub> d <sup>-1</sup> °C <sup>-1</sup>	4.90	4.98	4.45
Refreezing ratio	–	0.07	0.032	0.07
Temperature lapse rate ( $-\Gamma$ )	°C per 100 m	0.6	0.6	0.56
Precipitation/elevation gradient ( $g_z$ )	per 100 m	0.0936	0.207	0.0497
Rain-correction factor	–	1.32	1.32	1.28
Snow-correction factor	–	2.0	2.0	1.8
Precipitation-correction factor	–	2.265	1.119	1.633
Elevation of temperature station	m a.s.l.	641	641	16
Elevation of precipitation station	m a.s.l.	641	641	46
Starting elevation for precipitation gradient ( $z_0$ )	m a.s.l.	880	880	46
Reference $x$ -location for horizontal precipitation gradient ( $x_0$ )	km	445	510	626
Reference $y$ -location for horizontal precipitation gradient ( $y_0$ )	km	460	480	389
Horizontal precipitation gradient in east direction ( $g_x$ )	per km	0.0069	0.0208	0.0046
Horizontal precipitation gradient in north direction ( $g_y$ )	per km	-0.0187	-0.0163	-0.00818

used as initial geometry for the Breiðamerkurjökull ice flow basin. Apart from Breiðamerkurjökull, the spin-up led to stable, steady-state, reference ice geometries (Fig. 30c), which were used as initial geometries for transient simulations started in 1990.

### 5.3 Results

Figure 32 shows the simulated geometries of the ice caps in 1990, 2040, 2090 and 2190 and Figure 33 shows the simulated volume and area reduction and area-averaged runoff change from 2000 to 2200. The simulations from 1990 to 2005, forced with observed meteorological parameters (dashed lines in Fig. 33), agree fairly well with observations of volume changes and mass balance. The retreat rate is similar for Hofsjökull and Vatnajökull, but much faster for the lower and thinner Langjökull (Fig. 33; Table 3). Langjökull loses 35% of its initial volume after 50 model years when 75% of the volume is left for Vatnajökull and Hofsjökull (Figs. 32). Langjökull is predicted to disappear after 150 model years and only the highest peaks of Hofsjökull and Vatnajökull survive more than 200 years. The runoff increases as the climate warms, but peaks after 40–50 years from now and decreases again due to the reduced area of the glaciers (Fig. 33). Fast volume reduction and slow reduction in area until 2035 results in reduced surface elevation and fast runoff changes. Thereafter, the runoff increase is slowed down by a reduction in ice-covered area. The runoff increase is largest for Langjökull ( $\sim 2.8 \text{ m y}^{-1}$  increase relative to the average of 1981–2000). It is also high for Vatnajökull due to low lying areas that extend down to the sea level. A substantial part of the maximum runoff increase can be related



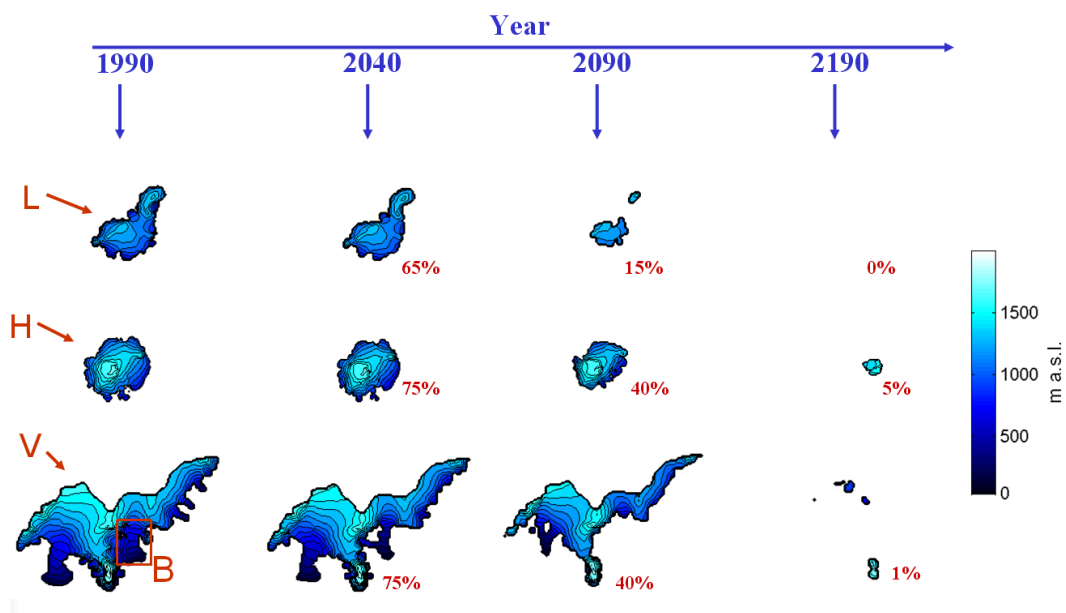


Figure 32: Response of Langjökull (L), Hofsjökull (H) and southern Vatnajökull (V) to the CE/VO-climate change scenario. The location of the Breiðamerkurjökull outlet glacier of southern Vatnajökull is indicated with a rectangle marked “B” in the leftmost map of Vatnajökull. The inset numbers are projected volumes relative to the initial stable ice geometries shown for the year 1990. Note that the figure shows only the southern part of the Vatnajökull ice cap, south of the main east-west ice divide, cf. Figure 29 where the outline of the whole ice cap and the location of the east-west ice divide are shown.

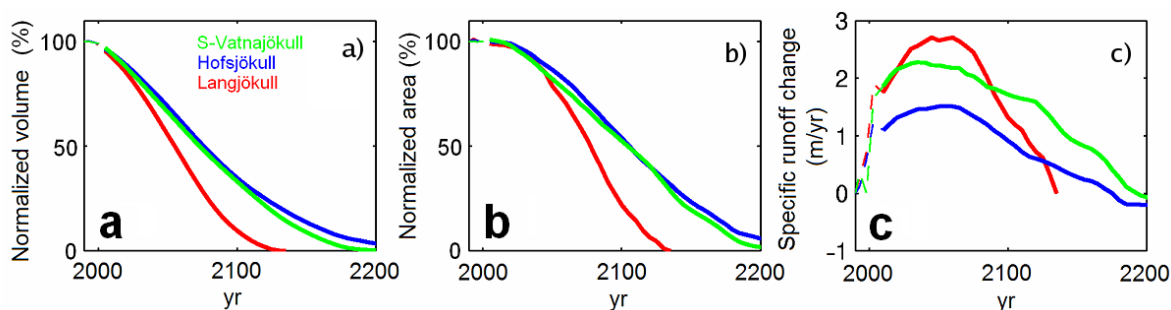


Figure 33: Volume and area reduction, normalised to present day values (Table 3), and area-averaged runoff change. The runoff is always from the present day ice-covered areas and consists of both glacier melting and precipitation. The enhanced glacier melting is the dominant contribution to the runoff change to begin with.

to the warming from 1990 to 2005 (dashed curves in Figure 33c) that has already taken place. The CE/VO scenario leads to more rapid glacier retreat and runoff increase than the earlier CWE and CCEP scenarios (Jóhannesson *et al.*, 2004; Aðalgeirsdóttir *et al.*, 2006; Jóhannesson, 1997; Sælhun *et al.*, 1998) due to the relatively high warming rates that are specified by the CE/VO scenario in the spring and fall.

#### 5.4 Contribution to hydrological modelling

Retreat and thinning of the main Icelandic ice caps near the end of the 21<sup>st</sup> century was extracted from the results of dynamic glacier simulations for use in hydrological modelling with the WaSiM model for the period 2071–2100. Digital terrain models describing the modified ice surface elevation and ice margin locations reflecting the retreat of the glaciers were prepared on the basis of the dynamic runs.

The altitude of new ice-free land was estimated from subglacial bedrock maps (Björnsson, 1988). Because of time constraints, dynamic results based on earlier CWE climate change scenario were used in this work (Jóhannesson *et al.*, 2004; Aðalgeirsdóttir *et al.*, 2006). Subsequently, dynamic simulations with the CE climate change scenario (see Section 3) showed a more rapid retreat of the Icelandic ice caps than the earlier CWE simulations, although the main character of the changes is the same. The effect of ice surface lowering and ice margin retreat may, therefore, be assumed to be somewhat underestimated in the hydrological simulations with the WaSiM model that are described in Section 6. This underestimate may, however, be assumed to be comparatively small because the main effect of the greater warming rate and different seasonality of the warming specified by the CE scenario lies in the direct effect of increased ablation and a higher proportion of the precipitation falling as rain rather than snow.

The dynamic simulations of Vatnajökull described by Aðalgeirsdóttir *et al.* (2006) are only for the southern part of the ice cap because of technical difficulties in obtaining a reasonable reference geometry for northern side of the ice cap due to surges in this part of Vatnajökull. Results from another dynamic model study of Vatnajökull (Flowers *et al.*, 2005; Marshall *et al.*, 2005) were used to estimate the geometry of the northern part of the ice cap near the end of the 21<sup>st</sup> century. The model used by Flowers *et al.* was different from the model of Aðalgeirsdóttir *et al.* in that a dynamic ice model is coupled to a model of the basal hydrology and basal sliding is based on modelled subglacial water pressure. This approach turns out to deal more successfully with the problems encountered on the northern side of the ice cap. A simulation based on a warming rate of 0.2° C per decade was chosen from the suite of simulations carried out by Flowers *et al.* as this warming rate was closest to the warming rate specified by the CE scenario.

## 6 Runoff modelling

### 6.1 Introduction

Discharge gauges can only supply information on runoff within a particular watershed for the period of gauge operation. Watershed models are, therefore, often used to fill in gaps in past discharge time-series and estimate discharge for ungauged watersheds. This section describes a new runoff map of Iceland for current climate conditions constructed by hydrological simulations (Jónsdóttir, in press). It also provides an evaluation of the possible effects of future climate change on water resources and hydropower potential. For a brief outline of the hydrology of Iceland and for earlier estimates of runoff in Iceland, the reader is referred to the description in Section 2 of this report. The results presented here show only one projection of how runoff and hydropower potential may change in the future, but the calibration of a watershed model for all of Iceland forms the basis for further work in this direction.

### 6.2 Background

One-way coupling of atmospheric and hydrological models has many advantages for distributed hydrological modelling. Hay *et al.* (2002) used output from the RegCM2 model (Giorgi *et al.*, 1996) as input to a distributed hydrological model for four basins in the USA. Their research indicated that precipitation averaged over a large area could have the daily variations necessary for basin scale modelling. Studies focusing on one-way coupling between atmospheric models and the WaSiM watershed model in alpine landscapes have earlier been reported by Jasper *et al.* (2002), Jasper and Kaufmann (2003) and by Kunstmann and Stadler (2005). The WaSiM model has further been integrated with a glacier sub-model (Klok *et al.*, 2001) to simulate the discharge of a heavily glaciated drainage basin. Jasper *et al.* (2002) compared WaSiM simulations that were driven by observed meteorological data, with simulations driven by data from high-resolution numerical weather prediction (NWP) models. Kunstmann and Stadler (2005) were able to reproduce observed stream flow reasonably well in an alpine and orographically complex basin in Germany by driving the WaSiM watershed model with MM5 output data.

In a study by Jónsdóttir and Þórarinnsson (2004), the HBV watershed model (Sælhun, 1996) was calibrated and driven both with observed and simulated data from the MM5 model. The main results were that the correlation between daily values of measured discharge and discharge calculated by the MM5 data was fairly good. The correlation was somewhat higher when data from nearby weather stations were used. Using the MM5 data, however, improved the water balance for each water year. Tómasson *et al.* (2005) simulated a short winter flood in the Þjórsá–Tungnaá river basin in S-Iceland, using precipitation as simulated by the MM5 model and the HEC–HMS (HEC, 2000) runoff model. They concluded that the runoff model results were in good agreement with observed discharge in the river basin. The MM5 model output has also been used as input to the University of Washington Distributed–Hydrology–Soil–Vegetation Model (DHSVM) to form an automated river flow forecasting system (Westrick *et al.*, 2002).

### 6.3 Data

The Hydrological Service currently operates approximately 170 water level gauges around Iceland. River discharge can be evaluated with a discharge rating curve at more than half of these gauges. The watersheds covered by discharge gauges now in operation cover roughly half of Iceland. Time-series of discharge from these gauges as well as discontinued series and discrete discharge data are collected in a database which was used for calibration of the hydrological model used in this study. 70 series were used for calibration of individual watershed models and 30 additional series were used for a crude comparison of measured and calculated water balance on the runoff map.

A 500 m digital elevation model (Icelandic Meteorological Office *et al.*, 2004), a soil map from the Agricultural University of Iceland and a digital vegetation map from the Icelandic Institute of Natural History were used for describing the watersheds in the hydrological model. The geographical data were all resampled to a 1x1 km spatial resolution.

The evaluation of projected runoff change between the periods 1961–1990 and 2071–2100 is based on the CE/VO climate change scenario as described in Section 3 and an estimate of future glacier geometry for the year 2085 that was produced with glacier models as described in Section 5.

## 6.4 Methods

The WaSiM (WATER balance SIMulation Model) hydrological model is a fully distributed catchment model using physically based algorithms and parameters for the description of hydrological processes (Jasper *et al.*, 2002, Jasper and Kaufmann, 2003). The model offers various methods of calculating the different water balance elements depending on the availability of input data. The temperature-based Hamon approach (Federer and Lash, 1983) was used for calculating evapotranspiration. A temperature-wind index method was used to account for higher melting of snow and ice when the wind speed is high. An extended melt approach (Hock, 1998, 1999) was used for simulation of melting on glaciers, using information on radiation. The soil model used Richards' equation (Richards, 1931; Philip, 1969) for the unsaturated zone but no groundwater model was applied.

In this study, eleven parameters describing the unsaturated zone, precipitation magnitude, snow accumulation and melt were adjusted to fit each watershed. An additional, six parameters were adjusted for glacier-covered areas. For the unsaturated zone, the following six parameters were adjusted: (1) storage coefficient of direct runoff  $k_d$ , (2) storage coefficient of interflow  $k_i$ , (3) drainage density  $d$ , (4) recession constant for baseflow  $k_b$ , (5) saturated hydrological conductivities of the uppermost aquifer, and (6) the fraction of surface runoff from snowmelt. A precipitation correction (7) was used to account for groundwater discharge to and from the watersheds, *i.e.* to scale precipitation to make modelled water balance fit with measured water balance. The same parameter was used for rain and snow. The four snow model parameters that were adjusted were (8) temperature limit for rain  $T_{R/S}$ , (9) temperature limit for snow melt  $T_0$ , (10) degree-day-factor without wind consideration  $c_1$ , and (11) degree-day-factor with wind consideration  $c_2$ . The six additional parameters that describe melting on glaciers are: (12) a melt factor  $MF$  with identical values for snow, firn and ice, (13–14) empirical radiation melt coefficients for snow and firn (identical)  $\alpha_{snow}$ , and for ice  $\alpha_{ice}$ , and (15–17) the specific storage coefficients for firn, snow and ice  $k_{firn}$ ,  $k_{snow}$  and  $k_{ice}$ .

For glacier-covered areas, model parameters estimated by Thorsteinsson *et al.* (2006) were considered and adjusted to fit runoff data as well as available information about accumulated mass balance of glaciers and ice caps over longer periods. Thorsteinsson *et al.* calibrated a glacier mass balance model on the basis of mass balance measurements from the Hofsjökull ice cap, the third largest glacier in Iceland, using meteorological data from the nearby Hveravellir weather station.

A one-way coupling between the MM5 model and the WaSiM model was applied by feeding the output data from MM5 directly into WaSiM. The MM5 output data were on an 8×8 km horizontal grid while the grid of the watershed model was set to 1×1 km resolution in order to catch more of the characteristics of the landscape. Each grid point in the MM5 model was treated as a meteorological station and data for each grid cell in WaSiM were evaluated by inverse distance weighting between the grid points of the MM5 model. The MM5 model data are available every six hours while the watershed model was run at a daily time step because of the time resolution of observed discharge data. The MM5 model data were therefore averaged or accumulated to a daily time step. In addition to simulated precipitation, the WaSiM model used simulated two-metre temperature, surface winds and incoming shortwave radiation as input fields.

Even though the MM5 model produces precipitation results that are in good agreement with obser-

vations, the use of a precipitation correction factor (7) in WaSiM is necessary because the model was not coupled to a groundwater module. This is due to a lack of data for calibration of the groundwater component. Without precipitation correction, the model does not produce good results for watersheds where a part of the precipitation seeps down and flows out of the watershed as groundwater. Similarly, a difference between the modelled and measured water balance arises for watersheds where ground water emerges within the watershed as spring water. The precipitation correction was determined for individual watersheds on the basis of the measured runoff and was found to be in the range 0.9–1.2 for about 50% of the watersheds. It reached as high as 4–6 for watersheds that receive large quantities of groundwater from neighbouring watersheds and it was set to zero for some watersheds without surface runoff. Although this methodology reproduces the observed runoff adequately, it can lead to large biases in internal physical parameters such as snow depth for watersheds where the precipitation correction is much larger or much smaller than 1. Also, since the precipitation correction is given a single value for each watershed, the modelled runoff is characterised by artificial discontinuities along watershed boundaries with large changes in precipitation correction.

The WaSiM model was calibrated for 70 watersheds, covering one third of the country. The calibration period for long series was the period 1971–1990. For shorter series, the calibration period varied between 5 to 20 years depending on the availability of measured data. The calibration process involved evaluation of a parameter set for each watershed, with the aim of catching the general characteristics of each basin and providing a good fit to the long-term water balance. The Nash–Sutcliffe coefficient  $R2$  (Nash and Sutcliffe, 1970) and  $R2log$  were used to measure how well the simulated runoff fits the observed runoff. Both coefficients  $R2$  and  $R2log$  range from 1 to  $-\infty$ , where a perfect fit corresponds to 1. The coefficient  $R2$  emphasises the fit of high flows and floods while  $R2log$  puts greater weights on how well low flows are simulated. Table C1 in Appendix C shows the  $R2$  and  $R2log$  coefficients as well as the fit of the water balance for periods with available data and Figure 34 shows a comparison

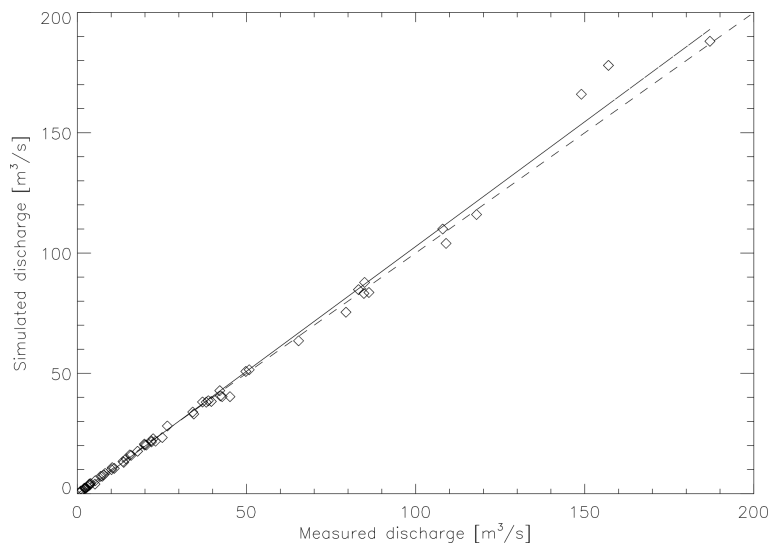


Figure 34: Measured and simulated (WaSiM/MM5) mean discharge [ $\text{m}^3 \text{s}^{-1}$ ] at the watershed gauges shown in Table C1. Dashed lines indicates a perfect fit, solid lines represents the linear best fit between the measured and simulated discharge.

between measured and simulated mean discharge. Inspection of the data in Table C1 shows that the difference between simulated and observed runoff was  $\leq 5\%$  for 58 of the 70 watersheds and  $\leq 2\%$  for 30 watersheds.

The classification of Iceland on a catchment basis by Halldórsdóttir *et al.* (2006) was used to transfer model parameters to ungauged watersheds (Fig. 35). The classification is based on available

geographical information; maps of geology and vegetation, an air temperature distribution model, the topography of the country, and on runoff characteristics. Catchments were divided into three groups: non-glaciated catchments with (1) high or (2) low hydrological permeability and (3) subglacial catchment areas. These three groups correspond to the three river types: groundwater-fed rivers, direct-runoff rivers, and glacial rivers, respectively. Subglacial catchment areas were further divided into areas with high and low hydrological permeability. The classification of non-glaciated catchment areas was more complex, reflecting the geographical variability within the country with regard to groundwater and snow storage reservoirs, wetland distribution, and vegetative patterns. The geographical extent of the calibrated watersheds was compared to the classes defined by the classification and the parameters that had been evaluated for each watershed were transferred to the class for which the watershed covered. If more than one gauged watershed overlays one continuous class, all parameter sets were evaluated. The parameter set was chosen that seemed to give the best fit to the measured discharge and/or that seemed to be comparable to parameter sets of the same class elsewhere. Parameters for disconnected classes were evaluated individually.

The WaSiM model was run for all of Iceland based on this division into classes for the period September 1, 1961 to August 31, 1991. The precipitation correction factor was further adjusted to account for groundwater flow to and from 100 watersheds by comparing calculated water balance to measured water balance. Parameters for glacier melt were also harmonised for each glacier. The resulting model of the whole country was then run for the reference period 1961–1990 and for the future period 2071–2100 based on the CE/VO scenario described in Section 3.

Tómasson (1981) divided Iceland up into 916 squares and estimated potential hydropower according to the following equation

$$P = gqAH, \quad (3)$$

where  $P$  [W] is the power,  $g$  [ $\text{m s}^{-2}$ ] is the acceleration of gravity of the Earth at its surface,  $q$  [ $\text{kg s}^{-1} \text{km}^{-2}$ ] is mean specific runoff,  $A$  [ $\text{km}^2$ ] is the area of the square and  $H$  [m] is height above

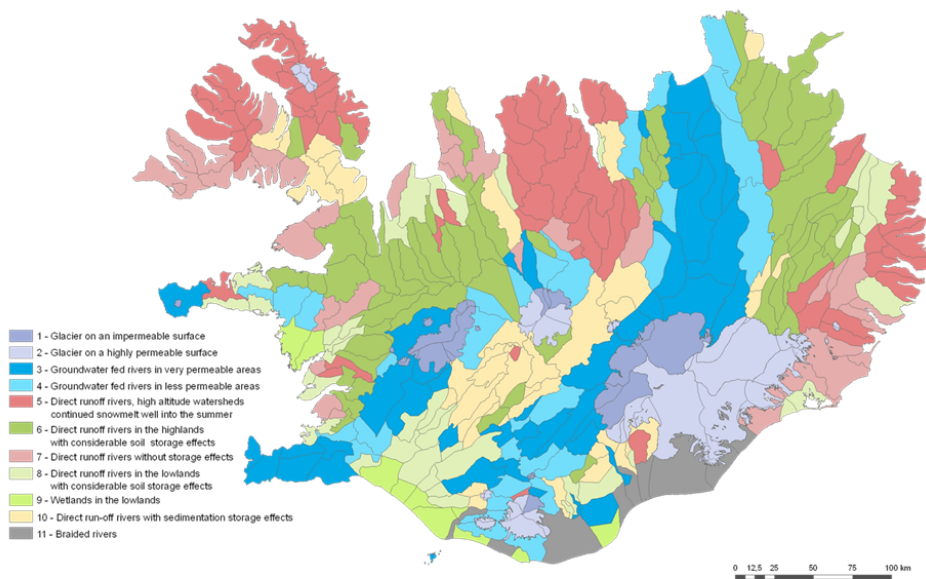


Figure 35: Classification of catchment types in Iceland.

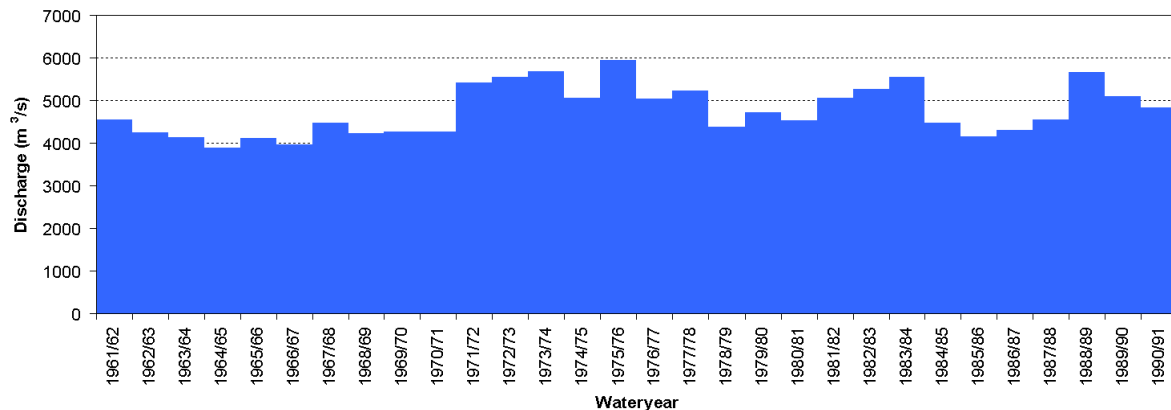


Figure 36: Simulated total annual runoff for all of Iceland (shown for water years, defined as September 1 to August 31) for the period 1961–1990.

sea level. The estimated power in runoff for the whole country is the sum of the power in each cell. The same method was used in this study to evaluate the gravitational potential power in runoff for all of Iceland.

## 6.5 Results of runoff modelling

Simulated average annual runoff for all of Iceland for the water years 1961–1990 (defined as September 1 to August 31) is shown in Figure 36. The average, annual runoff for these water years was found to be  $4770 \text{ m}^3 \text{ s}^{-1}$  or  $1460 \text{ mm y}^{-1}$ .

No measurements of actual evapotranspiration exist in Iceland. Rist (1956) estimated evapotranspiration to be in the range  $100\text{--}200 \text{ mm y}^{-1}$ ; Tómasson (1982) estimated average evaporation as  $310\text{--}414 \text{ mm y}^{-1}$  based on calculations of potential evapotranspiration by Einarsson (1972). According to this study, the average evapotranspiration of Iceland is  $280 \text{ mm y}^{-1}$ . When this model estimate of the evapotranspiration is added to the above runoff estimate of  $1460 \text{ mm y}^{-1}$ , one obtains  $1740 \text{ mm y}^{-1}$ . This is similar in magnitude to the average of the scaled precipitation, which was mentioned earlier in Section 4 in connection with the validation of the MM5 model, and approximately 2% lower than non-scaled average precipitation simulated by MM5 for the period 1961–1990. The total runoff is affected by the net balance of glaciated areas, which may be assumed to have been slightly positive on average in the period 1961–1990. The effect of the ice volume increase on average total runoff from the whole country is, however, likely to have been comparatively small in comparison with the uncertainty of the model simulations. The assumed ice volume increase “works in right direction” in the sense that it may be a part of the explanation for the precipitation simulated by MM5 which is not accounted for by the sum of the runoff and evapotranspiration.

Figure 37 shows the geographical distribution of annual average runoff within the country for the water years 1961–1990 and its seasonal distribution (autumn (SON), winter (DJF), spring (MAM) and summer (JJA)).

The projected runoff for the period 2071–2100 is shown in Figure D1 in Appendix D and the calculated difference in mean annual and seasonal runoff between the two 30-year periods is shown in Figure 38. Other results from the WaSiM model include a map of the change in mean annual evaporation between the two 30-year periods (Fig. D2) and maps of the number of days with snow cover per year (Figs. 39 and D3).

For the period 2071–2000, the WaSiM model simulates an average runoff of  $1800 \text{ mm y}^{-1}$ , almost 25% higher than runoff obtained for the period 1961–1990. Glacier-covered areas are then modelled

to be reduced by approximately 20%. Runoff from non-glaciated areas is projected to increase by 8%, partially because of the increased area of non-glaciated watersheds, while glacial runoff increases by 90%.

The modelled change in seasonality of runoff is shown in Figure 40 which is divided into three parts.

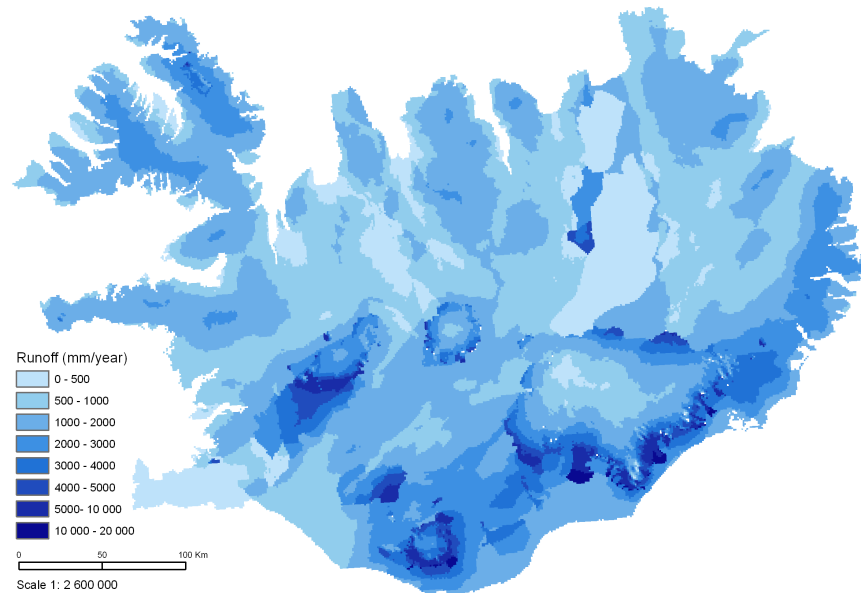
- a Total runoff from all of Iceland.
- b Runoff from non-glaciated areas. An increase is projected in all months except May–August. This change may be explained by the higher projected temperature during winter in 2071–2100, leading to less snow accumulation and hence less snow melt during May–August than during the reference period 1961–1990.
- c Runoff from glaciers. Even though glacier-covered areas are projected to decrease by 2400 km<sup>2</sup>, the simulated runoff from glaciers is substantially higher during the years 2071–2100 than during the period 1961–1990. The increased melting of glaciers and the consequent temporary increases in meltwater runoff are clearly the most pronounced aspects of the projected runoff change.

Gravitational potential power of runoff is modelled to be 220 TW h y<sup>-1</sup> for the whole country for the reference period 1961–1990 and 320 TW h y<sup>-1</sup> for the years 2071–2100, *i.e.* an increase of 45%.

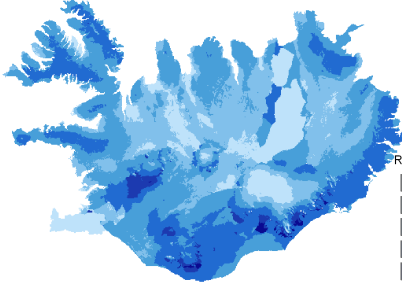
## 6.6 Summary and outlook

The WaSiM model has been run with simulated meteorological input from the MM5 model to evaluate the runoff of Iceland for the period 1961–1990 and to model the runoff during in the future period 2071–2100. Runoff is projected to increase by 25% when the climate has warmed by 2.8° C and annual precipitation has increased by 6%. By far the largest contribution to increased runoff was found to come from increased melting of glaciers caused by higher temperatures. This meltwater-induced increase in runoff is temporary, however. Projections of glacier retreat show that Icelandic glaciers may disappear almost completely within the next 200 years (Aðalgeirsdóttir *et al.*, 2006). A substantial increase in gravitational potential hydropower is projected for 2071–2100, indicating that there could be great changes in hydropower production potential associated with future climate change.

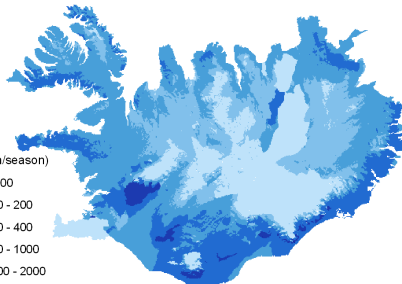




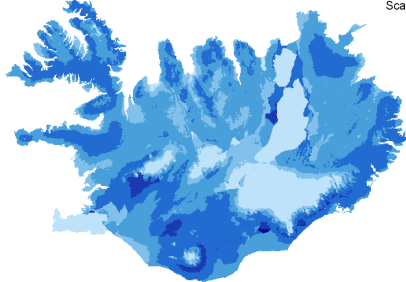
a) SON - Autumn



b) DJF - Winter



c) MAM - Spring



d) JJA - Summer

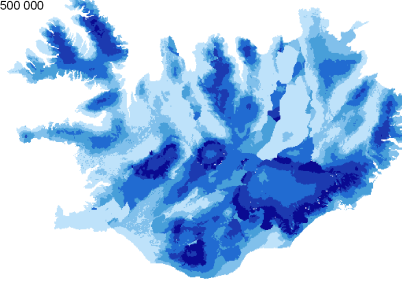


Figure 37: Modelled mean annual and seasonal runoff in Iceland for the water years 1961–1990.

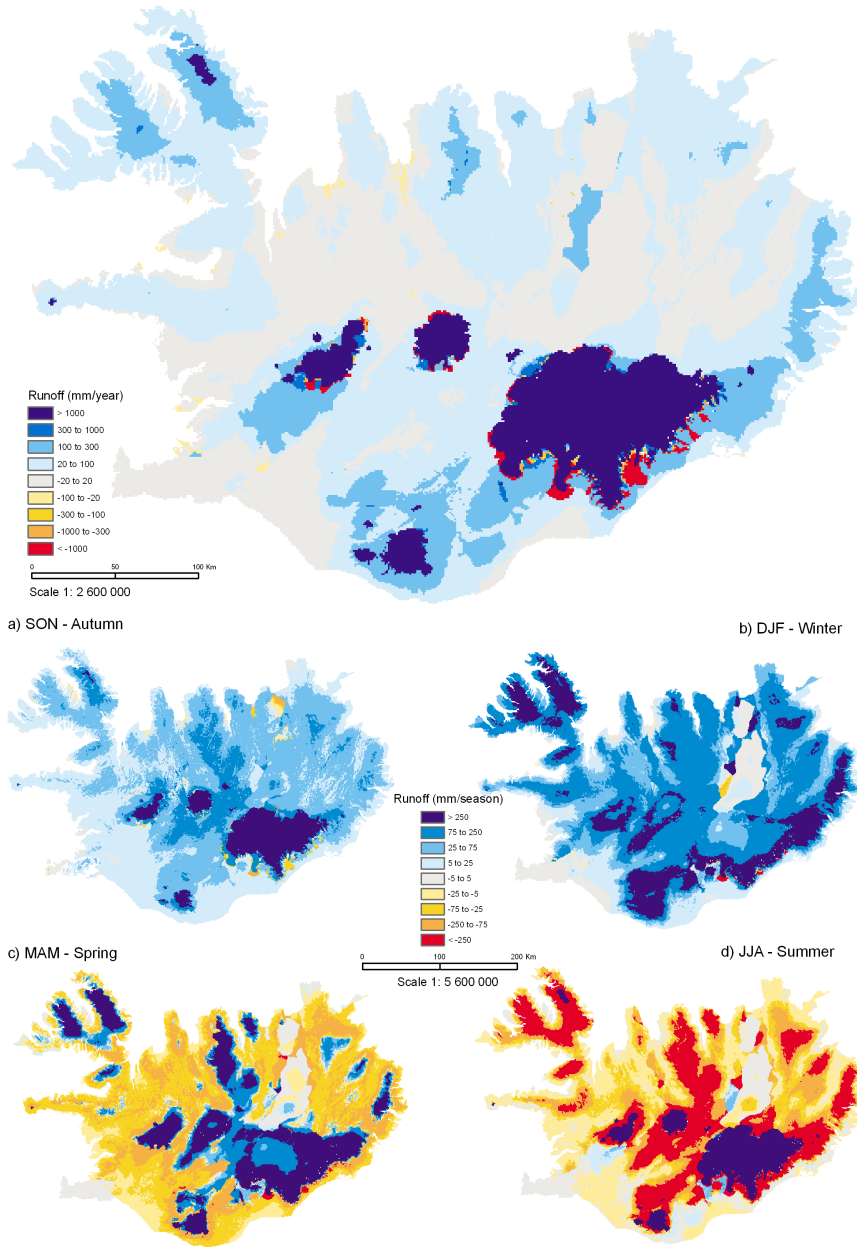


Figure 38: Projected change in mean annual and seasonal runoff from 1961–1990 to 2071–2100.

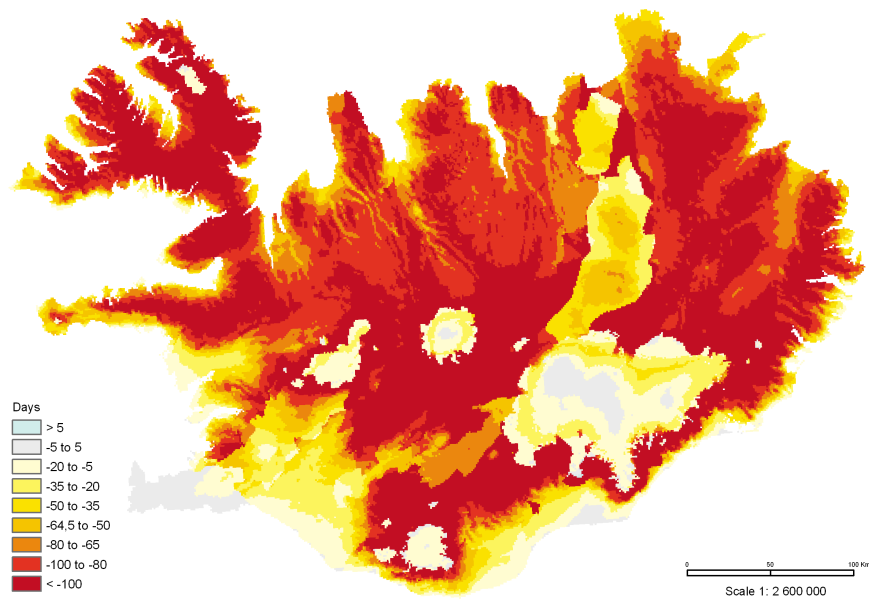


Figure 39: Projected change in mean annual number of days with snow covered ground from 1961–1990 to 2071–2100.

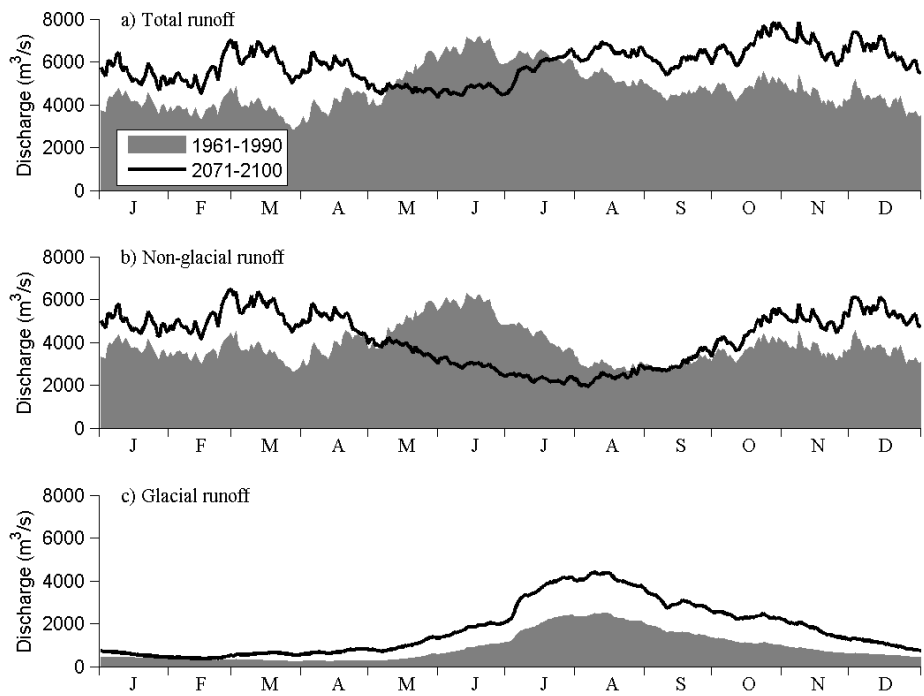


Figure 40: Mean seasonal variation in total runoff for the reference period 1961–1990 (dark gray area) and a future projection for the period 2071–2100 (curve). a) Runoff from all of Iceland. b) Runoff from non-glaciated areas (3% larger in area in the future period). c) Runoff from glaciated areas (20% smaller in area in the future period).



## 7 Energy production

### 7.1 The Icelandic power system

The transmission system and the largest power plants in Iceland are shown in Figure 41. Three curves on the map show how the country can be divided into different hydrological regions. Hydropower production in the easternmost region marked as red is commencing at the time of this writing and is the first of any significant size to be built in that region with its unique hydrology and flow patterns.

Most of the power plants shown are owned and operated by Landsvirkjun (The National Power Company). Some geothermal plants in the South-West are owned and operated by regional utilities that are presently planning and building a few hundred megawatts of additional geothermal plants there. For emergency service there are more than 100 MW of fossil fuel (oil) stations used for emergency service, most of them quite small. The main transmission system consists of 220 kV high tension lines connecting the power plants in the South-West to the main load centres around the capital city Reykjavík and a 132 kV line around the country with a radial to the North-Western peninsula, Vestfirðir. The three thick curves separating hydrological regimes cross the 132 kV ring where presently there are possible congestions that can be of significance when coordinating reservoir operations.

### 7.2 Implications for system planning and component design

Traditionally, hydropower companies base their estimates of power producing capability on the assumption that future runoff is a stationary, stochastic process having the same mean and other statistical properties as calculated from historical, measured flow series. This assumed stationarity has to be rejected if the greenhouse effect is accepted as the main underlying cause for current and future global climate trends. Hence, new methods for estimating future runoff must be devised and the methodology should take into account an increased risk with different statistical characteristics from that presently assumed.

As explained in Section 2.2 about the hydrology of Iceland, the flows in Icelandic rivers can be classified into three categories, direct-runoff, glacial runoff and groundwater flows (*cf.* Fig. 2). Figure 42 shows the different patterns of inflow into the two largest reservoirs of the Icelandic power system. The left graph shows the partial inflow to lake Þórisvatn in SW-Iceland where glacial inflows are filtered out by an upper albeit small reservoir. The inflow is characterised by a considerable groundwater

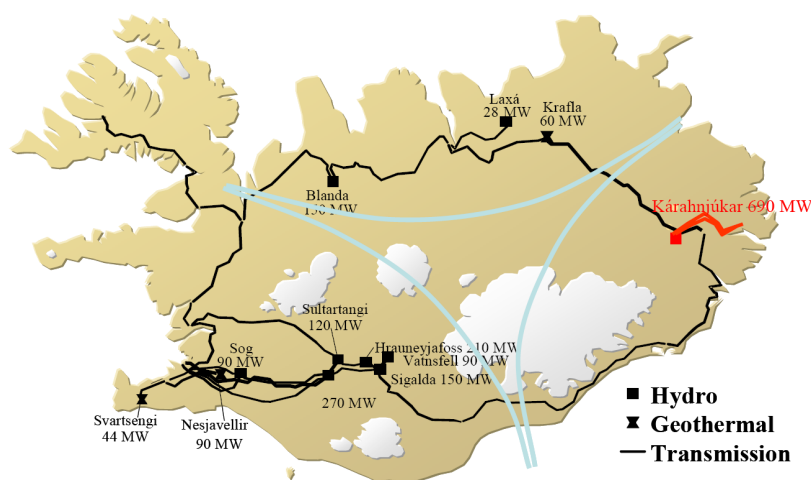


Figure 41: Key components of the Icelandic power system.

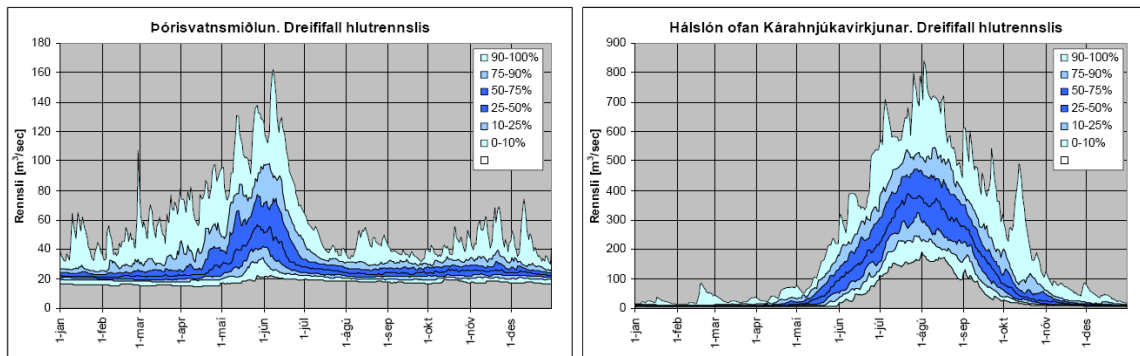


Figure 42: Different flow regimes. Left: Partial inflow Þórisvatn reservoir in the SW-Iceland. Right: Inflow to Háslón reservoir in the E-Iceland.

component and surface flows dominated by snowmelt in late winter and spring. Mid-winter peaks due to snowmelt are also common. The right hand side graph shows the inflow to the Háslón reservoir in E-Iceland with practically no ground water component and with surface flows dominated by glacial melting in late summer and autumn. Mid-winter snowmelt peaks are small and rare. Although all those components are present to some extent in all the three regions, glacial flows are most pronounced in the East and groundwater in the South-West.

The business of the hydropower industry is transport of energy from the rivers into storage reservoirs, where possible, and finally to the consumer through power plants and transmission facilities. Components of this system are expensive and their size is often carefully optimised to give the most economical performance under prevailing hydrological conditions. The most important flow properties, seasonal fluctuations and frequency are emphasized in Figure 42. The changes caused by global warming as foreseen now alter the outcome of the optimisation. These changes are more pronounced where glacial flows are dominant (highly temperature dependent) than for other types of flows, and thus different components are differently affected.

Looking first at storage reservoirs, the importance of those might be diminished somewhat where snowmelt is a decisive component, as in the Nordic countries. Shorter snow accumulation period and more frequent mid-winter warm spells result in more even or regulated inflow into storage reservoirs and thus lead to a shortening of the release period. Glacial flows on the other hand might with increased temperature become so much more intense in late summer and autumn that more storage capacity would actually be needed if the intention would be to harness the additional glacial runoff. Glacial melting in warm mid-winter spells will for large part continue to percolate into the winter snowpack on the glacier where it is refrozen instead of causing mid-winter floods.

In the planning and designing of new power plants, tunnels and other waterways that are difficult to enlarge should be planned for future rather than present flows. The powerhouse may have to be designed to accommodate larger turbines than presently economical or the layout might be such that expansions are easily constructed. Considerations for dam safety and spillway design might require considerable foresight.

Thermal power, fossil and nuclear stations are conveniently built close to industrial centers and large cities, while hydropower stations may be in remote regions needing a long and strong transmission network for transport to the market. The same holds true for wind power and wave power when that becomes economical. Adjustments of the transmission network to accommodate possible changes in the power production of remote existing plants might create some challenges in the future.

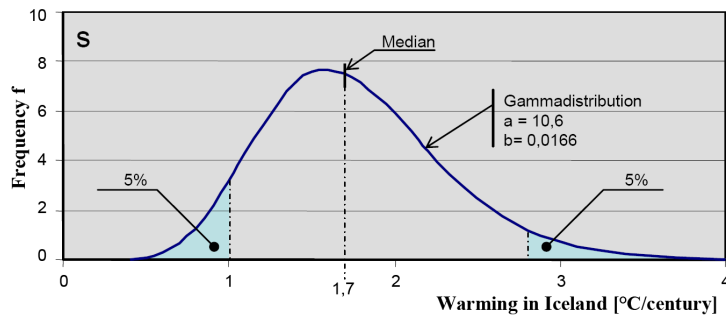


Figure 43: Statistical distribution of temperature trends in Iceland from middle of the 20<sup>th</sup> century and a decade into the 21<sup>th</sup> century in °C per century.

### 7.3 Magnitude of the climate trend

The CE/VO climate change scenario described in Section 3 may be used to make a first assessment of the magnitude of future river runoff changes at Icelandic power projects. The temperature scenario indicates from 2.5 to 3° C warming in the Icelandic highlands over a hundred and ten year period. This may be expected to lead to substantial changes in the seasonality and magnitude of surface and glacial runoff into the storage reservoirs of the power system. This estimated temperature change and its impacts on glacial runoff in addition to potential precipitation changes need to be accounted for in simulations of the Icelandic power system for future planning.

According to estimates of global warming, one may expect a comparatively slow human-induced development of the climate in the latter half of the last century, accelerating in the early half of the 21<sup>th</sup> century and then gradually decelerating after that. This indicates that within a normal planning horizon, *e.g.* planning for the period 2010–2015, and for interpretation of past runoff time-series as described below, one would generally use lower values for the warming rate than those described in Section 3 which are intended as averages for the whole period from 1961–1990 to 2071–2100.

The uncertainty of any quantitative estimate of future climate trends is clearly quite large. Indications of the spread of this estimate can be found in the Stern Review Report (Stern, 2006) and point to a distribution skewed upwards. The spread of trends for the years say 1950 to 2010 or 2015 is, however, much smaller than should be expected for the latter part of the century. In the former case, the period is mostly historical while in the latter case possible countermeasures to reduce greenhouse gas emissions or failure thereof contribute to additional uncertainty in addition to the uncertainty of the modelled temperature change.

Figure 43 depicts an estimate of the statistical distribution of warming rates for the Icelandic highlands for the period 1950 to 2010 or 2015 based on the above reasoning (hence the choice of the gamma distribution). It assumes a somewhat lower median warming rate than the CE/VO scenario and postulates that this warming rate is uncertain by almost a factor of two as indicated by the width of a 90% confidence interval. Although this distribution could lead to reasonable estimates of the mean and variance of present climate trends, care should be taken if the intention is to estimate trends for the next few decades. It would be more appropriate to use the CE/VO scenario for estimation of climate trends in the near future.

### 7.4 Runoff series

The runoff series used in Iceland for estimating power production capabilities are constructed using a series of conceptual hydrological watershed models created and maintained by the engineering firm Vatnaskil ehf. The models are calibrated using all available measurements of flow, precipitation,

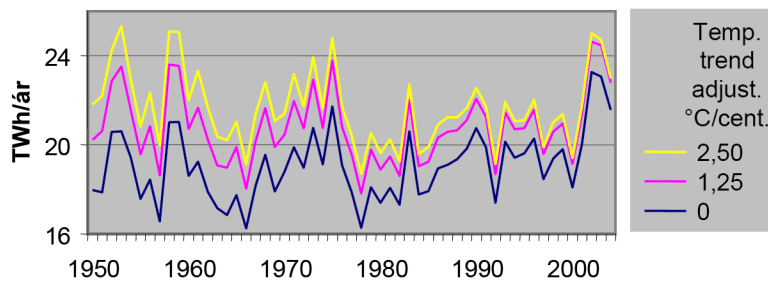


Figure 44: Possible energy supply in the runoff to power stations in Iceland as measured and adjusted for climate trends.

groundwater level and temperature. The calibrated models are then used to create flow series from 1950 for simulation purposes (Jóhannsson, 2006a). These models differ from most other hydrological models in the sense that they contain rather sophisticated 3D sub-models of groundwater flow.

Figure 44 shows the energy that could be extracted from the runoff series with unlimited market and the current installed power capacity in the present power stations. Three cases are shown, that is a baseline case using the 1950–2004 runoff series generated using historical data as an input into the conceptual hydrological models and two cases with assumed seasonal warming trend of 50% and 100%, respectively, of the CE/VO scenario (Jóhannsson, 2006b). More precisely, the historical temperature records from 1950–2004, that are used as input into the hydrological models, are de-trended with respect to the year 2010 by adding a 60 year warming trend to the year 1950, a 59 year warming trend to the year 1951, *etc.*, and a 6 year warming trend to the year 2004. The results are 55 years of runoff that can be considered approximately stationary with respect to the planning year 2010. As seen in the figure, there is a positive trend in runoff for the baseline case and that trend is statistically significant. For the two warming cases, the smaller warming trend of 1.25° C per century results in runoff series with a positive trend while the larger warming trend of 2.5° C per century results in runoff series with negative trend, neither trend is statistically significant. Based on these results, the expected seasonal warming rate for de-trending of historical time series in the Icelandic highlands for short term future planning should be in the range 1.25 and 2.5° C per century.

## 7.5 Risk analysis

In order to determine the load that can be scheduled for the power system in 2010 without an unacceptable risk we fix the load and use simulations to estimate the expected generation costs for different climatic trends from 1950 to 2010. The same procedure may then be repeated for a different load scenario *etc.* Figure 45 shows the results for a load scenario that is quite a bit higher than presently estimated for three possible of climatic trends. For each assumed trend, the 55 years of costs are ordered from highest to lowest obtaining a series of cost curves as shown in the figure. In the baseline case of no trend adjustment being made, very high costs are obtained, but very low if the seasonal trends corresponding to the full amplitude of the CE/VO scenario are assumed (annual average 2.5° C per century). The cost curves can then be added or weighted using the frequency function of Figure 43 to obtain a risk curve for estimation of optimum load based on different company-dependent specific criteria.

Alternatively, it is possible using conventional methods to calculate the power production capability attributable to each hypothetical climate trend to obtain a curve as shown in Figure 46. Based on Landsvirkjun's underlying assumptions and criteria, the preliminary risk analysis resulting in the curve shown Figure 46, would result in Landsvirkjun accepting power production capability for the year



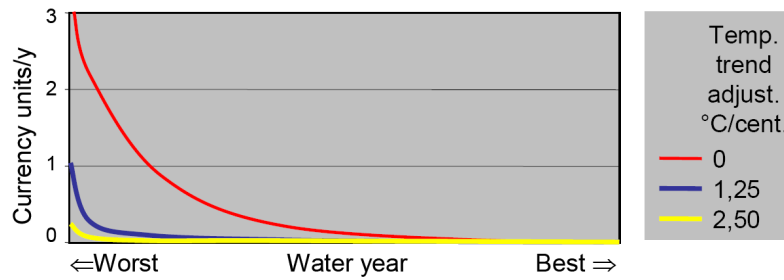


Figure 45: Generation costs obtained for a given load scenario for three possible climate trends from 1950 to 2010.

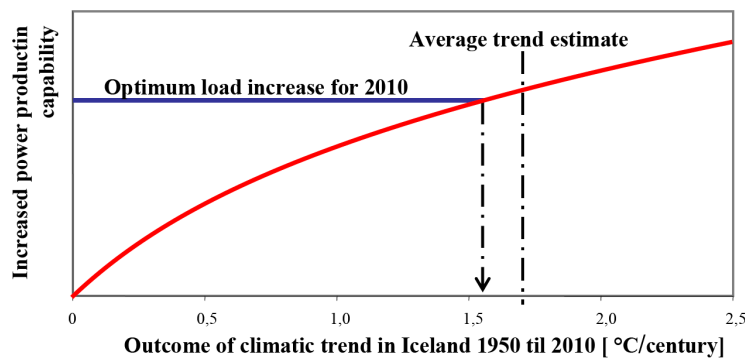


Figure 46: Power production capability as function of climatic trend.

2010 based on an assumed trend of  $1,56^{\circ}\text{C}$  per century (close to the mode of the gamma distribution in Figure 43).

## 7.6 Concluding remarks

Assuming future flows as stationary and ergodic extension of measured runoff series is no longer a probable scenario in a warming climate. For future planning, the use of uncorrected historical time-series may not be realistic and there is a need for developing mechanisms for adjustment of historical time-series based on historical and future trends in climate. Methods for sophisticated risk analysis accounting for climate change need be explored and extensively used.

Projections of future climate need to be utilised to develop business strategies for decisions on future hydropower development and for estimation of the impact on the existing hydropower installations. It has been demonstrated here how historical time series can be adjusted to make them suitable for use to support decisions about installations that will operate in a future climate. The uncertainty of such adjustments is closely related to the uncertainty of future climate scenarios.

Large-scale collaboration of the Nordic countries involving scientific institutions and companies and hydropower companies (as done in the CE project) results in procedures that are widely accepted. Such collaboration is further enhanced in the joint case studies that have been carried out for all countries involved, where the regional impact caused by potential climate change is estimated in a consistent manner and compared across the regions/countries. This also makes it possible to test the proposed procedures in different types of business environments and for different types of hydropower installations.



## 8 Summary and conclusions

Future climate change is likely to have pronounced effects on the hydrology and hydro-resources of Iceland. Some of the changes in the climate and hydrology of the country that have recently taken place are likely to be partly due to global greenhouse-induced climate change. The most conspicuous changes in this connection are a warming of more than 1° C over the last 20–30 years and an accelerating retreat of glacier margins since around the year 2000. Significant trends in precipitation have, on the other hand, not been observed. These changes are already impacting the design and operating environment of many constructions, such as hydropower plants, buildings in coastal areas, bridges and roads, and various institutes and government bodies are beginning to take them into account in practical design and operating decisions.

The main results of the VO research project as described in the preceding sections may be summarised as follows.

### Time-series

- The climate of Iceland has warmed by approximately 1.5° C since the latter part of the 19<sup>th</sup> century (based on a 10-year weighted running average of temperature time-series). It is likely that part of this warming is due to global warming. Warming during the last 20–30 years has been very rapid, much more rapid than is expected from scenarios of global warming or regional scenarios for the northern N-Atlantic region. The recent, rapid warming is likely to be partly related to a natural variation associated with a rebound from the cool 1970s and 1980s.
- Precipitation records since around 1900 are characterised by substantial decadal variations but precipitation does not show a distinct long-term trend.
- Discharge is characterised by substantial decadal variations, but trends turn out to be strongly dependent on the study period. An increase in the discharge of glacial rivers has recently taken place and there is a tendency for increased summer discharge in some non-glacial rivers.

### Precipitation modelling

- New precipitation maps of Iceland have been made based on meteorological simulations and hydrological and glaciological observations. The area-averaged, mean annual precipitation in Iceland in the reference period 1961–1990 is found to be in the range 1650–1800 mm y<sup>-1</sup>.
- The simulated area-averaged, annual precipitation time-series is characterised by similar decadal variations as observed precipitation and does not show a distinct long-term trend.
- Distributed data sets of daily precipitation on 1 × 1 km and 8 × 8 km grids for the period 1958–2006 have been generated and may be used for detailed runoff modelling of any watershed in Iceland.

### Climate change

- A climate change scenario for Iceland was defined based on a downscaling of coupled, global atmosphere–ocean simulations using the A2 and B2 emission scenarios.
- The temperature scenario specifies a 2.8° C annual average warming from 1961–1990 to 2071–2100, with the highest warming in the spring and fall.

- The precipitation scenario specifies a modest increase in annual precipitation of less than 10% on average for the whole of Iceland between 1961–1990 to 2071–2100. The change in precipitation varies from one part of the country to another and between seasons.
- The climate change scenario is only one out of a large number of possible scenarios which could be defined on the basis of the many global simulations and downscalings that are available. The statistical uncertainty of this scenario has not been explicitly assessed but it is considered a reasonable projection of the long-term climate development in Iceland over the next 100 years. Needless to say, there is a large uncertainty associated with the scenario.

### **Glacier modelling**

- Coupled mass balance/dynamic models of Langjökull, Hofsjökull and S-Vatnajökull indicate that the volume of the ice caps will be reduced by more than half within the next 100 years and that glaciers and ice caps in Iceland will essentially disappear in 100–200 years from now.
- Around 2030, annual average runoff from the areas currently covered by these ice caps is projected to have increased by approximately  $1.5\text{--}2.5 \text{ m}_{\text{w.e.}} \text{ y}^{-1}$  with respect to the runoff around the year 1990.
- The runoff increase reaches a comparatively flat maximum between 2025 and 2075 when the increasing contribution from the negative mass balance is nearly balanced by the counteracting effect due to the diminishing area of the ice caps.
- The response of the ice caps depends considerably on their altitude distribution. The downwasting of the lower and thinner Langjökull is projected to be more rapid than for the higher and thicker Hofsjökull and S-Vatnajökull.

### **Runoff modelling**

- A distributed runoff model forced by a meteorological model was calibrated and used to create a new runoff map for all of Iceland for the reference period 1961–1990. The average, annual runoff for this period was estimated to be  $4770 \text{ m}^3 \text{ s}^{-1}$  or  $1460 \text{ mm y}^{-1}$ . Average, annual evapotranspiration was simulated as  $280 \text{ mm y}^{-1}$ .
- Runoff is projected to increase by approximately 25% on average between 1961–1990 and 2071–2100, mainly due to increased melting of glaciers.
- The seasonality of runoff and flood characteristics are projected to change. There will in general be more autumn and winter runoff, and spring floods will be earlier and most likely smaller in amplitude.
- Subglacial watercourses and therefore outlet locations of glacial rivers are likely to change as a consequence of the thinning of ice caps and the retreat of glacier margins.
- A substantial increase in gravitational potential hydropower is projected.

### **Energy production**

- The use of uncorrected historical time-series may not be a realistic procedure for future planning in the energy sector. There is a need for developing mechanisms for adjustment of historical time-series based on historical and future trends in climate.

- Projections of future climate need to be utilised in decisions about future hydropower development and for estimation of the impact on the existing hydropower installations.

Hydropower is the most important renewable source of electricity in Iceland and it is the renewable energy source most strongly affected by climate. The results from the CE and VO projects show that this impact can be quite strong. Global warming will shorten the winter season, make it less stable and lengthen the ablation season on glaciers and ice caps. This leads to a more evenly distributed river flow the year around, a profitable situation for the industry.

There is also potential for increased hydropower production as the highest modelled increase in river flow is simulated in highland areas that are most important for hydropower. This implies that the projected hydrological changes may be expected to have practical implications for the design and operation of many hydropower plants, and also for other use of water, especially from glaciated highland areas.

One negative side is that the new annual rhythm in runoff indicated in the simulations will put more stress on spillways. They will probably have to be operated more often in winter as the unstable winter climate will generate more frequent sudden inflows when reservoirs may be full. This will also have an impact on the infrastructure with more frequent flooding problems downstream of the reservoirs. These areas are normally adapted to the present-day climate with stable winters and without high flows from autumn to spring.

In summary, the power industry will have to develop a new strategy characterised by flexibility because it must be possible to adapt the operation and even the design of power plants as climate change leads to changes in the discharge and seasonality and other hydrological characteristics. Continued research on climate change is essential to address the added uncertainty with which the industry is faced due to this situation and in order to supply the necessary information for proper adaptation to the evolving climate.



## 9 Suggestions for further research

Collaborative, Nordic research of the effect of climate change on renewable energy resources will continue in the “Climate and Energy Systems” (CES) project in the years 2007–2010 as mentioned in the introduction. This new research project will focus on changes in the period 20–40 years from now (*i.e.* in the period ca. 2030–2050). There will be less emphasis on changes with respect to a baseline period such as 1961–1990 than in the earlier CE project. Transient simulations will be carried out based on several alternative climate change scenarios spanning a range of possible future changes. Changes will be reported with respect to earlier periods such as 1961–1990, 1971–2000 or 1981–2000 with due respect to the fact that human-induced climate changes were probably already having a considerable effect on the climate during those periods.

The CES project will be complemented with national research projects in each participating country. The following paragraphs suggest focus points for research to be carried out in Iceland as a part of the new CES project and national projects in this field.

**Time-series** Time-series analyses will focus on the following points.

- The database of Nordic streamflow data will be updated with data until 2005.
- Variability in regional index series ( $P$ ,  $T$ ,  $Q$ )—monthly, seasonal and annual.
- Variability in extreme rainfall and flood frequency and intensity.
- Application of Bayesian techniques in flood frequency analysis.
- Variability in drought.
- Extreme value analysis, also linked to dam safety.
- Comparison of the last 10–15 years with the reference period (1961–1990) and scenarios.
- Studies of cyclic behaviour ( $P$ ,  $T$ ,  $Q$ ).
- Adjustment methods for input to Energy Systems Analysis.
- Uncertainty assessment.
- A distributed data set of daily temperature on a  $1 \times 1$  km grid will be derived from observations for the period 1949–2007.

**Precipitation modelling** The development of high-resolution, distributed precipitation models for Iceland will be continued.

- The LT model will be modified to run with 6-hourly time-resolution and time-varying parameterisation. The use of higher resolution ECMWF weather forecast analyses as input fields after 2002 will be further tested.
- The LT and MM5 models will be validated with precipitation observations from meteorological stations, and hydrological and glaciological data. Glaciological mass-balance data from other glaciers than Langjökull, Hofsjökull and Vatnajökull are important in this connection as they have not been used in the calibration of the models and therefore constitute an independent test of the model realism.

**Climate change** New and more diversified climate scenarios with shorter time horizon than in the earlier CE project will be used. The scenarios will be defined by dynamical downscaling of several global atmospheric simulations for the N-Atlantic region. The scenarios will cover several alternative emission scenarios.

The results obtained in the CE and VO projects underline the large spatial as well as a temporal variability of the climate. This is in particular true for precipitation, but it is also true for winds and temperature. Moving towards even higher spatial resolutions in describing past and future climate is therefore a very feasible option for future research. Dynamic and semi-dynamic downscaling of climate simulations should be undertaken for selected areas where a large spatial variability can be expected.

- To provide a coherent and consistent analysis, of a new generation of regional climate scenarios for the Nordic region, expressed in terms of ranges and conditional probabilities for the period of 2010–2050. Both climate change signals and climate variability will be addressed.
- Together with numerical efforts, there is an increasing need for observations at high spatial resolutions, particularly for precipitation and winds in complex terrain and vertical profiles of winds and temperatures.
- Further assessment of the natural variability of the elements of climate and the interaction of atmospheric processes at different spatial scales is needed.
- There is a need for the development of indices linking output from climate simulations to extreme events that may occur as a consequence of a complex combination of more than one meteorological parameter. Such events include for instance extremes in runoff, avalanches, mud flows and atmospheric icing. These efforts should be undertaken as a part of the exploitation of available regional downscaling of outputs from general circulation models.

**Glacier studies** The work will be concerned with modelling of glacier mass balance and ice flow dynamics in order to determine the response of glaciers and ice caps to climate change as specified by the climate scenarios defined in CES.

- Mass balance data sets collected in the CWE and CE projects will be extended to form the basis of the glacier mass-balance modelling. A special effort will be made to collect existing data on mass balance of Mýrdalsjökull, Drangajökull, glaciers in Tröllaskagi, as well as older data from Vatnajökull from before 1991.
- Degree-day mass-balance models with distributed precipitation will be calibrated for Vatnajökull, Hofsjökull and Langjökull. These models will be used to produce estimates of winter precipitation at stake locations on the ice caps, corrected to take liquid precipitation and/or winter ablation into account.
- An attempt will be made to develop a 2D glacier model that represents the role of sliding and surges (using subglacial water pressure) for the long-term geometry and dynamics of the surge-type outlet glaciers of N- and W-Vatnajökull.
- Dynamic 2D model simulations will be made for Vatnajökull, Hofsjökull and Langjökull. The effect of ice divide migration on runoff changes from the ice caps will be specially studied.
- Modelled changes in glaciated area and changes in the area distribution of the ice surface will be given to the hydrological modelling group as input for runoff modelling.
- Melt model parameters determined in the glacier modelling will also be reported to the hydrological modelling group for consideration in the calibration of hydrological models.



**Runoff modelling** The distributed WaSiM runoff model for Iceland, which was set up in the CE project, will be further developed.

- The groundwater module of the model will be configured and calibrated so that the arbitrary scaling of precipitation that is used in the current model configuration can be abandoned (*cf.* Section 6).
- Several transient runoff simulations until 2050 will be made based on different climate change scenarios.
- The orographic precipitation models of Iceland, that were developed as a part of the CE project, and possibly a distributed temperature data set derived from observations, will be used as an input for a new calibration of the WaSiM model.
- A special study of changes in seasonal and diurnal runoff variations from the Hofsjökull ice cap will be made with a hybrid radiation–degree-day mass-balance model.

### **Energy systems**

- Bridge the gap between scientists and corporate planners. That is, how can the scientific results be transferred to end users?
- Utilise prediction of future climate scenarios to develop business strategies for decisions on future hydropower development and for estimation of the impacts on the existing hydropower installations.
- Create joint case studies where the procedures and the results developed are put to use in a collaboration between hydropower companies involved in the project.

## 10 Acknowledgements

This study was carried out as a part of the projects *Climate and Energy* (CE), financed by Nordic Energy Research, and *Veður og orka* (VO) funded by the National Power Company of Iceland, the National Energy Fund of Iceland, the Ministry of Industry and the National Energy Authority and the project participants: the Hydrological Service of the National Energy Authority, the Icelandic Meteorological Office, the Institute of Earth Sciences at the University of Iceland, the Institute for Meteorological Research, and Vatnskil Consulting Engineers.

## 11 References

- Aðalgeirsdóttir, G. (2003) *Flow dynamics of the Vatnajökull ice cap, Iceland*. VAW/ETH Zürich, Mitteilungen No. 181.
- Aðalgeirsdóttir, G., G. H. Guðmundsson and H. Björnsson (2005) The volume sensitivity of Vatnajökull ice cap, Iceland, to perturbations in equilibrium line altitude. *J. Geophys. Res.*, **110**, F04001, doi: 10.1029/2005JF000289.
- Aðalgeirsdóttir, G., T. Jóhannesson, H. Björnsson, F. Pálsson and O. Sigurðsson (2006) The response of Hofsjökull and southern Vatnajökull, Iceland, to climate change. *J. Geophys. Res.*, **111**, F03001, doi: 10.1029/2005JF000388.
- Andreassen, L. M., H. Elvehøy, T. Jóhannesson, J. Oerlemans and S. Beldring (2006) Changes in runoff from glaciated areas due to climate change. Case studies of Storbreen and Engabreen, Norway. *Proc. The European Conference of Impacts of Climate Change on Renewable Energy Sources, Reykjavík, Iceland, June 5–6*.
- Barstad, I., and R. B. Smith (2005). Evaluation of an orographic precipitation model. *J. Hydrometeorol.*, **6**, 85–99.
- Beldring, S., J. Andréasson, S. Bergström, J. F. Jónsdóttir, S. Rogozova, J. Rosberg, M. Suomalainen, T. Tønning, B. Vehviläinen and N. Veijalainen (2006) Mapping water resources in the Nordic region under a changing climate. CE Rep. No. 3, The CE Project, Reykjavík.
- Beldring, S., J. Andréasson, S. Bergström, J. F. Jónsdóttir, S. Rogozova, J. Rosberg, M. Suomalainen, T. Tønning, B. Vehviläinen and N. Veijalainen (2006) Hydrological climate change maps of the Nordic region. *Proc. The European Conference of Impacts of Climate Change on Renewable Energy Sources, Reykjavík, Iceland, June 5–6*.
- Benoit, R., P. Pellerin, N. Kouwen, H. Ritchie, N. Donaldson, P. Joe and E. D. Soulis (2000) Toward the use of coupled atmospheric and hydrologic models at regional scale. *Mon. Wea. Rev.*, **128**(6), 1681–1706.
- Bergström, S., T. Jóhannesson, G. Aðalgeirsdóttir, A. Ahlstrøm, L. M. Andreassen, J. Andréasson, S. Beldring, H. Björnsson, B. Carlsson, P. Crochet, M. de Woul, B. Einarsson, H. Elvehøy, G. E. Flowers, P. Graham, G. O. Gröndal, S. Guðmundsson, S-S. Hellström, R. Hock, P. Holmlund, J. F. Jónsdóttir, F. Pálsson, V. Radic, N. Reeh, L. A. Roald, J. Rosberg, S. Rogozova, O. Sigurðsson, M. Suomalainen, Th. Thorsteinsson, B. Vehviläinen and N. Veijalainen (2007) *Impacts of climate change on river runoff, glaciers and hydropower in the Nordic area. Joint final report from the CE Hydrological Models and Snow and Ice Groups*. CE Rep. No. 6, The CE Project, Reykjavík.
- Björnsson, F. 1998. Samtíningur um jökla milli Fells og Staðarfjalls (Glacier variations between Fell and Staðarfjall, southeastern Iceland.) *Jökull*, **46**, 49–61.
- Björnsson, H., Jónsson, T., Gylfadóttir, S. S., and E. Ó. Ólason (2007a) Mapping the annual cycle of temperature in Iceland. *Meteorolog. Zeitschr.*, **16**(1), 45–56.
- Björnsson, H., E. Ó. Ólason, T. Jónsson and S. Henriksen (2007b) Analysis of a smooth seasonal cycle with daily resolution and degree-day maps for Iceland. *Meteorolog. Zeitschr.*, **16**(1), 57–69, doi: 10.1127/0941-2948/2007/0188.
- Björnsson, H., and T. Jónsson (2003) Climate and climatic variability at Lake Mývatn. *Aquatic Ecology*, **38**(1), 129–144.
- Björnsson, H. (1986) Surface and bedrock topography of ice caps in Iceland mapped by radio echo soundings. *A. Glaciol.*, **8**, 11–18.
- Björnsson, H. (1988) *Hydrology of Ice Caps in Volcanic Regions*. Soc. Sci. Isl., Reykjavík, **45**, 139 pp.
- Björnsson, H. (1996) Scales and rates of glacial sediment removal: A 20 km long, 300 m deep trench created beneath Breiðamerkurjökull during the Little Ice Age. *A. Glaciol.*, **22**, 141–146.
- Björnsson, H., G. Aðalgeirsdóttir, S. Guðmundsson, T. Jóhannesson, O. Sigurðsson and F. Pálsson (2006) Climate change response of Vatnajökull, Hofsjökull and Langjökull ice caps, Iceland. *Proc.*

- The European Conference of Impacts of Climate Change on Renewable Energy Sources, Reykjavík, Iceland, June 5–6.*
- Björnsson, H., S. Guðmundsson and F. Pálsson (2005) Glacier winds on Vatnajökull ice cap, Iceland and their relation to temperatures of its lowland environs. *A. Glaciol.*, **42**, 291–296.
- Björnsson, H., S. Guðmundsson, T. Jóhannesson, F. Pálsson, G. Aðalgeirsdóttir and H. H. Haraldsson (2006) Geometry, mass balance and climate change response of Langjökull ice cap, Iceland. *Proc. The International Arctic Science Committee (IASC), Working Group on Arctic Glaciology, Obergurgl, Austria, Jan. 30 – Feb. 3 2006* (PDF available at “[http://www.raunvis.hi.is/~sg/La\\_obergurgl.pdf](http://www.raunvis.hi.is/~sg/La_obergurgl.pdf)”, 19 April 2006).
- Björnsson, H., F. Pálsson, M. T. Guðmundsson and H. Haraldsson (1998) Mass balance of western and northern Vatnajökull, Iceland, 1991–1995. *Jökull*, **45**, 35–58.
- Björnsson, H., F. Pálsson and S. Guðmundsson (2001) Jökulsárlón at Breiðamerkursandur, Vatnajökull, Iceland: 20<sup>th</sup> century changes and future outlook. *Jökull*, **50**, 1–50.
- Björnsson, H., F. Pálsson and H. Haraldsson (2002) Mass balance of Vatnajökull (1991–2001) and Langjökull (1996–2001), Iceland. *Jökull*, **51**, 75–78.
- Bjørge, D., J. E. Haugen, and T. E. Nordeng (2000) *Future climate in Norway. Dynamical downscaling experiments within the RegClim project*. Res. Rep. No. 103, Norwegian Meteorological Institute, Oslo, Norway.
- Bromwich, D. H., L. Bai and G. G. Bjarnason (2005) High-resolution regional climate simulations over Iceland using polar MM5. *Mon. Wea. Rev.*, **133**, 3527–3547.
- Buzzi A., N. Tartaglione and P. Malguzzi (1998) Numerical simulations of the 1994 Piedmont flood: Role of orography and moist processes. *Mon. Wea. Rev.*, **126**, 2369–2383.
- Chen, F., and J. Dudhia (2001) Coupling an advanced land-surface/hydrology model with the Penn State/NCAR MM5 modeling system. Part I: Model Implementation and sensitivity. *Mon. Wea. Rev.*, **129**, 569–585.
- Chiao, S., Y.-L. Lin and M. L. Kaplan (2004) Numerical study of the orographic forcing of heavy precipitation during MAP IOP-2B. *Mon. Wea. Rev.*, **132**, 2184–2203.
- Crochet, P. (2007) A study of regional precipitation trends in Iceland using a high quality gauge network and ERA-40. *J. Climate*, **20**(18), 4659–4677, doi: 10.1175/JCLI4255.1.
- Crochet, P., T. Jóhannesson, T. Jónsson, O. Sigurðsson, H. Björnsson, F. Pálsson and I. Barstad (2007) Estimating the spatial distribution of precipitation in Iceland using a linear model of orographic precipitation. *J. Hydrometeorol.*, **8**(6), 1285–1306.
- Curry, R., B. Dickson and I. Yashayaev (2003) A Change in the Freshwater Balance of the Atlantic Ocean over the Past Four Decades. *Nature*, **426**, 826–829.
- de Woul, M. and R. Hock (2005) Static mass balance sensitivity of Arctic glaciers and ice caps using a degree-day approach. *A. Glaciol.*, **42**, 217–224.
- de Woul, M., R. Hock, M. Braun, T. Thorsteinsson, T. Jóhannesson and S. Halldórsdóttir (2006) Firn layer effect on glacial runoff—A case study at Hofsjökull, Iceland. *Hydrological Processes*, **20**, 2171–2185, doi: 10.1002/hyp.6201.
- Dickinson, R. E., R. M. Errico, F. Giorgi and G. T. Bates (1989) A regional climate model for the western United States. *Clim. Change*, **15**, 383–422.
- Einarsson, B. (2006) *Calibration of an HBV discharge model and evaluation of future runoff for the Tasiilaq basin, east Greenland*. CE Rep. No. 4, The CE Project, Hydrological Service, National Energy Authority, Reykjavík.
- Einarsson, M. Á. (1972) *Evaporation and potential evapotranspiration in Iceland*. Icel. Meteorol. Office, Reykjavík.
- Einarsson, M. Á. (1984) *Climate of Iceland*. In: van Loon, H., ed., *Climates of the Oceans*. Elsevier, Amsterdam, 673–697.

- Eythorsson, J. (1931) On the present position of the glaciers in Iceland. Some preliminary studies and investigations in the summer 1930. Reykjavík, Vísindafélag Íslendinga **X**, 35 pp.
- Eythorsson, J. (1963) Variations of Icelandic glaciers 1931-1960. *Jökull*, **13**, 31–33.
- Federer, C. A., and D. Lash (1983) *BROOK—A hydrologic simulation model for eastern forests*. Res. Rep. No. 19, Water Resour. Res. Center, Univ. of New Hampshire, Durham.
- Fenger, J., ed. (2007) *Impacts of Climate Change on Renewable Energy Sources. Their role in the Nordic energy System. A comprehensive report resulting from a Nordic Energy Research project*. Nord 2007:003, Nordic Council of Ministers, Copenhagen, 190 pp.
- Flowers, G. E., S. J. Marshall, H. Björnsson and G. K. C. Clarke (2005) Sensitivity of Vatnajökull ice cap hydrology and dynamics to climate warming over the next two centuries. *J. Geophys. Res.*, **110**, F02011, doi: 10.1029/2004JF000200.
- Førland, E. J., P. Allerup, B. Dahlström, E. Elomaa, T. Jónsson, H. Madsen, J. Perälä, P. Rissanen, H. Vedin and F. Vejen (1996) *Manual for operational correction of Nordic precipitation data*. DNMI Report No. 24/96 Klima, 66 pp.
- Giorgi, F. (1990) On the simulation of regional climate using a limited area model nested in a general circulation model. *J. Climate*, **3**, 941–963.
- Giorgi, F., L. O. Mearns, C. Shields and L. Mayer (1996) A regional model study of the importance of local versus remote controls of the 1988 drought and the 1993 flood over the central United States. *J. Climate*, **9**, 1150–1162.
- Giorgi, F., and L. O. Mearns (1999) Introduction to special section: Regional climate modeling revisited. *J. Geophys. Res.*, **104**(D6), 6335–6352.
- Grell, G. A., J. Dudhia and D. R. Stauffer (1995) *A description of the fifth-generation Penn State/NCAR Mesoscale Model (MM5)*. NCAR Tech. Note NCAR/TN-398+STR, 138 pp.
- Gröndal, G. O. (2006) *Effect of climate change on ice conditions in Lower Þjórsá*. Report, Almenna verkfræðistofan, Reykjavík.
- Guðmundsson, S., H. Björnsson, F. Pálsson and H. H. Haraldsson (2003) *Comparison of physical and regression models of summer ablation on ice caps in Iceland*. Rep. RH-15-2003, Science Institute, University of Iceland, and National Power Company of Iceland, Reykjavík (PDF available at “<http://www.raunvis.hi.is/~sg/emodels.pdf>”, 19 April 2006).
- Guðmundsson, S., H. Björnsson, G. Aðalgeirsdóttir, T. Jóhannesson, F. Pálsson and O. Sigurðsson (2007) Different response of two similar ice caps in Iceland to climate warming. *J. Glaciol.*, submitted.
- Halldórsdóttir, S. G., F. Sigurðsson, J. F. Jónsdóttir and Þ. Jóhannsson (2006) Hydrological classification for Icelandic waters. In: Refsgaard, C., and A. L. Højberg, eds., *XXIV Nordic Hydrological Conference (Nordic Water 2006, Vingsted, Denmark, 6–9 August 2006)*, NHP Report No. **49**, Auning, Denmark, 85–91.
- Hanna, E., T. Jónsson and J. E. Box (2004) An analysis of Icelandic climate since the nineteenth century. *Int. J. Climatol.*, **24**, 1193–1210.
- Hannachi, A. (2004) *A primer for EOF analysis of climate data*. Special Report, Dept. of Meteorology, University of Reading, UK.
- Haugen, J. E., and T. Iversen (2005) *Response in daily precipitation and wind speed extremes from HIRHAM downscaling of SRES B2 scenarios*. RegClim Tech. Rep. No. 8. Norw. Meteorol. Inst., Oslo.
- Hay, L. E., M. P. Clark, R. L. Wilby, W. J. Gutowsky, Jr., G. H. Leavesley, Z. Pan, R. W. Arritt and E. S. Takle (2002) Use of Regional Climate Model Output for Hydrological Simulations. *J. Hydrometeorol.*, **3**, 571–590.
- HEC (2000) *Hydrological Modeling system (HEC-HMS) - Technical Reference Manual*. Technical report, Hydrological Engineering Center, U.S. Army Corp of Engineers, Davis, California, USA, 157 pp.

- Hisdal, H., E. Holmqvist, J. F. J. Jónsdóttir, P. Jónsson, E. Kuusisto, G. Lindström and L. A. Roald (2006) Has streamflow changed in the Nordic countries? *Climate Res.*, submitted.
- Hock, R. (1998) *Modeling of Glacier Melt and Discharge*. Diss. ETH 12430, Verlag Geographisches Institut ETH, Zürich.
- Hock, R. (1999) A distributed temperature-index ice- and snowmelt model including potential direct solar radiation. *J. Glaciol.*, **45**(149), 101–111.
- Hock, R. (2006) *Distributed melt modelling: A model intercomparison on Storglaciären, Sweden*. Unpublished report, Stockholm University.
- Hock, R., P. Jansson, P. and L. Braun (2005) Modelling the response of mountain glacier discharge to climate warming. In: Huber, U. M., H. K. M. Bugmann and M. A. Reasoner, eds., *Global Change and Mountain Regions—A State of Knowledge Overview*. Advances in Global Change Series. Springer, Dordrecht, 243–52.
- Hock, R., M. de Woul, V. Radic, Th. Thorsteinsson, T. Jóhannesson and M. Braun (2006) The response of glaciers to climate change case studies on Storglaciären and Hofsjökull. *Proc. The European Conference of Impacts of Climate Change on Renewable Energy Sources, Reykjavik, Iceland, June 5–6*.
- Hock R., V. Radic and M. de Woul (2007) Climate sensitivity of Storglaciären, Sweden: An intercomparison of mass-balance models using ERA-40 re-analysis and regional climate model data. *A. Glaciol.*, **46**, 342–348.
- Hurrell, J. W., Y. Kushnir, G. Ottersen, M. Visbeck (2003) An Overview of the North Atlantic Oscillation. In: Hurrell J.W., Y. Kushnir, G. Ottersen and M. Visbeck, eds., *The North Atlantic Oscillation: Climatic significance and environmental impact*. American Geophysical Union, Washington, DC, 1–35.
- Icelandic Meteorological Office, National Land Survey of Iceland, Science Institute, University of Iceland, and National Energy Authority (2004) A 500x500m DTM of Iceland (Available at “<http://www.os.is/cefiles/glacier/island500x500.zip>”, 20 December 2006).
- IPCC (1990) *Climate change: The IPCC Scientific Assessment*. Houghton, J. T., G. J. Jenkins, and J. J. Ephraums, eds. Cambridge University Press, Cambridge, UK, 365 pp.
- IPCC (1996) *Climate change 1995: The Science of Climate Change. Contribution of Working Group I to the Second Assessment Report of the Intergovernmental Panel on Climate Change*. Houghton, J. T., L. G. Meira Filho, B. A. Callander, N. Harris, A. Kattenberg and K. Maskell, eds. Cambridge University Press, Cambridge, UK and New York, NY, USA, 572 pp.
- IPCC (2001) *Climate Change 2001: The Scientific Basis. Contribution of Working Group I to the Third Assessment Report of the Intergovernmental Panel on Climate Change*. Houghton, J. T., Y. Ding, D. J. Griggs, M. Noguer, P. J. van der Linden, X. Dai, K. Maskell and C. A. Johnson, eds. Cambridge University Press, Cambridge, UK, and New York, NY, USA, 881 pp.
- IPCC (2007) *Climate Change 2007: The Physical Science Basis. Contribution of Working Group I to the Fourth Assessment Report of the Intergovernmental Panel on Climate Change*. Solomon, S., D. Qin, M. Manning, Z. Chen, M. Marquis, K. B. Averyt, M. Tignor and H. L. Miller, Jr., eds. Cambridge University Press, Cambridge, UK, and New York, NY, USA, 996 pp.
- Jasper, K., J. Gurtz and H. Lang (2002) Advanced flood forecasting in Alpine watersheds by coupling meteorological observations and forecasts with a distributed hydrological model. *J. Hydrol.*, **267**, 40–52.
- Jasper, K., and P. Kaufmann (2003) Coupled runoff simulations as validation tools for atmospheric models at the regional scale. *Q. J. R. Meteorol. Soc.*, **129**, 673–692.
- Jóhannesson, T. (1997) The response of two Icelandic glaciers to climate warming computed with a degree-day glacier mass-balance model coupled to a dynamic model. *J. Glaciol.*, **43**(144), 321–327.

- Jóhannesson, T., G. Aðalgeirsdóttir, A. Ahlstrøm, L. M. Andreassen, H. Björnsson, M. de Woul, H. Elvehøy, G. E. Flowers, S. Guðmundsson, R. Hock, P. Holmlund, F. Pálsson, V. Radic, O. Sigurðsson and Th. Thorsteinsson (2006) The impact of climate change on glaciers and glacial runoff in the Nordic countries. *Proc. The European Conference of Impacts of Climate Change on Renewable Energy Sources, Reykjavík, Iceland, June 5–6.*
- Jóhannesson, T., G. Aðalgeirsdóttir, H. Björnsson, C. E. Bøggild, H. Elvehøy, S. Guðmundsson, R. Hock, P. Holmlund, P. Jansson, F. Pálsson, O. Sigurðsson and Þ. Þorsteinsson (2004) *The impact of climate change on glaciers in the Nordic countries.* CWE Rep. No. 3, The CWE Project, Reykjavík.
- Jóhannesson, T., H. Björnsson, P. Crochet, F. Pálsson, O. Sigurðsson and Th. Thorsteinsson (2006) Mass balance modeling of the Vatnajökull, Hofsjökull and Langjökull ice caps. *Proc. The European Conference of Impacts of Climate Change on Renewable Energy Sources, Reykjavík, Iceland, June 5–6.*
- Jóhannesson, T., O. Sigurðsson, B. Einarsson and Th. Thorsteinsson (2006) *Mass balance modelling of the Hofsjökull ice cap based on data from 1988–2004.* Rep. OS-2006/004, National Energy Authority, Reykjavík.
- Jóhannesson, T., O. Sigurðsson, T. Laumann and M. Kennett (1995) Degree-day glacier mass balance modelling with applications to glaciers in Iceland, Norway and Greenland. *J. Glaciol.*, **41**(138), 345–358.
- Jóhannesson, T., and O. Sigurðsson (1998) Interpretation of glacier variations in Iceland 1930–1995. *Jökull*, **45**, 27–33.
- Jóhannesson, S. (2006a) *Rennslisraðir til rekstrarhermana vatnsár 1950–2004. Tölfræðilegir eiginleikar (Runoff series for simulations, 1950–2004. Stochastic properties.* Rep. by Annað veldi ehf. for Landsvirkjun, Reykjavík.
- Jóhannesson, S. (2006b) *Orkugeta raforkukerfisins og hlýnandi veðurfar (Production capability of the power system and warming climate.* Rep. by Annað veldi ehf. for Landsvirkjun, Reykjavík.
- Johns, T. C., J. M. Gregory, W. J. Ingram, C. E. Johnson, A. Jones, J. A. Lowe, J. F. B. Mitchell, D. L. Roberts, D. M. H. Sexton, D. S. Stevenson, S. F. B. Tett and M. J. Woodageet (2003) Anthropogenic climate change for 1860 to 2100 simulated with the HadCM3 model under updated emission scenarios. *Clim. Dyn.*, **20**, 583–612, doi: 10.1007/s00382-002-0296-y.
- Jónasson, K. (2004) Spá um meðalhita í Reykjavík á 21. öld (Projection of mean temperature in Reykjavík in the 21<sup>st</sup> Century). *Raust*, **2**(4), 25–40.
- Jónasson, K., and T. Jónsson. 1997. *Fimmtíu ára snjódýpt á Íslandi (50-year snow depth in Iceland).* Icel. Meteorol. Office, rep. 97025.
- Jónsdóttir, J. F. (2007) *Water resources in Iceland—Impacts of climate variability and climate change.* Dept. of Water Resources Engineering, Lund Institute of Technology, Lund University, ISBN 978-91-628-7227-4.
- Jónsdóttir, J. F. (in press). A runoff map based on numerically simulated precipitation and a projection of future runoff in Iceland. *Hydrol. Sci. J.*
- Jónsdóttir, J. F., P. Jónsson and C.B. Uvo (2006) Trend analysis of Icelandic discharge, precipitation and temperature series. *Nord. Hydrol.*, **37**(4–5), 365–376.
- Jónsdóttir, J. F., and C. B. Uvo (2007) Long-term variability in precipitation and streamflow in Iceland and relations to atmospheric circulation. *Int. J. Climatol.*, revised.
- Jónsdóttir, J. F., C. B. Uvo and R. T. Clarke (2007) Trend analysis in Icelandic discharge, temperature and precipitation series by parametric methods. *Nord. Hydrol.*, under revision.
- Jónsdóttir, J. F., and J. S. Þórarinnsson (2004) *Comparison of HBV models, driven with weather station data and with MM5 meteorological model data.* Rep. OS-2004/17, National Energy Authority, Reykjavík.
- Jónsson, T. (1994) Precipitation in Iceland 1857–1992. In: Heino, R., ed., *Climate variations in Europe.* Publications of the Academy of Finland, **3/94**, Painatuskeskus, Helsinki, 183–188.

- Jónsson, T. (2002) *Langtímasveiflur I: Snjóhula og snjókoma (Long term variations II: Snowcover and snowfall)*. Icel. Meteorol. Office, rep. 02035.
- Jónsson, T. (2003) *Langtímasveiflur II: Úrkoma og úrkomutíðni (Long term variations II: precipitation and frequency of precipitation)*. Icel. Meteorol. Office, rep. 03010.
- Jónsson, T., and M. Miles (2001) Anomalies in the seasonal cycle of sea level pressure in Iceland and the North Atlantic oscillation. *Geophys. Res. Lett.*, **28**, 4231–4234.
- Kállberg, P., A. Simmons, S. Uppala and M. Fuentes (2004) *The ERA-40 archive ECMWF ERA-40*. Project Report Series No. 17, European Centre for Medium Range Weather Forecasts, Reading, England.
- Kjartansson, G. (1945) Íslenzkar vatnsfallstegundir. *Náttúrufræðingurinn*, **15**(3), 113–126.
- Klok, E. J., K. Jasper, K. P. Roelofsma, J. Gurtz, A. Badoux (2001) Distributed hydrological modelling of a heavily glaciated Alpine river basin. *Hydrol. Sci. J.*, **46**(4), 553–570.
- Kunstmann, H., and C. Stadler (2005) High resolution distributed atmospheric-hydrological modeling for Alpine catchments. *J. Hydrol.*, **314**, 105–124.
- Kuusisto, E. (2003) *Climate, Water and Energy. A summary of a joint Nordic project 2002–2003*. CWE Rep. No. 4, The CWE Project, Chiefs of the Hydrological Institutes in the Nordic Countries, Nordic Council of Ministers, Nordic Energy Research, Reykjavík.
- Liang, X.-Z., L. Li and K. E. Kunke (2004) Regional climate model simulation of U.S. precipitation during 1982–2002. Part I: Annual cycle. *J. Climate*, **17**, 3510–3529.
- Lorentz, E. N. (1956) *Empirical orthogonal functions and statistical weather prediction*. Report No. 1, Statistical forecasting project, Dept. of Meteorol., MIT.
- Marshall, S. J., H. Björnsson, G. E. Flowers and G. K. C. Clarke (2005) Simulation of Vatnajökull ice cap dynamics. *J. Geophys. Res.*, **110**, F03009, doi: 10.1029/2004JF000262.
- Meehl, G. A., T. F. Stocker, W. D. Collins, P. Friedlingstein, A. T. Gaye, J. M. Gregory, A. Kitch, R. Knutti, J. M. Murphy, A. Noda, S. C. B. Raper, I. G. Watterson, A. J. Weaver and Z.-C. Zhao (2007) Global Climate Projections. In: Solomon, S., D. Qin, M. Manning, Z. Chen, M. Marquis, K. B. Averyt, M. Tignor and H. L. Miller, Jr., eds., *Climate Change 2007: The Physical Science Basis. Contribution of Working Group I to the Fourth Assessment Report of the Intergovernmental Panel on Climate Change*. Cambridge University Press, Cambridge, UK, and New York, NY, USA.
- Meier, F. M., M. B. Dyurgerov, U. K. Rick, S. O’Neel, W. T. Pfeffer, R. S. Anderson, S. P. Anderson and A. F. Glazovsky (2007) Glaciers Dominate Eustatic Sea-Level Rise in the 21<sup>st</sup> Century. *Science*, **317**, 1064–1067, doi: 10.1126/science.1143906.
- Nakicenovic, N., and R. Swart, eds., (2000) *Emissions Scenarios. A Special Report of Working Group III of the Intergovernmental Panel on Climate Change*. Cambridge University Press, UK, 570 pp.
- Nash, J. E., and J. V. Sutcliffe (1970) River flow forecasting through conceptual models part I—A discussion of principles, *J. Hydrol.*, **10**(3), 282–290.
- Nick, F. M., J. van der Kwast and J. Oerlemans (2007) Simulation of the evolution of Breiðamerkurjökull in the late Holocene. *J. Geophys. Res.*, **112**, B01103, doi: 10.1029/2006JB004358.
- Ogilvie, A. E. J., and T. Jónsson (2001) “Little ice age” research: A perspective from Iceland. *Climatic Change*, **48**(1), 9–52, doi: 10.1023/A:1005625729889.
- Ólafsson, J. (1999) Connections between oceanic conditions off N-Iceland, Lake Mývatn temperature, regional wind direction variability and the North Atlantic Oscillation. *Journal of the Icelandic Marine Research Institute (Rit Fiskideildar)*, **16**, 41–57.
- Ólafsson, H., og T. Arason (2007) Observed trends in the orographic precipitation gradient, Proc. Int. Conf. Alpine Meteorol. 2005, 23–27 May 2005, Zadar, Croatia (ICAM), *Croatian Meteorol. Journ.*, **40**.
- Paterson, W. S. B. (1994) *The Physics of Glaciers*. 3<sup>rd</sup> ed., Elsevier, New Youk, 480 pp.
- Pálsson, F., E. Magnússon and H. Björnsson (2002a) *The surge of Dyngjujökull 1997–2000. Mass transport, ice flow velocities, and effects on mass balance and runoff*. Reykjavík, Science Institute,



- RH-01-2002.
- Pálsson, F., H. Björnsson, H. H. Haraldsson and E. Magnússon (2002b) *Afkomu- og hraðamælingar á Langjökli jökulárið 2001–2002*. Reykjavík, Science Institute, RH-26-2002.
- Pálsson, F., H. Björnsson and E. Magnússon (2004a) *Afkomu- og hraðamælingar á Langjökli jökulárið 2003–2004*. Reykjavík, Science Institute, RH-18-2004.
- Pálsson, F., H. Björnsson and H. H. Haraldsson (2004b) *VATNAJÖKULL: Mass balance, meltwater drainage and surface velocity of glacial year 2001–2002*. Reykjavík, Science Institute, RH-21-2004.
- Pálsson, F., H. Björnsson, E. Magnússon and H. H. Haraldsson (2004c) *VATNAJÖKULL: Mass balance, meltwater drainage and surface velocity of glacial year 2002–2003*. Reykjavík, Science Institute, RH-22-2004.
- Pálsson, F., H. Björnsson, E. Magnússon and H. H. Haraldsson (2004d) *VATNAJÖKULL: Mass balance, meltwater drainage and surface velocity of the glacial year 2003–2004*. Reykjavík, Science Institute, RH-23-2004.
- Pálsson, H., Ó. Rögnvaldsson and H. Ólafsson (2005) *Calculations of predicted precipitation changes in Iceland*. Inst. Meteorol. Res., Tech. memo.
- Qian, J.-H., A. Seth and S. Zebiak (2003) reinitialized versus continuous simulations for regional climate downscaling. *Mon. Wea. Rev.*, **131**, 2857–2874.
- Philip, J. R. (1969) The theory of infiltration. In: Chow, V. T., ed., *Advances in Hydrosciences*, 216–296. Academic Press, New York.
- Phillips, I. D., and J. Thorpe (2006) Icelandic precipitation—North Atlantic sea-surface temperature associations. *Int. J. Climatol.*, **26**, 1201–1221, doi: 10.1002/joc.1302.
- Radic, V. and R. Hock (2006) Modelling mass balance and future evolution of glaciers using ERA-40 and climate models—A sensitivity study at Storglaciären, Sweden. *J. Geophys. Res.*, **111**, F03003, doi: 10.1029/2005JF000440.
- Radic, V. (2006) *Modeling future sea level rise from the retreat of glaciers*. Licentiat thesis, Department of Physical Geography and Quaternary Geology, Stockholm university.
- Richards, L. A. (1931) Capillary conduction of liquids through porous medium. *Physics*, **1**, 318–333.
- Rist, S. (1956) *Íslensk vötn (Icelandic fresh waters)*. Raforkumálastjóri, Vatnamælingar, Reykjavík, Iceland.
- Rist, S. (1990) *Vatns er þörf (a general description of the hydrology of Iceland)*. Menningarsjóður, Reykjavík, 248 pp.
- Rummukainen, M. (2006) The CE regional climate scenarios. *Proc. The European Conference of Impacts of Climate Change on Renewable Energy Sources, Reykjavík, Iceland, June 5–6*.
- Rögnvaldsson, Ó., P. Crochet and H. Ólafsson (2004) Mapping of precipitation in Iceland using numerical simulations and statistical modeling. *Meteorol. Zeitschrift*, **13**(3), 209–219, doi: 10.1127/0941-2948/2004/0013-0209.
- Rögnvaldsson, Ó., and H. Ólafsson (2005) The response of precipitation to orography in simulations of future climate. Proc. Int. Conf. Alpine Meteorol. 2005, 23–27 May 2005, Zadar, Croatia (ICAM), *Croatian Meteorol. Journ.*, **40**, 526–529.
- Rögnvaldsson, Ó., J. F. Jónsdóttir and H. Ólafsson (2007) Numerical simulations of precipitation in the complex terrain of Iceland—Comparison with glaciological and hydrological data. *Meteorol. Z.*, **16**(1), 71–85.
- Salas, J. D. (1993) Analysis and modeling of hydrologic time series. In: Maidment, D. R., ed., *Handbook of Hydrology*. McGraw-Hill, New York, chapter 19.
- Schuler, T., R. Hock, M. Jackson, H. Elvehøy, M. Braun, I. Brown and J.-O. Hagen (2005) Distributed mass balance and climate sensitivity modelling of Engabreen, Norway. *A. Glaciol.*, **42**, 395–401.
- Schulla, J., and K. Jasper (2001) *Model description WaSiM-ETH*. Available at “<http://www.iac.ethz.ch/~staff/verbunt/Down/WaSiM.pdf>”.

- Serreze, M. C., F. Carse, R. G. Barry (1997) Icelandic Low cyclone activity: Climatological features, linkages with the NAO, and relationships with recent changes in the Northern Hemisphere circulation. *J. Climate*, **10**(3), 453–464, doi: 10.1175/1520.
- Sigurðsson, O., and Ó. J. Sigurðsson (1998) *Afkoma nokkurra jökla á Íslandi 1992–1997 (Mass balance of a number of Icelandic glaciers 1992–1997)*. Rep. OS-98082 (in Icelandic), National Energy Authority, Reykjavík.
- Sigurðsson, O. (1998) Glacier variations in Iceland 1930–1995—From the database of the Iceland Glaciological Society. *Jökull*, **45**, 3–25.
- Sigurðsson, O. (2005) Variations of termini of glaciers in Iceland in recent centuries and their connection with climate. In: Caseldine, C., A. Russell, J. Harðardóttir and Ó. Knudsen, eds., *Iceland—Modern processes and past environment*. Elsevier, Amsterdam, 241–255 and 408.
- Sigurðsson, O., T. Jónsson and T. Jóhannesson (2007) Relation between glacier-termini variations and summer temperature in Iceland since 1930. *A. Glaciol.*, **42**, 395–401.
- Sigurðsson, O., Th. Thorsteinsson, S. M. Ágústsson and B. Einarsson (2004) *Afkoma Hofsjökuls 1997–2004. (Mass balance of Hofsjökull 1997–2004.)* Rep. OS-2004/029, National Energy Authority, Reykjavík.
- Smith, R. B., and I. Barstad (2004) A linear theory of orographic precipitation. *J. Atmos. Sci.*, **61**, 1377–1391.
- Smith, W. H. F., and P. Wessel (1990) Gridding with continuous curvature splines in tension. *Geophysics*, **55**, 293–305.
- Smith, T.M., and R. W. Reynolds (2004) Improved extended reconstruction of SST (1854–1997). *J. Climate*, **17**(12), 2466–2477, doi: 10.1175/1520.
- Snorrrason, Á., H. Björnsson and H. Jóhannesson (2000) Causes, characteristics and predictability of floods in regions with cold climates. In: Parker, D. J., ed., *Floods*. Routledge, London, 198–215.
- Stern, N. (2006) Stern review on the economics of climate change, pre-publication edition: Available at
- Sælthun, N. R. (1996) *The “Nordic” HBV model-version developed for the project “Climate Change and Energy Production”*. NVE Publ. No. 7, Norwegian Water Resources and Energy Administration, Oslo.
- Sælthun, N. R., P. Aittoniemi, S. Bergström, K. Einarsson, T. Jóhannesson, G. Lindström, P.-E. Ohlsson, T. Thomsen, B. Vehviläinen, K. O. Aamodt (1998) *Climate change impact on runoff and hydropower in the Nordic countries—Final report from the project “Climate change and energy production”*. TemaNord 1998:552, Nordic Council of Ministers, Copenhagen.
- Thorsteinsson, Th., B. Einarsson, T. Jóhannesson and R. Hock (2006) Hofsjökull mass balance simulated with a degree-day model: Calibration and effects of including potential direct radiation. *Proc. The European Conference of Impacts of Climate Change on Renewable Energy Sources, Reykjavík, Iceland, June 5–6*.
- Thorsteinsson, Th., B. E. Einarsson, T. Jóhannesson and R. Hock (2006) *Comparison of degree-day models of the mass balance of the Hofsjökull ice cap*. Rep. OS-2006/014, National Energy Authority, Reykjavík.
- Tómasson, H. (1981) Vatnsafl Íslands, mat á stærð orkulindar (Hydropower in Iceland, an estimate of the size of an energy resource). In: *Orkuþing 81. Erindi flutt á Orkuþingi 9., 10. og 11. júní, 1981*. Vol. 2.
- Tómasson, H. (1982) Vattenkraft i Island och dess hydrologiska förutsättningar (Hydropower in Iceland and its hydrological prerequisites). In: *Den nordiske hydrologiske konferense, NHK-82, Förde 28.–30. juni 1982*. Rep. OS-82059/VOD-10, National Energy Authority, Reykjavík.
- Tómasson, G. G., H. Ólafsson and Ó. Rögnvaldsson (2005) Meteorological and hydrological modeling of an extreme precipitation event in S-Iceland. *Proc. Int. Conf. Alpine Meteorol. 2005*, 23–27 May 2005, Zadar, Croatia (ICAM), *Croatian Meteorol. Journ.*, **40**, 558–561 (PDF available at

- [“http://www.map.meteoswiss.ch/map-doc/icam2005/pdf/poster-session-d/D41.pdf”](http://www.map.meteoswiss.ch/map-doc/icam2005/pdf/poster-session-d/D41.pdf)).
- Uppala, S.M., and 45 co-authors (2005) The ERA-40 re-analysis. *Q. J. R. Meteorol. Soc.*, **131**, 2961–3012.
- Warner, T. T., R. A. Peterson and R. E. Treadon (1997) A tutorial on lateral boundary conditions as a basic and potentially serious limitation to regional numerical weather prediction. *Bull. Amer. Meteorol. Soc.*, **78**(11), 2599–2617.
- Westrick, K. J., P. Storck and C. F. Mass (2002) Description and evaluation of a hydro-meteorological forecast system for mountainous watersheds. *Wea. Forecasting*, **17**, 250–262.

## A The LT orographic precipitation model

The LT model (Smith and Barstad, 2004; Barstad and Smith, 2005) can be summarised by the following transfer function representing the Fourier transform of the distribution of precipitation rate

$$\widehat{P}(k, l) = \frac{C_w i \sigma \widehat{h}(k, l)}{(1 - imH_w)(1 + i\sigma\tau_c)(1 + i\sigma\tau_f)}. \quad (\text{A1})$$

In (A1), the air is assumed to be saturated with vapour,  $C_w$  is a coefficient depending on surface humidity and lapse rate and relating condensation rate to vertical motion,  $\widehat{h}(k, l)$  is the Fourier transform of the terrain elevation,  $k$  and  $l$  are the horizontal components of the wavenumber,  $i = \sqrt{-1}$ ,  $\sigma = Uk + Vl$  is the intrinsic frequency with  $U$  and  $V$  the eastward and northward components of the regionally averaged horizontal wind-vector,  $\tau_c$  is the conversion time from cloud water to hydrometeors and  $\tau_f$  the fallout time of hydrometeors to the ground,  $H_w$  is the thickness of the moist layer and  $m$  is the vertical wave number,

$$m = \left\{ \left[ \frac{N_m^2 - \sigma^2}{\sigma^2} \right] (k^2 + l^2) \right\}^{1/2}, \quad (\text{A2})$$

with  $N_m$  the moist buoyancy frequency. The precipitation field,  $P$ , in  $x, y$  space is then retrieved using an inverse Fourier transform

$$P(x, y) = \max\left(\int \int \widehat{P}(k, l) e^{i(kx+ly)} dkdl + P_\infty, 0\right), \quad (\text{A3})$$

where  $P_\infty$  represents the background precipitation field in the large-scale weather system. The truncation of negative precipitation values in (A3) that may be generated by the model in downslope regions simulates the effect of lee-side evaporation.

The input parameters to the model are  $U$ ,  $V$ ,  $P_\infty$ , the regionally averaged surface temperature, the terrain elevation  $h(x, y)$ ,  $\tau_c$ ,  $\tau_f$  and  $N_m$ . The main limitations are that the model is not suitable when unstable atmospheric conditions prevail and it is not capable to deal with flow blockings.

This model has been used by Crochet *et al.* (2007) with input meteorological information from ERA-40 (Uppala *et al.*, 2005) to estimate the detailed spatial distribution of precipitation in Iceland over the period 1958–2002. The LT model was run with a 6h time step to produce 6-hourly precipitation with a 1-km horizontal resolution, that was then accumulated over a day or longer. As the model development assumes saturated conditions, it is run only when the relative humidity ( $RH$ ) is greater or equal to 90%. This calculation has recently been extended to 2006 using input information from the available ECMWF analyses. As the ECMWF NWP model has changed from 2002 to 2006 and its horizontal resolution is getting finer, its capacity to simulate orographic precipitation has improved. The background precipitation used as input of the LT model may in fact already contain some orographic precipitation that needs to be identified and removed before running the LT model so that it is not “counted twice”. In order to deal with this matter and define an homogeneous procedure for the entire period 1958–2006, the following procedure was used.

i) The orographic component that may be present in the background precipitation is identified by running the LT model with orography ( $h_{NWP}$ ) corresponding to the NWP model to be downscaled

$$\widehat{P}_{NWP}(k, l) = \frac{C_w i \sigma \widehat{h}_{NWP}(k, l)}{(1 - imH_w)(1 + i\sigma\tau_c)(1 + i\sigma\tau_f)}, \quad (\text{A4})$$

$$P_{NWP}(x, y) = \begin{cases} \max\left(\int \int \widehat{P}_{NWP}(k, l) e^{i(kx+ly)} dkdl, 0\right) & \text{if } RH \geq 90\% \text{ and } P_\infty(x, y) > 0 \\ 0 & \text{if } RH < 90\% \text{ or } RH \geq 90\% \text{ and } P_\infty(x, y) = 0 \end{cases} \quad (\text{A5})$$

ii) The identified orographic precipitation (if any) already present in the background precipitation field is removed

$$P'_\infty = \max(P_\infty - P_{NWP}, 0) . \quad (\text{A6})$$

iii) The LT model precipitation is computed using the new background precipitation field

$$P(x, y) = \begin{cases} \max(\int \int \widehat{P}(k, l) e^{i(kx+ly)} dk dl + P'_\infty, 0) & \text{if } RH \geq 90\% \text{ and } P_\infty(x, y) > 0 \\ P_\infty(x, y) & \text{if } RH < 90\% \text{ or } RH \geq 90\% \text{ and } P_\infty(x, y) = 0 \end{cases} \quad (\text{A7})$$

## B Daily validation of simulated precipitation

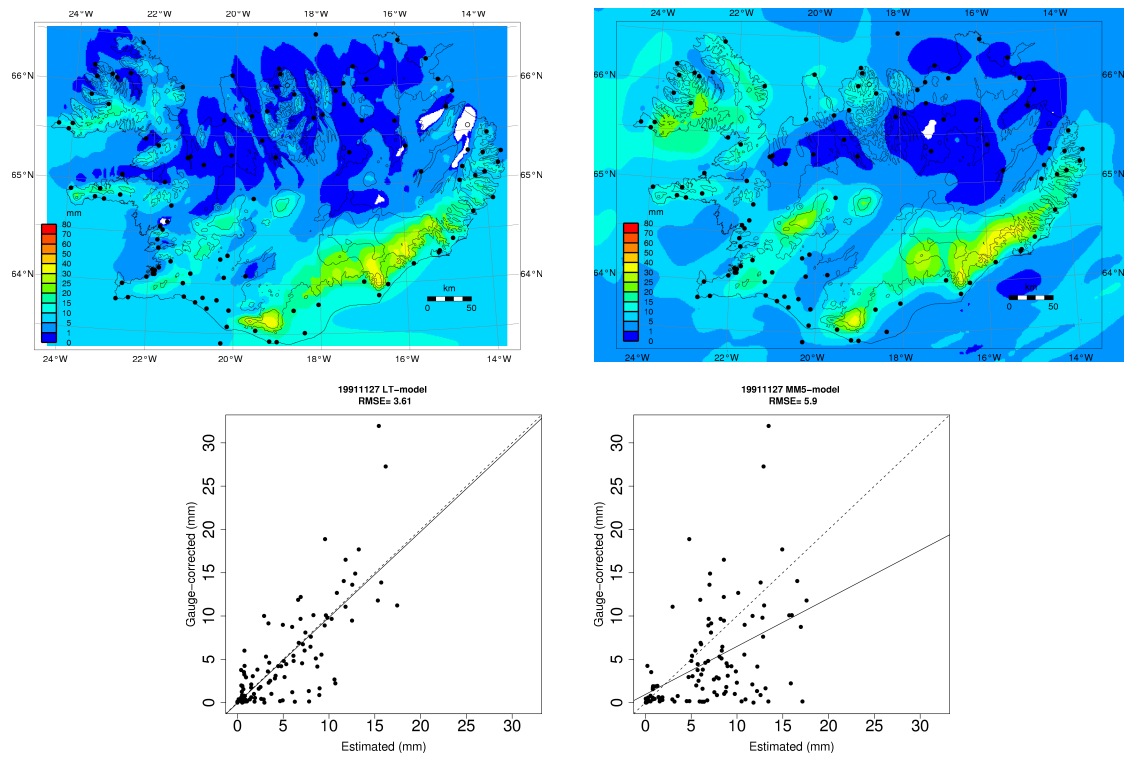


Figure B1: 1991-11-27: LT-model (left), MM5-model (right). The wind direction was from S.

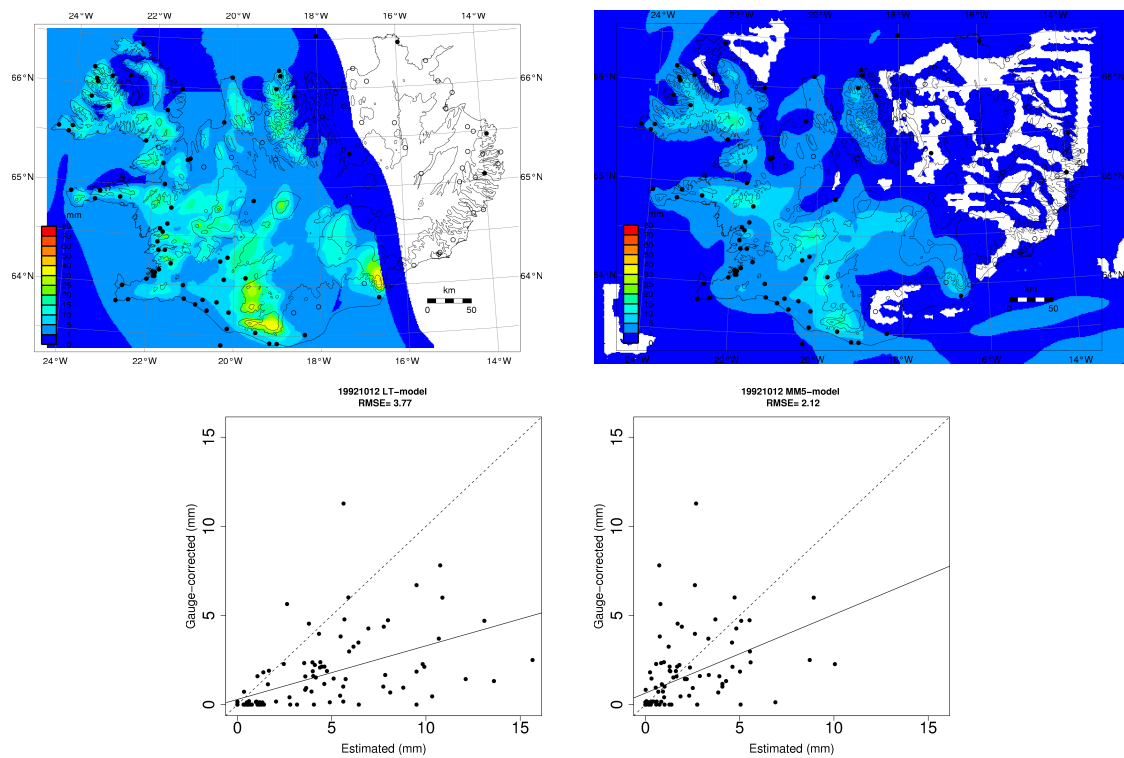


Figure B2: 1992-10-12: LT-model (left), MM5-model (right). The wind direction was from SW.

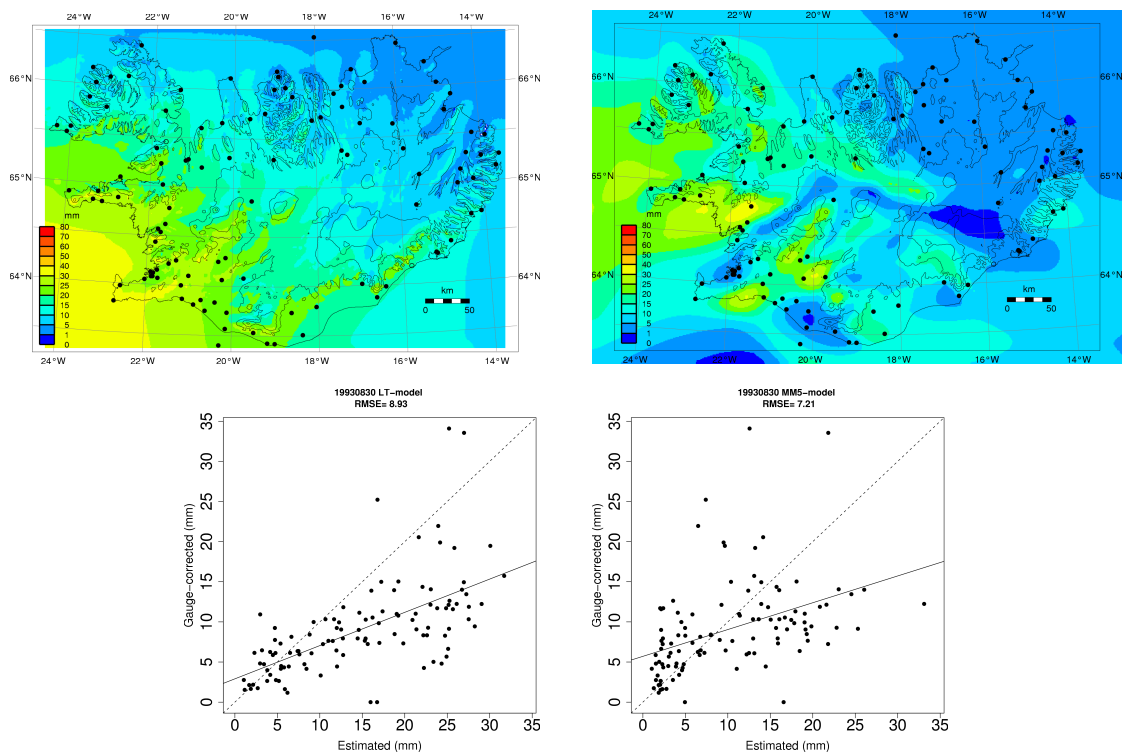


Figure B3: 1993-08-30: LT-model (left), MM5-model (right). The wind direction was from SE.

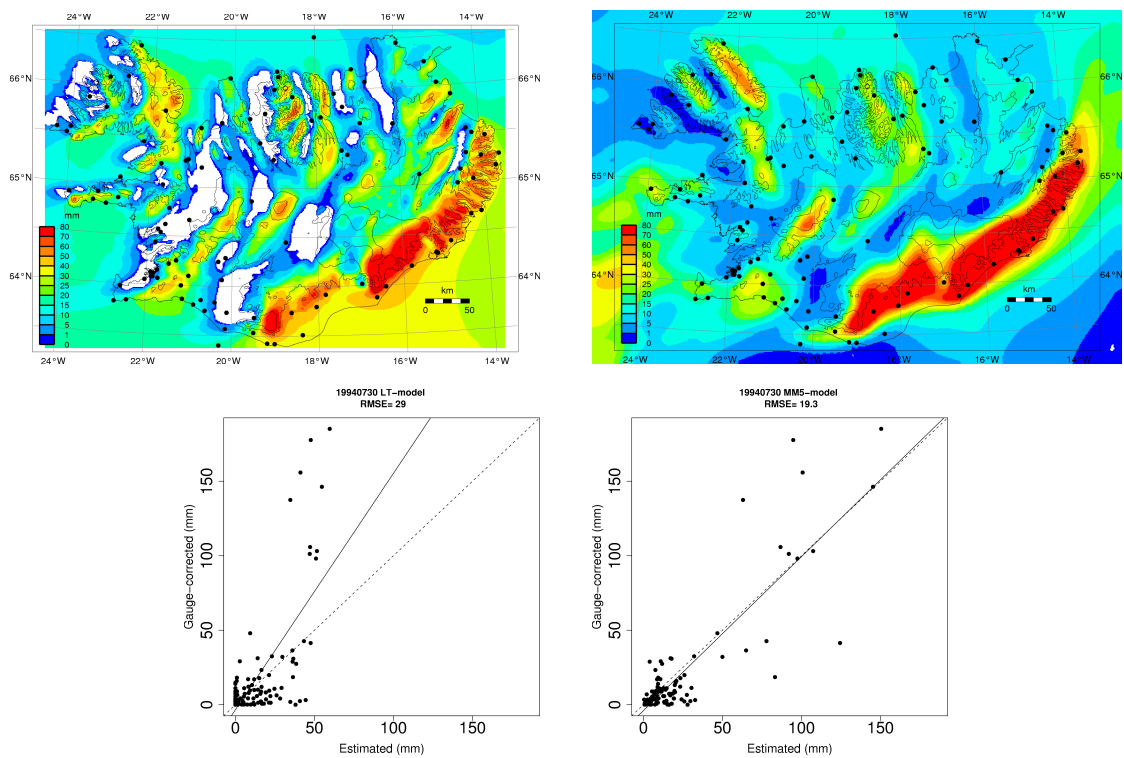


Figure B4: 1994-07-30: LT-model (left), MM5-model (right). The wind direction was from E.

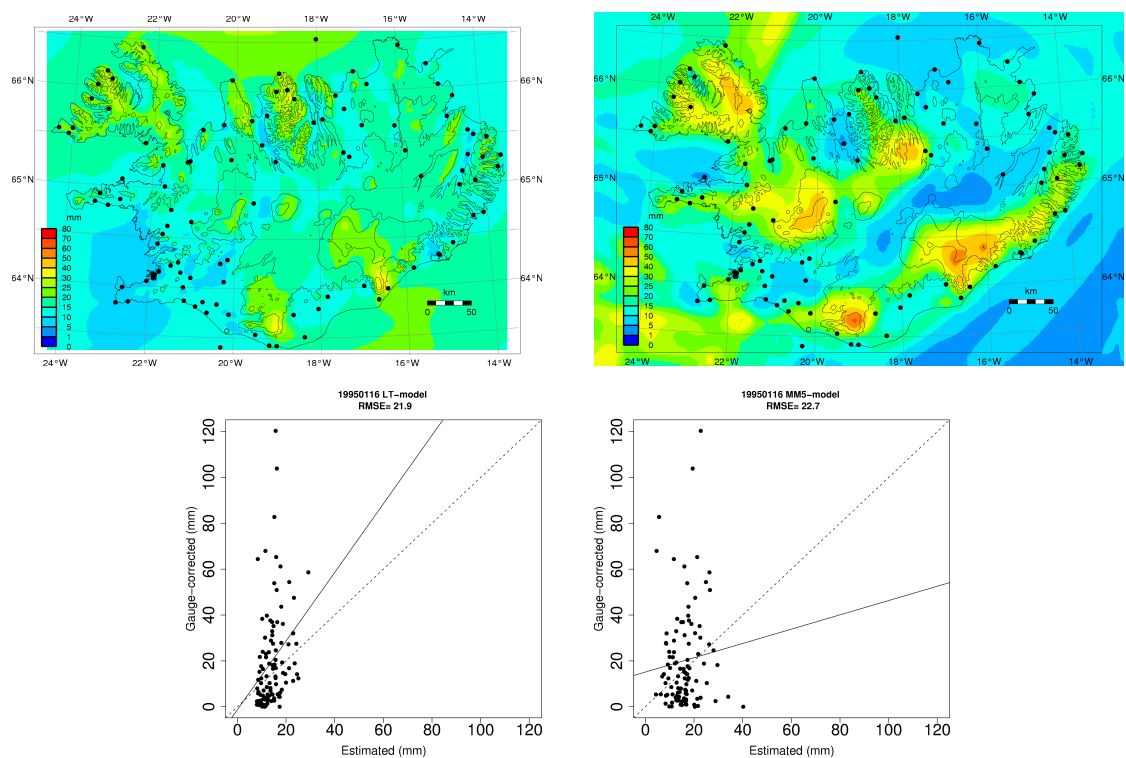


Figure B5: 1995-01-16: LT-model (left), MM5-model (right). A deep cyclon was off the north coast. The strongest wind was from N in NW-Iceland.

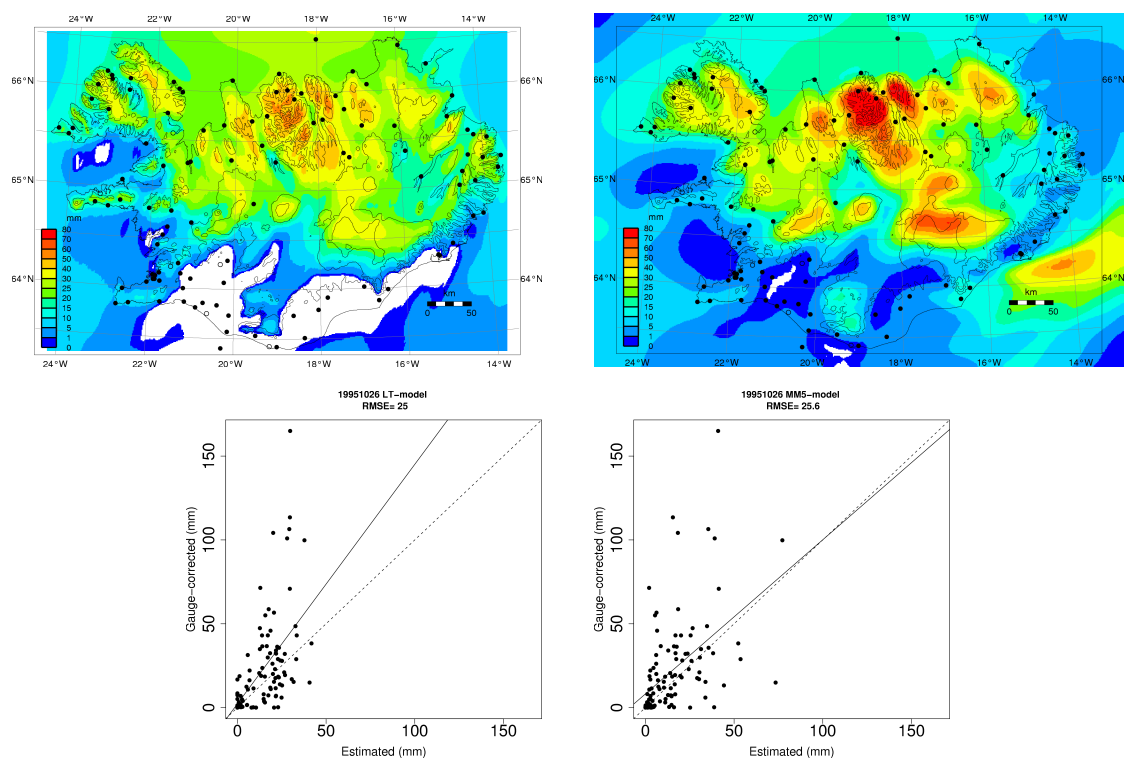


Figure B6: 1995-10-26: LT-model (left), MM5-model (right). The wind direction was from N.



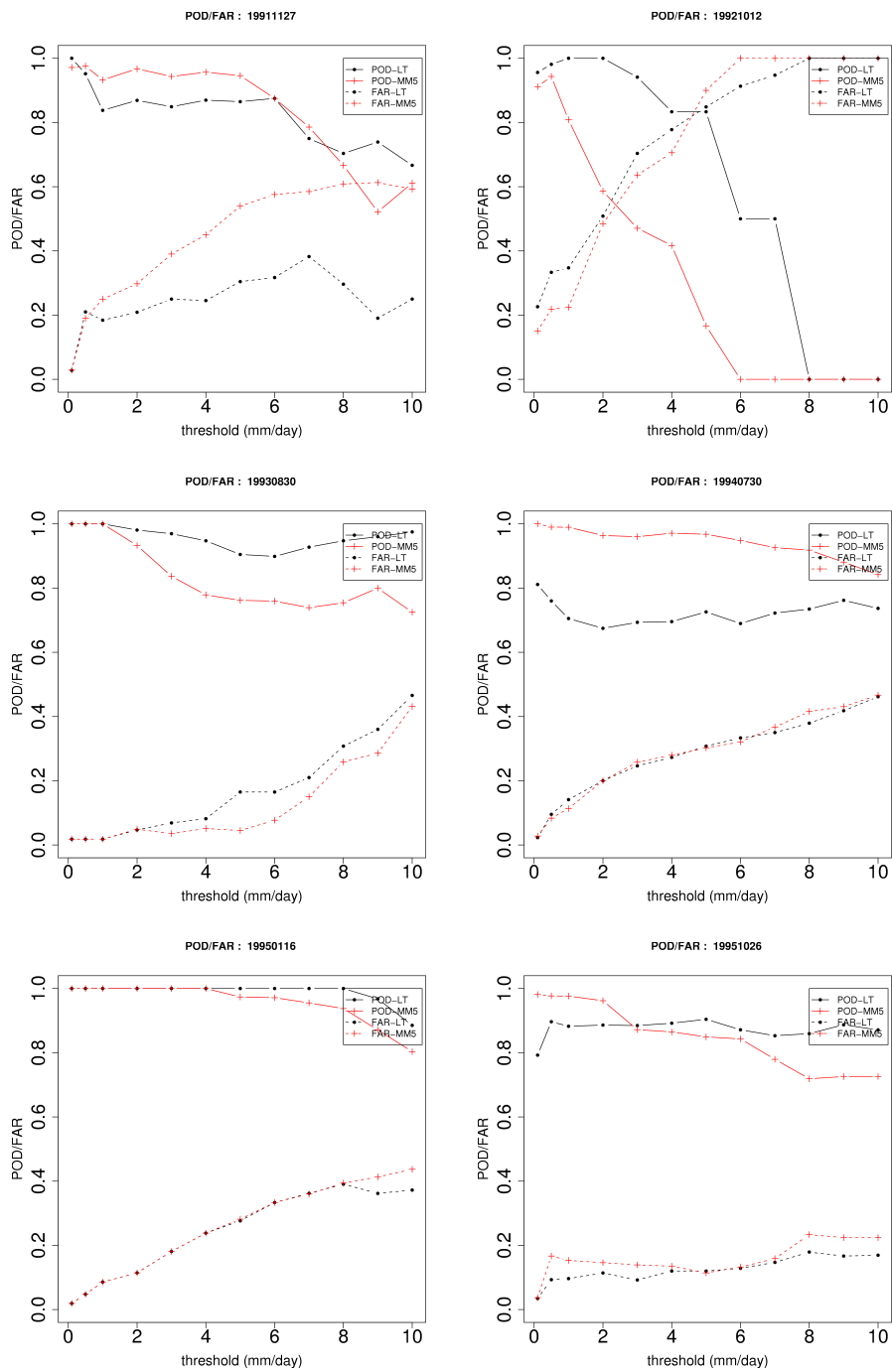


Figure B7: POD/FAR for the six validation days: LT-model (black), MM5-model (red).

## C $R2$ and $R2log$ coefficients for measured and simulated discharge

Table C1: The fit of water balance,  $R2$  and  $R2log$  at the watershed gauges used for calibration of the WaSiM watershed model.  $Q_{meas}$  is the measured discharge [ $m^3 s^{-1}$ ] during years when measured data exist for the whole year within the specific period.  $Q_{calc}$  is the calculated discharge during the same period. Difference between the two data sets is shown in percentages and  $R2$  and  $R2log$  are the Nash–Sutcliffe coefficients of fit for each gauge and period specified. Data are from Jónsdóttir (in press).

Station	Period	$Q_{meas}$	$Q_{calc}$	Difference	$R2$	$R2log$
10	1963–2001	10.9	10.5	-4%	0.62	0.58
12	1963–2001	6.9	7.2	3%	0.41	0.31
16	1963–2001	2.4	2.4	-2%	0.45	0.46
19	1963–2001	3.0	2.9	-5%	0.54	0.56
26	1965–2001	13.5	13.4	-1%	0.43	0.15
32	1971–2001	42.3	40.6	-4%	0.07	-0.03
38	1964–2001	2.3	2.3	0%	0.60	0.70
43	1963–2001	65.4	63.5	-3%	0.29	0.23
45	1963–2001	10.3	10.8	5%	0.54	0.46
48	1996–2001	21.9	21.5	-2%	0.16	0.12
50	1963–1997	84.7	83.2	-2%	0.52	0.59
51	1963–2001	10.1	10.0	-1%	0.62	0.5
54	1963–1989	42.1	42.8	2%	0.47	0.46
59	1973–2001	50.8	51.5	1%	0.26	0.25
60	1963–2001	20.4	20.2	-1%	0.39	0.44
66	1963–2001	79.4	75.4	-5%	0.18	-0.01
70	1963–2001	109	104	-5%	0.52	0.48
71	1981–2001	42.8	40.3	-6%	0.67	0.68
81	1963–2001	1.5	1.4	-1%	0.43	0.10
83	1963–2002	3.4	3.3	-2%	0.60	0.62
87+68	1964–2001	149	166	12%	0.42	0.46
96	1963–2001	83.1	84.8	2%	0.57	0.60
102	1963–2001	187	188	1%	0.75	0.73
104	1966–1983	2.6	2.4	-5%	0.58	0.61
105	1971–2001	37.0	38.1	3%	0.13	0.10
108	1963–1998	38.1	38.0	0%	-1.01	-1.41
109	1963–2001	34.1	33.9	-1%	0.68	0.67
110	1963–2001	157	178	13%	0.64	0.65
116	1963–2001	19.8	20.6	4%	-0.69	-0.60
128	1971–2001	22.4	22.8	2%	0.58	0.56
135	1966–2001	0.8	0.8	3%	0.62	0.69
144	1971–2001	38.7	38.6	0%	0.70	0.70
145	1971–2001	21.8	22.0	1%	0.54	0.61
146	1969–2001	5.3	5.4	2%	0.52	0.51
148	1963–2001	8.2	8.4	1%	0.59	0.60
150	1968–2001	26.6	28.1	6%	0.72	0.72
162	1984–2001	86.2	83.6	-3%	0.80	0.70

<b>Station</b>	<b>Period</b>	<b>Q<sub>meas</sub></b>	<b>Q<sub>calc</sub></b>	<b>Difference</b>	<b>R2</b>	<b>R2log</b>
164	1971–2001	118	116	-2%	0.78	0.76
167	1984–2001	23.1	21.8	-6%	0.42	0.67
185	1971–2001	2.1	2.3	6%	0.15	-0.36
198	1976–2001	15.5	16.1	4%	0.51	0.53
200	1976–2001	39.6	38.3	-3%	0.51	0.53
204	1976–2001	7.8	7.86	1%	0.62	0.61
205	1991–2003	15.9	15.9	0%	0.65	0.71
221	1981–2001	25.1	23.3	-7%	0.61	0.60
231	1984–2001	34.4	33.1	-4%	0.34	0.37
232	1984–2001	7.4	7.24	-2%	0.33	0.60
233	1985–2001	45.1	40.3	-11%	0.31	0.50
235	1985–2001	84.9	87.8	-3%	0.64	0.64
237	1986–2002	13.7	13	-5%	0.67	0.60
238	1988–2001	49.8	50.8	2%	0.46	0.56
254	1991–2004	3.9	4.2	8%	0.48	0.63
265	1991–2004	19.9	20.2	2%	0.66	0.71
266	1997–2002	5.2	3.96	-24%	0.71	0.70
269	1998–2004	3.0	2.83	-5%	0.41	0.27
271	1971–2001	108	110	2%	0.33	0.30
276	1991–1997	14.4	14.5	1%	0.56	0.63
278	1992–2004	1	1.1	10%	0.50	0.56
332	1997–2002	7.7	7.74	1%	0.29	0.17
365	1998–2004	3.7	3.62	-1%	0.61	0.56
366	1997–2004	3.6	4.06	12%	0.03	-0.40
411	2000–2004	17.8	17.6	-1%	0.46	0.65

## D Runoff maps

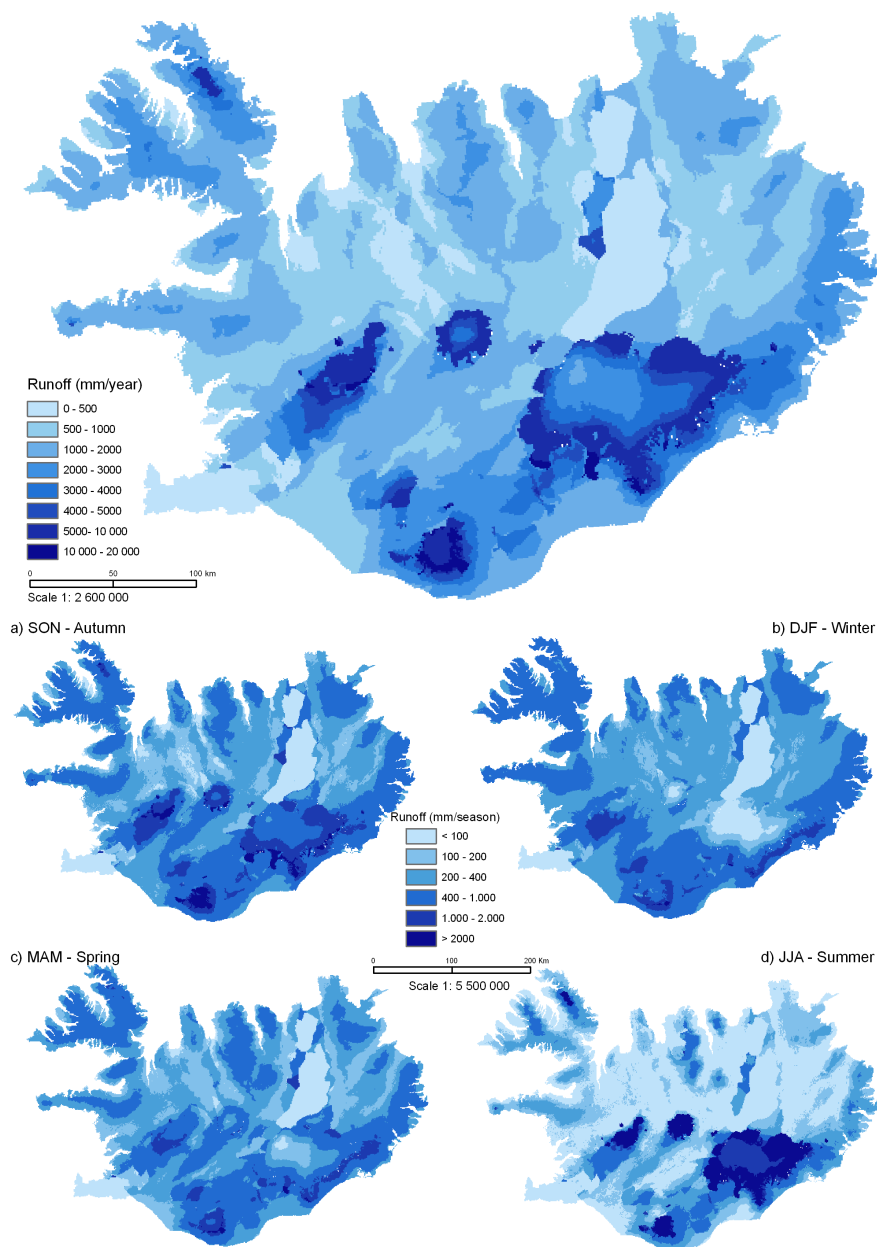


Figure D1: Projected mean annual and seasonal runoff in Iceland 2071–2100.

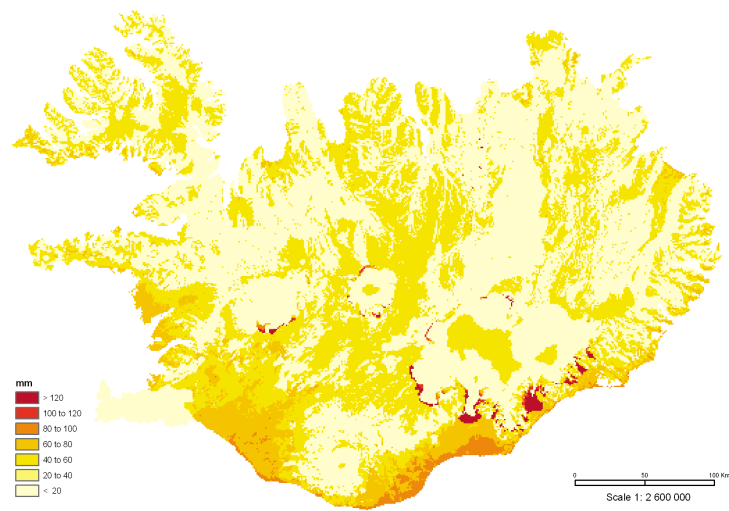


Figure D2: Projected change in mean annual evaporation from 1961–1990 to 2071–2100.

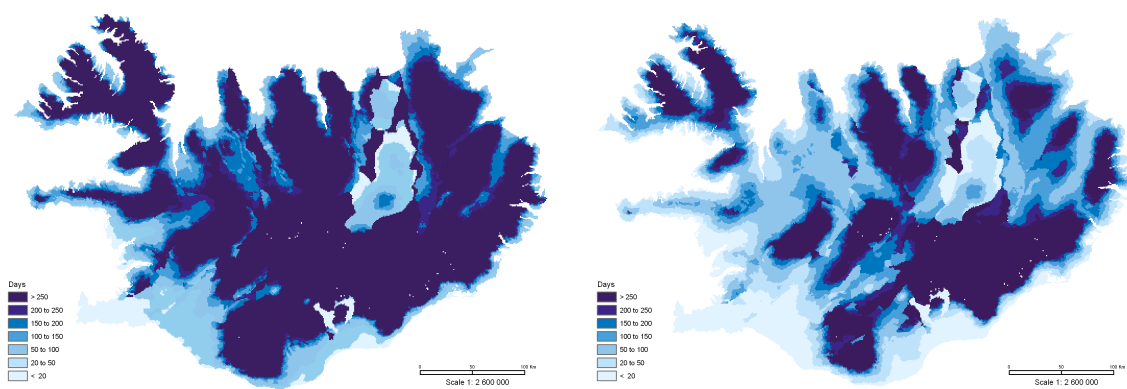


Figure D3: Mean annual number of days with snow covered ground. Left: Modelled for the reference period 1961–1990. Right: Projected for the period 2071–2100.

